Cretaceous large igneous provinces: from volcanic formation to environmental catastrophes and biological crises

L. M. E. Percival[1,2]*, H. Matsumoto[3], S. Callegaro[4], E. Erba[5], A. C. Kerr[6], J. Mutterlose[7] and K. Suzuki[3]

[1]Archaeology, Environmental Changes and Geo-Chemistry (AMGC), Vrije Universiteit Brussel, Pleinlaan 2, 1050 Brussels, Belgium

[2]Department of Earth Sciences, Faculty of Science, Vrije Universiteit Amsterdam, De Boelelaan 1085, 1081 HV Amsterdam, Netherlands

[3]Japan Agency for Marine-Earth Sciences and Technology, Natsushima, Yokosuka, Kanagawa 237-0061, Japan

[4]The Centre for Planetary Habitability, University of Oslo, Sem Sælands vei 2, 0371 Oslo, Norway

[5]Dipartimento di Scienze della Terra, Università degli Studi di Milano, 20133 Milan, Italy

[6]School of Earth and Environmental Sciences, Cardiff University, Park Place, Cardiff CF10 3AT, UK

[7]Institut für Geologie, Mineralogie und Geophysik, Ruhr-Universität Bochum, Universitätsstraße 150, 44801 Bochum, Germany

LMEP, 0000-0002-9377-1589

*Correspondence: l.m.e.percival@vu.nl

Abstract: The Cretaceous Period was marked by the formation of numerous large igneous provinces (LIPs), several of which were associated with geologically rapid climate, environmental and biosphere perturbations, including the early Aptian and latest Cenomanian oceanic anoxic events (OAEs 1a and 2, respectively). In most cases, magmatic CO_2 emissions are thought to have been the major driver of climate and biosphere degradation. This work summarizes the relationships between Cretaceous LIPs and environmental perturbations, focusing on how volcanism caused climate warming during OAE 1a using osmium-isotope and mercury concentration data. The new results support magmatic CO_2 output from submarine LIP activity as the primary trigger of climate warming and biosphere stress before/during OAE 1a. This submarine volcanic trigger of OAE 1a (and OAE 2), two of the most climatically/biotically severe Cretaceous events, highlights the capacity of oceanic LIPs to impact Earth's environment as profoundly as many continental provinces. Cretaceous magmatism (and likely output of CO_2 and trace-metal micronutrients) was apparently most intense during those OAEs; further studies are needed to better constrain the eruption histories of those oceanic plateaus. Another open question is why the Cretaceous Period overall featured a higher rate of magmatic activity and LIP formation compared with before and afterwards.

Supplementary material: Geochemical datasets from Deep Sea Drilling Project (DSDP) Site 398 and Alstätte-1 and a summary of Cretaceous Os isotope literature are available at https://doi.org/10.6084/m9.figshare.c.7026011

Large igneous provinces (LIPs) represent the formation of huge volumes of igneous material emplaced into and/or onto the Earth's continental or oceanic crust over a geologically short time interval (Coffin and Eldholm 1994). This emplacement occurs through a combination of both intrusive magmatism and extrusive volcanic activity: the latter is most famously in the form of continental flood basalts, some of which featured individual lava flows with an aerial extent on the order of 10^4 km^2 (e.g. Coffin and Eldholm 1994; Bryan and Ernst 2008; Bryan and Ferrari 2013; Ernst 2014). Several different formal definitions for large igneous provinces have been proposed, characterizing them as magmatic provinces with high volumes of igneous material that can form in a range of intraplate tectonic settings, with the majority of magmas emplaced over a geologically short space of time (e.g. >0.1 Mkm^3 in pulses of *c.* 1–5 Myr; Bryan and Ernst 2008; or >0.1 Mkm^3, frequently >1 Mkm^3, in <5 Myr, often <2 Myr; Ernst *et al.* 2021).

The history of LIP formation over the last 300 Myr, since the formation of the Pangaean supercontinent, is relatively well established. Several

From: Hart, M. B., Batenburg, S. J., Huber, B. T., Price, G. D., Thibault, N., Wagreich, M. and Walaszczyk, I. (eds) *Cretaceous Project 200 Volume 1: the Cretaceous World*. Geological Society, London, Special Publications, **544**, https://doi.org/10.1144/SP544-2023-88

provinces are preserved as flood basalt units and/or large-scale intrusive sill and dyke swarms on the continents, or as oceanic plateaus in the Pacific and Indian ocean basins (see e.g. Coffin and Eldholm 1994; Ernst 2014; Kerr 2014; Ernst *et al.* 2021). These LIPs are generally better preserved than those that formed prior to 300 Ma, and are typically estimated to have had original volumes of emplaced magma greater than 0.1 Mkm^3; frequently above 1 Mkm^3 (Bryan and Ernst 2008; Ernst *et al.* 2021). However, the Greater Ontong–Java Plateau in the western Pacific Ocean may have been an order of magnitude more voluminous still (Gladczenko *et al.* 1997; Taylor 2006; Hoernle *et al.* 2010). The rapid emplacement of most provinces (within *c.* 1 Myr; see Kasbohm *et al.* 2021, and references therein) highlights that the rate of magma production during LIP formation was typically both higher and sustained for longer time periods than for any observed volcanic activity in human history. In this context, it is notable that the large majority of geologically rapid changes to Earth's global climate and environment during the Phanerozoic Aeon, particularly in the last 300 Myr, broadly coincided with an interval of LIP formation. These events include at least four of the so called 'Big Five' mass extinctions (e.g. Wignall 2001; Courtillot and Renne 2003; Bond and Wignall 2014; Ernst *et al.* 2021; Kasbohm *et al.* 2021).

The Cretaceous Period (143–66 Ma; Gale *et al.* 2020) was marked by the highest rate of LIP formation in at least the last 300 Myr. Numerous provinces were emplaced into both the continental and oceanic crust, and estimates of the total number of Cretaceous LIPs vary (but see recent lists by e.g. Torsvik 2019; Ernst *et al.* 2021). However, there are seven major Cretaceous LIPs that comprise both high volumes of igneous material and have been widely linked with climate/environmental change and/or elevated biotic stress/extinction during that period (Fig. 1). Continental flood-basalt provinces include the Paraná–Etendeka LIP, the High Arctic LIP (HALIP), the Madagascan LIP, and the Deccan Traps (although the latter three also comprise offshore components). Additionally, the Greater Ontong–Java, Kerguelen, and Caribbean plateaus were emplaced into continental margins and ocean crust to form oceanic plateaus, which are considered to represent large areas of elevated and thickened basaltic ocean floor formed through mantle-plume activity rather than seafloor spreading-related magmatic processes (Kerr 2014). Indeed, owing to the subduction of most pre-Jurassic crust, many currently known oceanic LIPs are Cretaceous in age, including those that are best preserved and most extensively investigated (see Kerr 2014). This work reviews the seven major Cretaceous LIPs that are thought to have impacted Earth's environment and/or biosphere, and the relationship between these phenomena, utilizing both new datasets for one such environmental episode, the Early Aptian oceanic anoxic event (OAE 1a), and published datasets relating to this and other Cretaceous intervals and LIPs.

Cretaceous LIPs and episodes of environmental change

The Paraná–Etendeka LIP and Valanginian 'Weissert' Event

The Paraná–Etendeka LIP covers an area of *c.* 4 Mkm^2 in western South America (principally Brazil, but also Paraquay, Uruguay and Argentina) and western Africa (Namibia and Angola), and has long been associated with the opening of the South Atlantic Ocean (Peate 1997). Extrusive magmas largely comprise tholeiitic basalt flows, with some silicic and alkaline units and intrusive sills and dyke swarms, particularly in the South American Paraná part of the province (e.g. Erlank *et al.* 1984; Milner *et al.* 1992, 1995; Peate 1997; Marsh *et al.* 2001; De Min *et al.* 2018; see also Gomes and Vasconcelos 2021, and references therein). The volatile budget of Paraná–Etendeka magmas may have been relatively low compared with other LIPs, as calculated from phenocrysts and measured from melt inclusions (maximum of 900–1100 ppm S, 125 ppm Cl and 450 ppm F; Callegaro *et al.* 2014; Marks *et al.* 2014). Moreover, the magmas were emplaced within or erupted on to country rocks that largely consisted of aeolian sandstones, organic-lean shales and crystalline basement (Barreto *et al.* 2016; Jones *et al.* 2016). These lithologies were all probably volatile depleted and would not have been a major source of thermogenic carbon or sulfur following heating by the intruding magmas (cf., Svensen *et al.* 2004, 2009; Heimdal *et al.* 2018).

Paraná–Etendeka volcanism is widely attributed to have caused an episode of prolonged environmental perturbation during the Valanginian Stage (137.7–132.6 Ma), known as the Weissert Event (Erba *et al.* 2004). This episode of environmental change is characterized in the upper Valanginian stratigraphic record by a positive carbon-isotope ($\delta^{13}C$) excursion of ~1.5–2 ‰ in carbonate and up to 4 ‰ in bulk organic matter (e.g. Lini *et al.* 1992; Weissert *et al.* 1998; Erba *et al.* 2004; Price and Mutterlose 2004; Gröcke *et al.* 2005; McArthur *et al.* 2007; Bornemann and Mutterlose 2008; Littler *et al.* 2011; Price *et al.* 2018; Jelby *et al.* 2020). The end of the Weissert Event is marked by the maximum value of the positive carbon-isotope excursion in upper Valanginian strata (Erba *et al.* 2004), although the $\delta^{13}C$ values decrease gradually through lower Hauterivian strata. This $\delta^{13}C$ shift was initially hypothesized to result from enhanced burial of

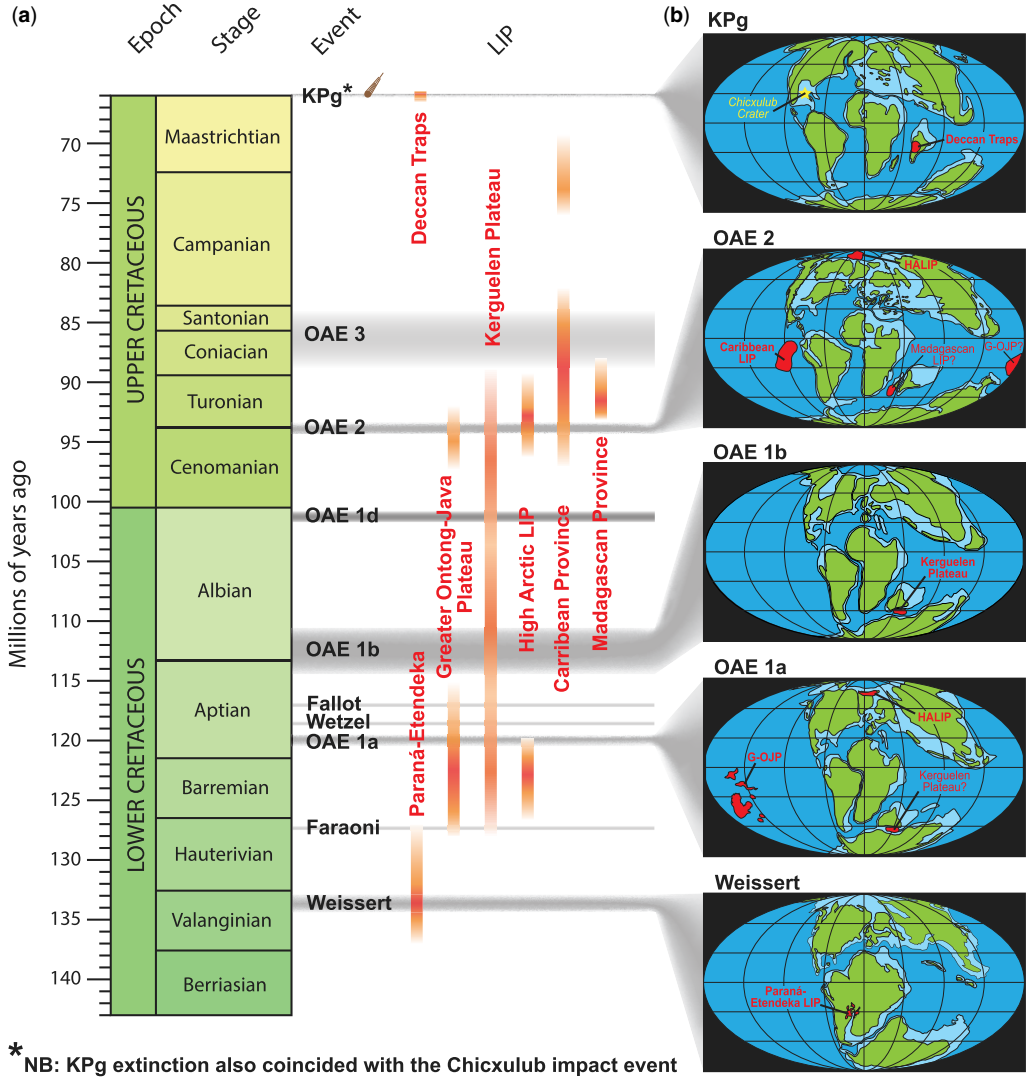

Fig. 1. (**a**) Occurrence of large igneous province (LIP) volcanism (vertical orange bars), and episodes of major environmental change (horizontal grey bars), during the Cretaceous Period. Ages and durations of volcanic activity are primarily based on Jiang *et al.* (2023) (the range of the Ontong-Java is extended into the Aptian to account for palaeontological and geochemical evidence of activity at that time). Ages and durations of major events from Wagreich (2012), Jenkyns (2010), Schulte *et al.* (2010), Eldrett *et al.* (2015), Cavalheiro *et al.* (2021), Matsumoto *et al.* (2022) and Martinez *et al.* (2023). (**b**) Palaeogeographic maps show the reconstructed continental positions during the Weissert Event, oceanic anoxic events (OAEs) 1a, 1b and 2, and the Cretaceous–Paleogene (KPg) transition, with the LIPs that have been associated with each event indicated in red (with the Chicxulub impact crater also indicated by the yellow star for the KPg). Sources: Palaeogeographical reconstructions are modified from the following sources: Weissert Event from Möller *et al.* (2020) and Charbonnier *et al.* (2020*b*); OAE 1a from Percival *et al.* (2021*b*) and Kocsis and Scotese (2021); OAE 1b from Kocsis and Scotese (2021); OAE 2 from Du Vivier *et al.* (2015); and the KPg from Claeys *et al.* (2002).

organic carbon (which is isotopically light) in sediments as they were deposited, leaving the residual seawater carbon inventory, and any carbonates or organic material subsequently formed from it, isotopically heavier (Weissert *et al.* 1998; Erba *et al.* 2004). However, while some Valanginian strata do preserve organic-rich facies consistent with this hypothesis, the majority do not. Thus,

enhanced primary productivity and burial of organic carbon in terrestrial sediments have been proposed as alternative contributors towards the carbon-cycle change (Westermann *et al.* 2010).

The nature of climate change during the Weissert Event is debated. The Early Valanginian interval prior to and during the onset of the Weissert Event was marked by a warm global climate (Littler *et al.* 2011), and evidence for surface warming at that time has been documented from bulk-rock oxygen-isotope ($\delta^{18}O$) records in some NW Tethyan and proto-Atlantic archives (Duchamp-Alphonse *et al.* 2007; Charbonnier *et al.* 2020*c*). Clay mineralogy and calcareous nannofossil and spore–pollen assemblages also indicate enhanced humidity in and around the former region (Kujau *et al.* 2013; Möller *et al.* 2020; Charbonnier *et al.* 2020*c*). Thus far, this warming has not been as clearly recorded by other palaeotemperature proxies or robustly documented in other areas around the world, with only modest temperature increases of at most 1°C that largely do not significantly exceed pre-event variations (e.g. Littler *et al.* 2011; Price *et al.* 2018; Charbonnier *et al.* 2020*c*; Cavalheiro *et al.* 2021). In contrast, in several Valanginian records, particularly those from the Boreal Realm but also in the NW Tethys and southern high latitudes, the turning point in $\delta^{13}C$ values at the peak of the positive excursion stratigraphically correlates with evidence for the onset of a transient fall in surface temperatures, (e.g. Erba *et al.* 2004; McArthur *et al.* 2007; Meissner *et al.* 2015; Price *et al.* 2018; Cavalheiro *et al.* 2021). This correlation between the $\delta^{13}C$ peak and onset of temperature decrease is consistent with enhanced atmospheric CO_2 sequestration through the hypothesized increase in organic-carbon burial. However, proto-Atlantic sea-surface temperature reconstructions based on the biomarker-based TEX_{86} palaeothermometer suggest that stable warm conditions persisted throughout the Valanginian in that low-latitude environment (Littler *et al.* 2011), potentially highlighting a steepening of global temperature gradients during the Weissert Event (Charbonnier *et al.* 2020*c*; Cavalheiro *et al.* 2021).

Age constraints for Paraná–Etendeka volcanism are based on magnetostratigraphy and both argon–argon ($^{40}Ar/^{39}Ar$) and uranium–lead (U–Pb) geochronology. Collectively, these data suggest a duration of at least 2–3 Myr of effusive volcanic activity for the LIP as a whole, with Etendeka magnetostratigraphy suggesting even more protracted eruptions in that part of the province (see compilations by Mena *et al.* 2011; Dodd *et al.* 2015; Gomes and Vasconcelos 2021; Bacha *et al.* 2022; Jiang *et al.* 2023). Uranium–lead and $^{40}Ar/^{39}Ar$ dating of Paraná and Etendeka units by several studies have outlined a pronounced pulse of volcanic activity that probably reached its maximum between 134 and 135 Ma (Renne *et al.* 1992, 1996; following recalculation by Thiede and Vasconcelos 2010; also Ernesto *et al.* 1999; Janasi *et al.* 2011; Pinto *et al.* 2011; Florisbal *et al.* 2014; Almeida *et al.* 2018; Gomes and Vasconcelos 2021; Bacha *et al.* 2022). These magmatic ages broadly overlap with the onset date of the Weissert Event based on both magnetostratigraphic (133.9 Ma; Cavalheiro *et al.* 2021) and cyclostratigraphic (134.56 Ma; Martinez *et al.* 2023) age modelling. However, recent high-precision U–Pb dating of Paraná rocks has shown that at least part of the intense volcanic activity postdated the start of the Weissert Event (Rocha *et al.* 2020). To what extent the older v. younger dates of Paraná–Etendeka magmas are representative of rates of extrusive volcanic activity across the province as a whole is unclear. Because the majority of dated rocks are coeval with the onset of the Weissert Event, it is widely assumed that there was a causal relationship between the two phenomena (e.g. Erba *et al.* 2004; Martinez *et al.* 2015, 2023; Gomes and Vasconcelos 2021; Bacha *et al.* 2022), although it cannot be excluded that significant Paraná–Etendeka volcanism occurred later, potentially questioning the nature of any link (Rocha *et al.* 2020).

The Greater Ontong–Java Plateau and Early Aptian OAE (OAE 1a)

The total magmatic volume comprised by the Greater Ontong–Java Plateau (G-OJP) is debated, but is often defined as the Ontong–Java Plateau together with subsidiary nearby flood-basalt provinces such as the Nauru, East Mariana, Manihiki and Hikurangi (after Ingle and Coffin 2004; Charbonnier and Föllmi 2017; see also Svensen *et al.* 2019, and references therein). These provinces were collectively emplaced on to the western Pacific oceanic crust during the Early Cretaceous, covering an area over 2 Mkm^2, and comprising a combined total volume of several tens of millions of cubic kilometres, significantly greater than any other preserved LIP (Taylor 2006; Hoernle *et al.* 2010). Moreover, part of the original plateau has likely been subducted since its emplacement (see Schlanger *et al.* 1981; Larson 1991). Accreted and exposed Ontong–Java magmas in Malaita (Solomon Islands) consist of massive sheeted and pillowed basalt flows, with basaltic rocks also recovered from ODP drill sites on the plateau (e.g. Saunders *et al.* 1996; Tejada *et al.* 1996; Neal *et al.* 1997; Fitton and Godard 2004). It is likely that much of the G-OJP was emplaced via submarine volcanic activity (Saunders *et al.* 1996). However, preservation of phreatomagmatic deposits at Ocean Drill Program (ODP) Site 1184 in the Eastern Salient of the Ontong–Java Plateau shows that at least some eruptions occurred near

or above the sea surface (Chambers *et al.* 2004; Thordarson 2004).

Geochronological $^{40}Ar/^{39}Ar$ studies on Ontong–Java basalts and volcaniclastic sediments from southern Malaitia, Ramos Island and ODP sites 289, 807 and 1184 indicate a pulse of volcanic activity that covered a huge area around 122 Ma (Mahoney *et al.* 1993; Tejada *et al.* 1996, 2002; Chambers *et al.* 2004). Submarine eruptions of a broadly similar age have also been reported from studies of whole rock basalts recovered from the Manihiki and Hikurangi plateaus (Ingle *et al.* 2007; Hoernle *et al.* 2010; Timm *et al.* 2011). Recently, this geochronology has been challenged by Davidson *et al.* (2023), on the basis that older ages might be affected by recoil, while plagioclase $^{40}Ar/^{39}Ar$ dates from Ontong–Java and Manihiki plateau rocks have ages closer to 110 Ma than 120 Ma. However, those authors do not discount the possibility that the G-OJP had a protracted emplacement over several million years across the late Barremian to early Albian interval, in which their dates are from volcanic rocks that were erupted towards the end of the plateau's formation. Mahoney *et al.* (1993) and Tejada *et al.* (1996) also report eruption ages of *c.* 90 Ma at Sigana Island and ODP Site 803, potentially highlighting a second major pulse of volcanism on the G-OJP. Plateau formation through two distinct spells of volcanism 30 Myr apart is at odds with the mantle plume model of LIP emplacement, and it has been suggested that the younger dates are also affected by argon recoil, and may represent minimum ages (Chambers *et al.* 2002).

The 122 Ma pulse of volcanism has long been associated with OAE 1a (121 Ma), based on the broad temporal correlation between the two phenomena (e.g. Larson and Erba 1999; Courtillot and Renne 2003; Erba *et al.* 2015). The Early Aptian oceanic anoxic event was marked by the development of marine anoxia/euxinia across the global ocean for approximately 1–1.4 Myr (Li *et al.* 2008; Malinverno *et al.* 2010; Leandro *et al.* 2022). Widespread oxygen-depleted conditions were initially interpreted from the preservation of laminated, organic-rich, mudstones around the world, dubbed the Selli Level in the Umbria–Marche Basin of central Italy (e.g. Schlanger and Jenkyns 1976; Weissert 1989; Jenkyns 1995; Pancost *et al.* 2004; Föllmi *et al.* 2006; van Breugel *et al.* 2007; see also reviews by Jenkyns 2010 and Robinson *et al.* 2017). Global stratigraphic records of OAE 1a are further characterized by a series of $\delta^{13}C$ excursions, reflecting sequential carbon-cycle perturbations during the Early Aptian (Weissert 1989; Jenkyns 1995; Menegatti *et al.* 1998; Gröcke *et al.* 1999; Ando *et al.* 2008; Robinson *et al.* 2008; Vickers *et al.* 2016). These $\delta^{13}C$ excursions have been subdivided into segments (C3–C7) based on Tethyan archives (Menegatti *et al.* 1998). Following a relatively stable $\delta^{13}C$ signature through uppermost Barremian–lowermost Aptian strata (C1–C2), a sharp negative shift is documented at the base of the OAE 1a level (C3), highlighting a large influx of isotopically light carbon to the Earth's surface from one or more of volcanic activity, thermogenic emissions, and methane clathrate destabilization (e.g. Jahren *et al.* 2001; Méhay *et al.* 2009; Kuhnt *et al.* 2011; Naafs *et al.* 2016; Bauer *et al.* 2017; Adloff *et al.* 2020). The negative isotopic signature is followed by a positive rebound (C4), another stable spell (C5), a second positive excursion at the top of the OAE level (C6) and a continuation of elevated $\delta^{13}C$ values that remain high above it (C7), with these later shifts probably reflecting the widespread deposition of organic carbon (Jenkyns 2010). The various carbon-cycle perturbations impacted Earth's surface climate during OAE 1a, with overarching climate warming and transient interludes of cooling during the event interpreted from palaeontological and geochemical evidence (e.g. Menegatti *et al.* 1998; Jenkyns 2003, 2018; Dumitrescu *et al.* 2006; Ando *et al.* 2008; Kuhnt *et al.* 2011; Bottini *et al.* 2015; Naafs and Pancost 2016). As well as oceanic anoxia and global temperature changes, OAE 1a is thought to have been marked by seawater acidification, biospheric stress, accelerated hydrological cycling and enhanced continental weathering (e.g. Erba 2004; Erba *et al.* 2010, 2015; Bottini *et al.* 2012; Mutterlose *et al.* 2014; Lechler *et al.* 2015; Naafs and Pancost 2016).

The Kerguelen Plateau and Aptian–Albian OAE (OAE 1b)

The Kerguelen Plateau began to form during the break-up of India from Australia and Antarctica during the Early Cretaceous, and today encompasses an area of elevated oceanic crust comprising >2 Mkm^3 of mainly basaltic rock, with some dacites and rhyolites (Kerr 2014). Additional fragments of the plateau such as Broken Ridge and Ninetyeast Ridge are preserved in the Indian Ocean (see Wallace *et al.* 2002, and references therein). Some older magmas that formed during the initial break-up of southern Gondwana are also preserved in NE India and western Australia (Frey *et al.* 1996; Coffin *et al.* 2002; Kent *et al.* 2002). Unlike many LIPs, the Kerguelen Plateau has a long volcanic history, commencing in the Early Cretaceous and continuing (less voluminously) to the present day (see Coffin *et al.* 2002; Jiang *et al.* 2021). The onshore volcanics all date to 114 Ma or older; Baksi 1995; Frey *et al.* 1996; Coffin *et al.* 2002; Kent *et al.* 2002). The oldest part of the main oceanic province is the Southern Kerguelen Plateau, for which $^{40}Ar/^{39}Ar$ dates suggest that volcanic activity commenced by 125 Ma

at least, and possibly earlier (Jiang *et al.* 2022). Volcanic activity on the Southern Kerguelen Plateau continued until 110 Ma (Whitechurch *et al.* 1992; Coffin *et al.* 2002; Duncan 2002; Jiang *et al.* 2022), with later eruptions occurring on the Central Kerguelen Plateau and Elan Bank (100.4 $\pm$ 0.7 and 107.7 Ma, respectively; Duncan 2002). Further north, Broken Ridge samples have been dated to *c.* 95 Ma (Duncan 2002), while ages for rocks from Ninetyeast Ridge and Skiff Bank are younger still (*c.* 85–35 Ma; Duncan 1978, 1991, 2002).

Jiang *et al.* (2022, 2023) have recently proposed a revision of the temporal magmatic history of Kerguelen, and argue that the volcanism commenced at 125 Ma or earlier. As such, these authors suggest that early volcanic activity on the plateau may have contributed towards the environmental change associated with OAE 1a, while acknowledging that Kerguelen carbon emissions were unlikely to have caused the OAE alone. More frequently, a link has been postulated between the Kerguelen Plateau and more moderate environmental change during the Aptian–Albian transition (*c.* 113 Ma), often referred to as OAE 1b, based on a better age correlation between the two phenomena (e.g. Trabucho Alexandre *et al.* 2011; Erba *et al.* 2015; Sabatino *et al.* 2018; Matsumoto *et al.* 2020). This interval of marine anoxia is documented in the Vocontian Basin (SE France) and NW Tethys by the preservation of four main discrete organic-rich shale intervals (the Jacob, Kilian, Paquier or Urbino level, and Leenhardt levels; Bréhéret 1988; Coccioni *et al.* 2014). Some of these shale horizons have also been identified in Atlantic sites (e.g. Erbacher *et al.* 2001; Herrle *et al.* 2004; Trabucho Alexandre *et al.* 2011). Of those four shale levels, the Kilian and Paquier horizons are the two that have been the most widely identified around the world (see overviews in Coccioni *et al.* (2014); Bodin *et al.* 2023), with OAE 1b sometimes referred to as the Paquier Event (Jenkyns 2010). Upper Aptian–lower Albian strata also document a series of $\delta^{13}C$ excursions, with the Kilian and Paquier levels both marked by sharp negative carbon-isotope shifts of 2–3‰ that have been used to identify OAE 1b strata at sites around the world not marked by deposition of organic-rich sediments (e.g., Gröcke *et al.* 1999; Millán *et al.* 2014; Tsikos *et al.* 2004*b*; Herrle *et al.* 2015; Navarro-Ramirez *et al.* 2015; Phelps *et al.* 2015; Li *et al.* 2016; Zhao *et al.* 2022). Upper Aptian palaeotemperature records from the North Atlantic indicate a prolonged cooling pulse prior to/during the onset of OAE 1b (McAnena *et al.* 2013), and a cold pulse has also been postulated from study of Vocontian Basin and NW Tethys Ocean sites (Herrle and Mutterlose 2003; Bottini and Erba 2018). However, there is no clear evidence for a similar fall in temperatures in the South Atlantic (Jenkyns *et al.* 2012). In contrast, the Paquier level (or its stratigraphic equivalent) is marked by evidence for climate warming in the Vocontian Basin, North Atlantic and NW Tethys (Erbacher *et al.* 2001; Herrle *et al.* 2003; Huber *et al.* 2011; Bottini and Erba 2018).

The Caribbean LIP and the latest Cenomanian OAE (OAE 2)

The Caribbean (or Caribbean–Colombian) LIP was an oceanic plateau that is preserved today as obducted fragments outcropping in Ecuador, Colombia (including Isla Gorgona), Costa Rica, and several Caribbean islands, most prominently Haiti, Jamaica, Curaçao, and Aruba (Kerr *et al.* 1997). The plateau also comprises a substantial proportion of the thickened oceanic crust of the Caribbean (Mauffret and Leroy 1997). The fragmentary nature of the remnants of this LIP hinders determination of its original volume, although 4–4.5 Mkm^3 has been estimated (see Courtillot and Renne 2003; Kerr *et al.* 2003; Kuroda *et al.* 2007). It is widely accepted that the plateau formed on the Farallon (proto-Pacific) plate and possibly represents the 'head' phase of the Galápagos plume (Kerr *et al.* 2003; Boschman *et al.* 2014; Nerlich *et al.* 2014). After its formation, the southern part of the plateau collided with and accreted onto the NW margin of South America, while the northern portion moved into the inter-American gap that had been opening between north and south America since the Jurassic (see reviews in Kerr *et al.* 2003; Boschman *et al.* 2014). Studies of the exposed outcrop and recovered rocks from ODP sites indicate that the emplaced magmas largely consist of tholeiitic pillow basalts, with some basaltic and dolerite sills in addition to picritic and komatiitic lavas also preserved (Kerr *et al.* 2003). While it is evident that the plateau predominantly formed through submarine volcanism, Buchs *et al.* (2018) reported layered tuffs with accretionary lapilli and interbedded lahar deposits with rounded clasts of basalt in accreted oceanic plateau sequences from western Colombia. These tuffs indicate that, like other Cretaceous Pacific plateaus, the Caribbean LIP became subaerial. The preservation of corals and carbonized tree-trunk fragments in sediments interbedded with LIP basalts in the Western Cordillera of Colombia supports the occurrence of eruptions in either shallow water depths or a subaerial context (Hall *et al.* 1972; Moreno-Sanchez and Pardo-Trujillo 2003). Dating of Caribbean LIP samples through $^{40}Ar/^{39}Ar$ and Re–Os geochronology has highlighted a wide range of ages spanning the Cretaceous to the Early Paleogene (see Kerr *et al.* 2003). However, $^{40}Ar/^{39}Ar$ ages from Deep Sea Drilling Project (DSDP) Leg 15, Haiti, Gorgona Island, Costa Rica, Hispaniola, Western Colombia

and Curaçao all suggest a major pulse of volcanism between 93 and 88 Ma (Walker *et al.* 1991, 1999; Sinton *et al.* 1998; Kerr *et al.* 2004; Snow *et al.* 2005; see also Kasbohm *et al.* 2021).

The Cenomanian–Turonian boundary has been dated to 93.9 Ma (Meyers *et al.* 2012), and records another interval of widespread oceanic anoxia (OAE 2), which has been widely linked to the coeval Caribbean volcanism (e.g. Sinton and Duncan 1997; Kerr 1998; Snow *et al.* 2005; Turgeon and Creaser 2008; Du Vivier *et al.* 2014, 2015; Scaife *et al.* 2017; Percival *et al.* 2018). Stratigraphic archives of this episode of global environmental perturbation are characterized by a positive $\delta^{13}C$ excursion of up to 6‰ in all of carbonates, bulk-, and compound-specific organic matter (e.g. Scholle and Arthur 1980; Hasegawa 1997; Tsikos *et al.* 2004*a*; Erbacher *et al.* 2005; Sageman *et al.* 2006; Jarvis *et al.* 2011). Well-preserved laminated organic-rich shales have been reported from uppermost Cenomanian–lowermost Turonian strata in numerous sites, particularly in the Atlantic, NW Tethys and Boreal Realm (Schlanger and Jenkyns 1976; Arthur *et al.* 1987; Linnert *et al.* 2010; see also reviews by Jenkyns 2010; Robinson *et al.* 2017). Thus, this isotopic shift is typically interpreted as reflecting enhanced organic-carbon burial in the global ocean. Palaeotemperature reconstructions based on carbonate oxygen-isotope (and in some locations, TEX_{86}) trends indicate a rise in temperatures at the onset of OAE 2, with both proxies highlighting that the warm conditions continued after the end of the event (Paul *et al.* 1999; Forster *et al.* 2007; Jarvis *et al.* 2011; van Helmond *et al.* 2014, 2015; O'Connor *et al.* 2020).

However, the elevated temperatures were punctuated by a transient interval of climate cooling (and seawater re-oxygenation) across large parts of the marine realm, dubbed the Plenus Cold Event owing to its initial recognition by the southward migration of the boreal belemnite species *Praeactinocamax plenus* (Gale and Christensen 1996). This cooling/reoxygenation pulse is further documented by multiple geochemical palaeothermometers, a shift in the abundance of specific nannofossils (notably cold-water species), and often a return to pre-OAE lithologies and the disappearance of organic-rich shales (e.g. Tsikos *et al.* 2004*a*; Forster *et al.* 2007; Sinninghe-Damsté *et al.* 2008; Linnert *et al.* 2010; van Helmond *et al.* 2014, 2015, 2016; Desmares *et al.* 2016; O'Connor *et al.* 2020). The transient temperature decrease probably resulted from sequestration of organic carbon caused by one or both of the documented organic-carbon burial and enhanced silicate weathering (Pogge von Strandmann *et al.* 2013; Robinson *et al.* 2019; Percival *et al.* 2020; Papadomanolaki *et al.* 2022). However, this fall in temperatures did not occur synchronously across the world, suggesting that local oceanographic and climatic conditions significantly influenced the regional manifestation of any cooling (O'Connor *et al.* 2020; Percival *et al.* 2020).

The High Arctic LIP (HALIP) and its relation to the Cretaceous OAEs

Numerous studies have documented the preservation of Cretaceous magmatic units across much of the High Arctic, spanning Svalbard, Franz Josef Land, Novaya Zemlya, the Barents Sea, Northern Greenland, the Canadian Arctic islands, and New Siberian Islands, together with the offshore Alpha-Mendeleev Ridge and Chukchi Plateau (see e.g. Tarduno 1998; Maher 2001; Buchan and Ernst 2006; Tegner *et al.* 2011; Corfu *et al.* 2013; Senger *et al.* 2014; Naber *et al.* 2021; Bédard *et al.* 2021*a*, *b*; Senger and Galland 2022). Comprising both extrusive volcanic units and intrusive dyke swarms in particular, these magmatic formations have been postulated to collectively represent the HALIP (Tarduno 1998). Thus far, geochronology studies of the HALIP have primarily focused on areas in Arctic Canada (particularly the islands of Axel Heiberg and Ellesmere), with U–Pb and $^{40}Ar/^{39}Ar$ dates indicating that the LIP formed through numerous spells of emplacement over a 40 Myr interval of the Cretaceous (Tegner *et al.* 2011; Dockman *et al.* 2018). In particular, two major magmatic pulses at 135–120 Ma and 105–90 Ma have been identified (e.g. Corfu *et al.* 2013; Evenchick *et al.* 2015; Estrada *et al.* 2016; Polteau *et al.* 2016; Dockman *et al.* 2018; Kingsbury *et al.* 2018; Naber *et al.* 2021; Deegan *et al.* 2022). Dating of alkaline HALIP rocks in Northern Greenland potentially indicates a later episode of HALIP-related alkaline volcanism between 85 and 70 Ma (Tegner *et al.* 2011; Thórarinsson *et al.* 2015). Recognized magmatic pulses of HALIP overlap in age with both OAEs 1a and 2; consequently, the province has been linked with both episodes of environmental change (e.g. Tegner *et al.* 2011; Zheng *et al.* 2013; Polteau *et al.* 2016; Adloff *et al.* 2020). In the case of OAE 1a, this link may be related to the emission of thermogenic carbon following intrusion of organic-rich sedimentary rocks by basaltic sills, providing a source of isotopically light carbon to the Earth's surface that could have caused the C3 negative excursion in $\delta^{13}C$ (Polteau *et al.* 2016; Adloff *et al.* 2020; Deegan *et al.* 2022).

The Madagascan LIP

The Madagascan LIP largely comprises tholeiitic flood basalt sequences, with minor alkaline and silicic units, and associated sill and dyke swarms and intrusive complexes, and has been attributed to the

Marion plume prior to the separation of Madagascar from the Indian subcontinent (e.g. Storey *et al.* 1995; Torsvik *et al.* 1998, 2000; Kumar *et al.* 2001). Remnants of the province are well exposed and preserved along Mahajanga and the eastern coastal area, and in the Morondava sedimentary basins in western Madagascar (Mahoney *et al.* 1991; Storey *et al.* 1995; Melluso *et al.* 2001; Cucciniello *et al.* 2022). Further volcanism is also recorded through intrusions into and extrusions onto Precambrian basement. The original volume of the province is poorly constrained, but probably exceeded 1 Mkm^3, including the Madagascar Plateau flanking the south coast of the island, as well as the Conrad Rise (Storey *et al.* 1995). Age estimates for Madagascar LIP volcanism largely range between *c.* 93 and 86 Ma, based largely on $^{40}Ar/^{39}Ar$ and some U–Pb dating, together with biostratigraphic constraints based on interbedded sedimentary rocks (Storey *et al.* 1995; Torsvik *et al.* 2000; Melluso *et al.* 2001, 2005; Pande *et al.* 2001; Mahoney *et al.* 2008; Cucciniello *et al.* 2010, 2011, 2013, 2022; see also Jiang *et al.* 2023). Because these ages are close to that of the Cenomanian–Turonian boundary, it has been postulated that the Madagascan LIP might have contributed to environmental change associated with OAE 2. However, statistical appraisals of the available ages shows that volcanic activity initially peaked in northern Madagascar and spanned 3 Myr between 93 and 90 Ma (Cucciniello *et al.* 2022), slightly postdating OAE 2. Thus, it is unlikely that the Madagascan LIP played a major role in triggering environmental change associated with that OAE.

The Deccan–Traps and the Cretaceous–Paleogene interval

Major eruptions associated with the Deccan Traps (western India) commenced during the latest Maastrichtian, 300–400 kyr prior to the end of the Cretaceous Period (66.04 Ma; Gale *et al.* 2020) and continued into the earliest Paleogene (Schoene *et al.* 2019; Sprain *et al.* 2019 and references therein). It has been suggested that a smaller-scale phase of Deccan eruptions occurred earlier in the Cretaceous (68–67 Ma; see Chenet *et al.* 2007; Parisio *et al.* 2016). However, subsequent data have cast doubt on the occurrence of major eruptions significantly prior to the main-phase of Deccan volcanism (Schoene *et al.* 2015). By far the most intensely studied part of the Deccan Traps is the Western Ghats region, which comprises a cumulative thickness of *c.* 3000 m of tholeiitic basalts in multiple flood basalt units stratigraphically separated by oxidized 'red-bole' palaeosols (Widdowson *et al.* 1997, and references therein). Magnetostratigraphic studies of the Western Ghats basalts show that the main phase of Deccan volcanism began just prior to the start of the C30n–C29r chron reversal (66.38 Ma), and concluded just after the C29r–C29n reversal at 65.7 Ma (Courtillot *et al.* 1986, 2000; Chenet *et al.* 2009). This <1 Myr duration is supported by numerous recent geochronological investigations utilizing both $^{40}Ar/^{39}Ar$ ages of Deccan basalts (66.31–65.72 Ma; e.g. Renne *et al.* 2015; Sprain *et al.* 2019) and U–Pb dating of zircons preserved in the red boles interbedded between with them (66.26–65.63 Ma; e.g. Schoene *et al.* 2015, 2019; Eddy *et al.* 2020). Recent modelling of eruption rates in the Western Ghats, based on $^{40}Ar/^{39}Ar$ geochronology, highlighted a pronounced rise in eruption volume between the Bushe and Poladpur formations, around the time of the Cretaceous–Paleogene (KPg) transition and Chicxulub impact (Renne *et al.* 2015; Sprain *et al.* 2019). An acceleration in volcanism beginning with Poladpur eruptions is also shown by U–Pb-based modelling, but manifesting as a series of discrete pulses that began 50–100 kyr prior to the KPg event and bolide impact (Schoene *et al.* 2019). However, U–Pb geochronology of red-bole zircons from the Malwa plateau indicate that there were highly voluminous Deccan eruptions occurring in the northern part of the province up to 350 kyr prior to the KPg event (Eddy *et al.* 2020). Additionally, some of the Deccan magmas are preserved offshore from the Indian coast and may comprise a volume significantly greater than the well-studied onshore volcanics, with little known regarding their eruptive history (Mittal *et al.* 2022).

The last 300–400 kyr of the Cretaceous were marked by up to 2–3°C of climate warming (the Late Maastrichtian Warming Event), which has been documented in shallow and deep marine settings around the world by both oxygen-isotope and TEX_{86} data (e.g. Li and Keller 1998*a*; Westerhold *et al.* 2011; Esmeray-Senlet *et al.* 2015; Vellekoop *et al.* 2016; Barnet *et al.* 2018; Woelders *et al.* 2017, 2018; Hull *et al.* 2020). Cyclostratigraphic and magnetostratigraphic age models across a number of these sites demonstrate that the warming commenced coevally with the onset of Deccan volcanism, supporting a causal link between the two phenomena (Barnet *et al.* 2018; Woelders *et al.* 2017; Hull *et al.* 2020; Gilabert *et al.* 2022). Intriguingly, temperatures then declined around 100–200 kyr before the end of the Cretaceous, despite continuing Deccan activity (Vellekoop *et al.* 2016; Barnet *et al.* 2018; Woelders *et al.* 2017, 2018; Hull *et al.* 2020). A rise in SO_2 contents of Deccan basalts from 750 to 1800 ppm, and thus of assumed volatile emissions, just prior to the end of the Cretaceous may have aided this cooling pulse (Callegaro *et al.* 2023). A second (geologically brief) warming pulse in the final 10 s kyr of the period has been postulated, although evidence for this second temperature

increase has been reported from only a few locations (Stüben *et al.* 2003; Keller *et al.* 2020; O'Connor *et al.* 2023; cf., Vellekoop *et al.* 2016; Woelders *et al.* 2017; Barnet *et al.* 2018; Hull *et al.* 2020). It is assumed that these temperature changes occurred in response to carbon cycle disturbances following Deccan CO_2 emissions (e.g. Li and Keller 1998*a*; Robinson *et al.* 2009; Esmeray-Senlet *et al.* 2015; Vellekoop *et al.* 2016; Hull *et al.* 2020). However, there is no clear $\delta^{13}C$ excursion in upper Maastrichtian strata comparable in magnitude with those of the Cretaceous OAEs (Woelders *et al.* 2017; Barnet *et al.* 2018). The lack of a negative isotopic shift may result from Deccan carbon output being primarily magmatic in origin, rather than thermogenic, although whether magmatic volatiles alone could have caused the warming is unclear (Self *et al.* 2006; see also Ganino and Arndt 2009).

The KPg boundary, which marks the most recent of the 'Big Five' Phanerozoic mass extinctions (Raup and Sepkoski 1982), also overlapped in time with Deccan volcanism. This extinction has been compellingly linked to the coeval Chicxulub impact by global enrichment of iridium and other platinum group elements in the extinction horizon, together with documented microspherules, shocked-quartz grains and tsunami sediments (e.g. Alvarez *et al.* 1980; Schulte *et al.* 2010; Goderis *et al.* 2021). Nonetheless, it has been hypothesized that Deccan eruptions contributed towards causing this biospheric crisis, either in combination with the Chicxulub impact or independently (e.g. Courtillot and Renne 2003; Keller 2012; Font *et al.* 2016; Petersen *et al.* 2016; Callegaro *et al.* 2023; Cox and Keller 2023). The different hypotheses proposed regarding the links between the Chicxulub impact, Deccan Traps and the extinction event are outlined in more detail elsewhere (see e.g. Schulte *et al.* 2010; Hart *et al.* 2012, 2019; Richards *et al.* 2015; Punekar *et al.* 2016; Leighton *et al.* 2017; Schoene *et al.* 2019; Hull *et al.* 2020; Callegaro *et al.* 2023; Cox and Keller 2023; Senel *et al.* 2023), and are not further discussed here.

The link between LIP volcanism and environmental change

Many major environmental perturbations during the Cretaceous were marked by pronounced climate warming on a global scale (with the Weissert Event and parts of OAE 1b the likely exceptions), and LIP-related emissions of carbon dioxide are widely accepted to have been a key trigger of these temperature rises (e.g. Weissert and Erba 2004; Jenkyns 2010; Bond and Wignall 2014; Bodin *et al.* 2015). Carbon outgassing of LIP basalts remains poorly constrained, however, and it is uncertain whether magmatic emissions would have been sufficient to greatly impact atmospheric CO_2 levels (see Self *et al.* 2006, 2014; Black *et al.* 2021). As noted above, thermogenic carbon emissions associated with the heating of organic-rich sediments by intruding magmas have been proposed as an additional/alternative trigger of climate warming during OAE 1a (Polteau *et al.* 2016; Deegan *et al.* 2022). This mechanism has also been suggested for the Late Maastrichtian Warming Event (Eddy *et al.* 2020; Hernandez Nava *et al.* 2021), although the limited evidence for organic-rich sediments that were intruded by Deccan magmas and the lack of a $\delta^{13}C$ negative excursion in uppermost Cretaceous strata do not support this hypothesis. Regardless of the specific carbon source, any episode of Cretaceous climate warming probably resulted in acceleration of the global hydrological cycle, enhancing continental weathering and nutrient runoff to the oceans, and consequently stimulating eutrophication and seawater oxygen depletion, aided by ocean stratification and stagnation directly caused by oceanic temperature increase (see Jenkyns 2010; Bond and Sun 2021, and references therein). The carbon emissions themselves could also have directly resulted in ocean acidification and associated environmental stress, at least during some events (Erba *et al.* 2010).

Establishing better constraints on the timing of volcanic activity from sedimentary records that document surface temperature fluctuations and/or changes in environmental and biospheric conditions is key to resolving the complex relationships between LIP emplacement and their impact on Earth's climate and environment. In recent years, the development of several geochemical proxies of volcanism has enabled reconstruction of the timing of LIP activity in the stratigraphic archives that record episodes of environmental and/or biota perturbation. Osmium-isotope compositions (specifically $^{187}Os/^{188}Os$) and mercury (Hg) concentrations represent two such proxies (see reviews by Grasby *et al.* 2019; Dickson *et al.* 2021; Percival *et al.* 2021*a*). Differences in the compatibility of osmium and rhenium (Re) within silicates result in mantle rocks and LIP basalts derived from mantle-plume volcanism typically being enriched in primitive osmium compared with rhenium, giving them an unradiogenic Os-isotope composition ($^{187}Os/^{188}Os \approx 0.13$; Allègre *et al.* 1999). Thus, intense LIP volcanism and/or the weathering (or submarine alteration) of juvenile basalts should cause a geologically rapid increase in the flux of unradiogenic Os to the global ocean relative to the comparatively constant background input from mid-ocean ridges and extraterrestrial material, lowering seawater $^{187}Os/^{188}Os$ ratios (e.g. Peucker-Ehrenbrink and Ravizza 2000). Conversely, the felsic crust is marked by higher Re/Os ratios, with decay of ^{187}Re to ^{187}Os over long geological timescales,

eventually resulting in a more radiogenic osmium-isotope composition of continental material and the riverine runoff derived from its erosion (average $^{187}Os/^{188}Os \approx 1.4$ today; Peucker-Ehrenbrink and Jahn 2001). Thus, seawater $^{187}Os/^{188}Os$ ratios can also increase if continental weathering rates increase. Because osmium has a seawater residence time of tens of thousands of years, any significant change in the oceanic $^{187}Os/^{188}Os$ composition should be recorded in the hydrogenous phase of sedimentary rocks deposited throughout the global ocean, apart from hydrographically restricted basins where local sources may dominate (e.g. Paquay and Ravizza 2012; Dickson *et al.* 2015).

Mercury is emitted to the atmosphere as a volcanic volatile, with this source acting as a major natural source of the element to the Earth's surface today (Pyle and Mather 2003). In the stratosphere, mercury has a residence time of 0.5–2 years, enabling it to be distributed over a hemispherical–global scale before being deposited in sediments (Schroeder and Munthe 1998; Selin 2009). Hence, numerous studies have utilized Hg contents as a proxy for volcanic activity in Earth's past, normalizing against total organic carbon (TOC) to account for the element typically being bound to organic compounds during deposition (see reviews by Grasby *et al.* 2019; Shen *et al.* 2020; Percival *et al.* 2021*a*). Under highly euxinic conditions where free sulfides precipitate in the water column, Hg may be associated with that phase (Shen *et al.* 2019, 2020). Mercury may be adsorbed onto clay minerals if neither organic carbon or sulfides are present (Kongchum *et al.* 2011; Shen *et al.* 2020). Adsorption onto iron–manganese oxides or hydroxides has also been reported in oxidized settings, particularly for some riverine, lacustrine and estuarine environments (e.g. Quémerais *et al.* 1998; Driscoll *et al.* 2013; Maher *et al.* 2020), although studies of other sites have reported preferential binding onto organic compounds (e.g. Feyte *et al.* 2010; Cossa *et al.* 2021).

Any or all of remobilization of sedimentary mercury related to water-column and/or sediment redox changes, input from wildfires or enhanced terrigenous runoff, variation in organic matter type (from marine to terrestrial) and diagenetic removal of sedimentary TOC can alter sedimentary Hg contents and Hg/TOC ratios independently of volcanism (e.g. Hammer *et al.* 2019; Them *et al.* 2019; Charbonnier *et al.* 2020*a*; Frieling *et al.* 2023). Thus, reconstructing a volcanically triggered perturbation to the global mercury cycle depends on documenting stratigraphically correlative Hg enrichments in multiple sites distributed across the world and considering any potential local inputs of the element. Moreover, submarine volcanic activity may have a very limited dispersal range of mercury owing to the rapid scavenging and transformation of mercury species in hydrothermal vents, resulting in an apparent near-field drawdown of Hg emitted directly into seawater (within hundreds of kilometres; Bowman *et al.* 2015; see also Scaife *et al.* 2017; Percival *et al.* 2018, 2021*b*).

Despite the advances in tracking LIP volcanism in stratigraphic records of major climate/environmental change, relatively few studies have combined geochemical proxies of volcanism and surface temperature in the same site (but see Robinson *et al.* 2009; Bottini *et al.* 2015; Schoene *et al.* 2019; Percival *et al.* 2020). Thus, questions remain regarding the extent to which volcanic activity triggered climate warming and consequent environmental degradation during the Cretaceous. These questions particularly pertain to OAE 1a, with magmatic CO_2, thermogenic carbon, and methane clathrate release all suggested as a cause of climate warming during the onset of the event (e.g. Jahren *et al.* 2001; Méhay *et al.* 2009; Naafs *et al.* 2016; Adloff *et al.* 2020; Deegan *et al.* 2022). Moreover, hydrothermal nutrient (e.g. Fe, V, Cu) output from submarine G-OJP volcanism may have directly enhanced primary productivity and triggered widespread marine anoxia during OAE 1a independently of global temperature change (see Erba *et al.* 2015). Here, the record of LIP volcanism during OAE 1a is investigated at two sites that have been previously studied for palaeotemperature trends (Fig. 2): DSDP Site 398 (Vigo Seamount, Atlantic Ocean) and Alstätte-1 (Lower Saxony Basin, NW Germany). The documented relationship between volcanism and environmental change during OAE 1a is placed into the wider context of how LIP activity impacted the global climate during that event. This scenario is then discussed in a broader overview of the geochemical records and environmental and biotic impacts of large igneous provinces during the Cretaceous Period.

Study sites

The expanded Early Aptian stratigraphic record recovered from DSDP Site 398 consists of repeating dark grey-green turbiditic sedimentary sequences spanning several tens of metres in thickness. The strata are composed primarily of dark mudstones and claystones with some layers of calcareous sandstones and graded quartz-based sandstones–mudstones, deposited on the southern flank of the Vigo Seamount, just off the Iberian Margin (Ryan *et al.* 1979; Sigal 1979). Preservation of terrigenous material (including terrestrial organic matter) indicates that the sediments were probably deposited as part of a submarine fan, potentially related to deltaic progradation (Arthur 1979). However, a generally low BIT (branched and isoprenoid tetraether) index of

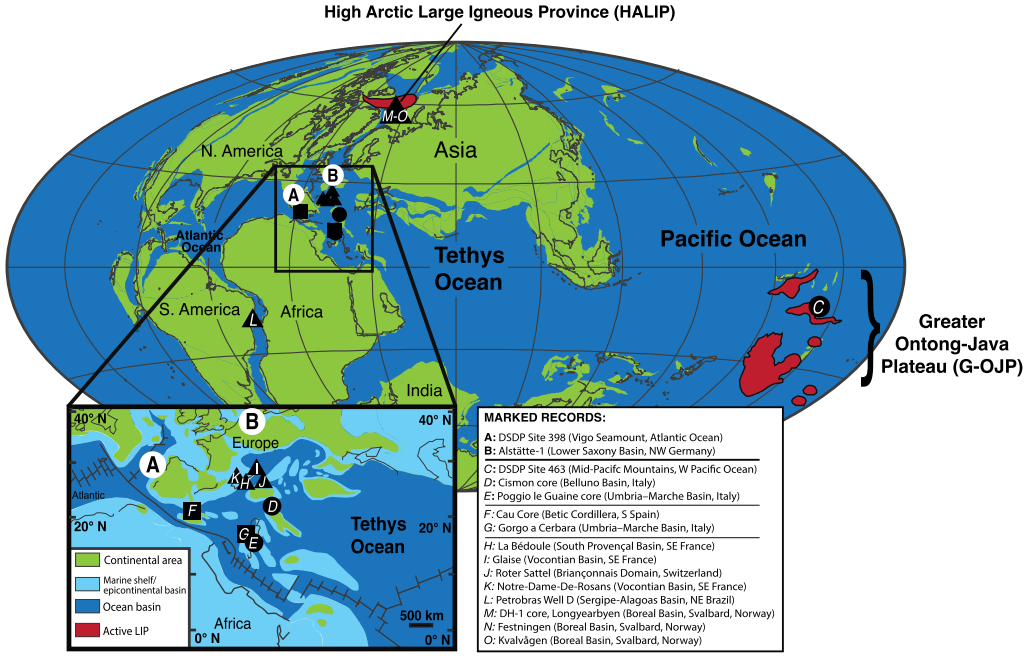

Fig. 2. Palaeogeographic map of the Barremian–Aptian interval, adapted from Percival *et al.* (2021*b*), after van Breugel *et al.* (2007) and Giraud *et al.* (2018). The reconstructed locations of the HALIP and G-OJP are shown in red. Sites investigated in this study for mercury and osmium data shown by white circles: (**a**) DSDP Site 398; (**b**) Alstätte-1. Sites previously investigated using both proxies are shown by black circles (**c–e**), just for osmium isotopes with black squares (**f–g**), and just for mercury by black triangles (**h–o**).

organic matter studied from the sediments suggests that terrestrial organics do not dominate the setting (Naafs and Pancost 2016). There is no black-shale layer at this locality comparable with those typically associated with Lower Aptian stratigraphic records (Arthur 1979). Instead, OAE 1a strata have been identified by trends in the $\delta^{13}C$ composition of organic matter, in combination with calcareous nannofossil biostratigraphy (Bralower *et al.* 1994; Li *et al.* 2008). Palaeoenvironmental reconstructions from this site, based on TEX_{86}, have highlighted warm sea-surface temperatures prior to OAE 1a, which rose slightly during the event but significantly declined after it (Naafs and Pancost 2016).

The Alstätte-1 section represents a boreal record of OAE 1a, and primarily consists of organic-rich laminated mudstones and marlstones that were deposited into the epicontinental Lower Saxony Basin during the Early Aptian (Hoffmann and Mutterlose 2011). Palaeogeographic reconstructions, geochemical data, palaeontological findings and the preservation of organic-rich sediments deposited under anoxic conditions all indicate that the basin was probably hydrographically restricted to some degree during Barremian–Aptian times, potentially including the OAE 1a interval (Pauly *et al.* 2013). However, Aptian fauna recovered from strata below and in the OAE 1a interval are mainly of Boreal endemic composition and co-occur with cosmopolitan taxa (ammonites, belemnites), with the earliest cosmopolitan species documented a few metres below the OAE 1a level. Highly distinctive Tethyan belemnites are preserved directly above OAE 1a strata, suggesting strong sea-way connectivity and faunal exchange with the NW Tethys immediately following the event (Mutterlose 1998; Mutterlose and Böckel 1998). Lower Aptian strata and the OAE 1a interval have been identified from a combination of belemnite, ammonite and nannofossil biostratigraphy, integrated with $\delta^{13}C$ studies (Bottini and Mutterlose 2012). TEX_{86}-derived sea-surface temperature reconstructions highlight a sharp rise from $<30°C$ prior to OAE 1a to 33°C during the event, but mild cooling during the middle of the OAE and after it had concluded (Mutterlose *et al.* 2014). The initial warming is potentially supported

by a negative excursion in belemnite $\delta^{18}O$ correlative with the shift in TEX_{86} (Mutterlose *et al.* 2014).

Methodology

Osmium-isotope analysis

Osmium abundances and isotopic values were determined by isotope dilution and negative thermal ionization mass spectrometry on a Thermo Fisher Scientific TRITON at the Japan Agency for Marine-Earth Science and Technology (JAMSTEC), Japan. Sample preparation followed the protocol described in Ishikawa *et al.* (2014) and Matsumoto *et al.* (2020), and broadly follows the procedures developed by Cohen and Waters (1996) and Birck *et al.* (1997). Briefly, powdered samples were spiked with a ^{185}Re- and ^{190}Os-rich solution and sealed in quartz glass tubes with 4 ml of inverse aqua regia. After being heated at 230°C for 48 h, osmium was separated and purified by CCl_4 extraction, HBr back-extraction and standard micro-distillation techniques. Rhenium was purified from the aqua regia phase through anion chromatography, with Re concentrations determined via quadrupole inductively coupled plasma mass spectrometry (Thermo Fisher Scientific iCapQ) at JAMSTEC. Procedural blanks averaged 0.10 ± 0.08 pg Os and 22 ± 10 pg Re, with a $^{187}Os/^{188}Os$ ratio of 0.166 ± 0.004 (1 SD, $n = 3$). Analytical uncertainty and precision were monitored through repeated measurements of the JMC Os standard, giving $^{187}Os/^{188}Os$ values of 0.10691 ± 0.00008 (1 SD, $n = 3$), consistent with previously reported values ($^{187}Os/^{188}Os = 0.106838 \pm 0.000015$; Nozaki *et al.* 2012). The past seawater Os-isotope composition at the time of deposition ($^{187}Os/^{188}Os_{(i)}$) is calculated from the modern-day measured $^{187}Os/^{188}Os$ and $^{187}Re/^{188}Os$ compositions of a sedimentary rock sample and its age in order to account for the post-depositional decay of ^{187}Re to ^{187}Os (Cohen *et al.* 1999). The initial sedimentary Os concentration at the time of deposition [$Os_{(i)}$] is determined by utilizing the determined $^{187}Os/^{188}Os_{(i)}$ ratio together with the measured $^{187}Os/^{188}Os$ composition and Os and ^{192}Os concentrations of a rock sample, assuming a $^{192}Os/^{188}Os$ of 3.08271 (Percival *et al.* 2021*b*).

Mercury concentrations

Mercury concentrations were determined on an Advanced Mercury Analyser 254.7 at the Vrije Universiteit Brussel (VUB), Belgium, following the procedure outlined in Liu *et al.* (2021). The limit of detection for the Advanced Mercury Analyser based on repeated blank analyses ($n = 33$ across the two sample sets) was 0.09 ng, calculated as 3 times the standard deviation on the blank measurements, one to two orders of magnitude below the content in a measured sample. A 100 ± 2 mg aliquot of powdered sample was used per analysis, with repeatability of the results monitored through at least two measurements for each sample. Analytical accuracy was further tested through repeated measurements of the certified reference materials MESS-3 (marine sediment) and JP-1 (peridotite), yielding average concentrations of 89.51 ± 1.89 ng/g (1 SD, $n = 25$) and 4.86 ± 0.38 ng/g (1SD, $n = 13$), respectively, across analysis of the two sample sets, consistent with established compiled values (MESS-3 = 91 ± 9 ng/g; JP-1 = 5.3 ng/g).

Total organic carbon and total sulfur contents

Total organic carbon and total sulfur (TS) contents were determined on a Nu Instruments Horizon 2 isotope ratio mass spectrometer coupled to a Eurovector elemental analyser, EuroEA3000, at the VUB. Prior to TOC analyses, the samples were decarbonated with 10% HCl following the procedure outlined in Liu *et al.* (2021), in order to remove inorganic carbon (assumed to be entirely in carbonate form). Carbon content calibration was performed using the certified reference material IAEA-CH-6 (sucrose). Data accuracy and reproducibility were monitored through repeated analyses of international standards IVA33802151 (organic-rich sediment) and IVA33802153 (organic-poor soil), with analytical uncertainty typically better than ±0.1 wt% (1 SD). The measured carbon content in decarbonated aliquots of each sample was converted to a bulk rock TOC value by accounting for the percentage sample mass lost following decarbonation. The TS contents were measured on bulk-rock powder samples without any chemical pre-treatment. Sulfur content calibration on the isotope ratio mass spectrometer was performed using the certified reference material IAEA-S-1 (silver sulfide), with data accuracy and reproducibility again better than ±0.1 wt% (1 SD) based on repeated analyses of international standards: IVA33802151 and MESS-2 (estuarine sediment).

Results

Early Aptian strata from DSDP Site 398 record a shift in $^{187}Os/^{188}Os_{(i)}$ ratios from a mean background of *c.* 0.60 to a highly unradiogenic composition of *c.* 0.20 across the OAE 1a level, before a return towards more radiogenic pre-event values above it (Fig. 3a). The sample with the most unradiogenic Os-isotope composition is also marked by a large enrichment in $[Os]_{(i)}$ (1323 pg/g, compared

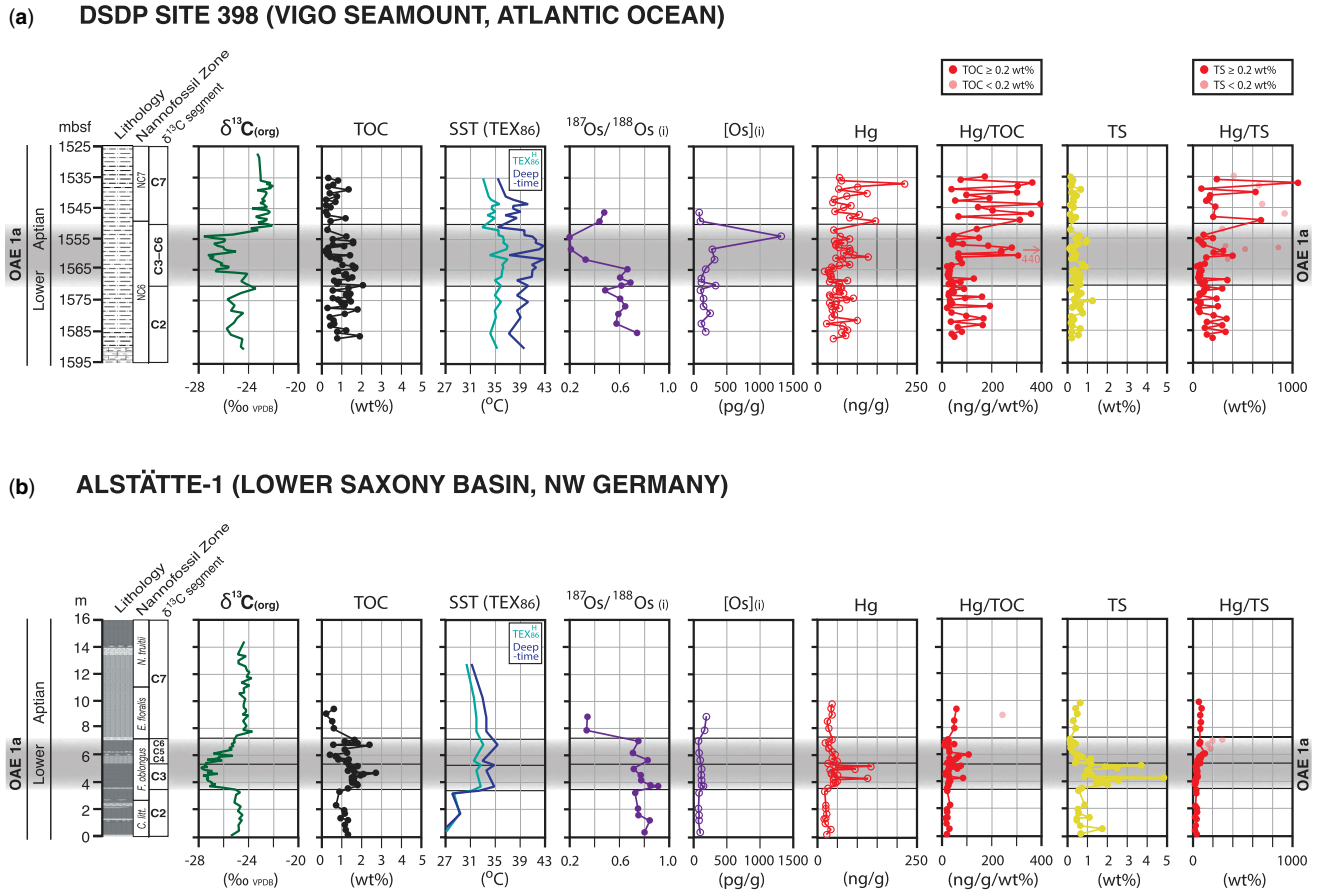

Fig. 3. Stratigraphic trends in $\delta^{13}C$, total organic carbon (TOC) and sea-surface temperature (SST) based on TEX_{86}, $^{187}Os/^{188}Os_{(i)}$, $[Os]_{(i)}$, Hg, Hg/TOC and Hg/TS for (**a**) DSDP Site 398 and (**b**) Alstätte-1. Vertical scales are in metres. The stratigraphic extent of the OAE 1a level (here defined as strata spanning the C3–C6 segments) is marked by the horizontal grey bars. TS, Total sulfur. Sources: For DSDP Site 398, the lithological column is from Jenkyns (2018), the biostratigraphic and $\delta^{13}C$ information are from Li *et al.* (2008); the SST trends are from Naafs and Pancost (2016); all other data from this study. For Alstätte-1, the lithological, biostratigraphic, $\delta^{13}C$, TOC and SST information are from Mutterlose *et al.* (2014); all other data are from this study. Sea-surface temperature trends based on both the widely applied TEX_{86}^{H} calibration of Kim *et al.* (2010) and the deep-time analogue outlined by Tierney and Tingley (2014) are presented, as calculated by Naafs and Pancost (2016). A lower reliability limit of 0.2 wt% for TOC follows the protocol of Grasby *et al.* (2016), and is also applied here for TS.

with a mean of 173 pg/g for the rest of the record). A transient rise in $^{187}Os/^{188}Os_{(i)}$ up to 0.69 in basal OAE1a strata is superimposed onto the initial unradiogenic signal. Mercury concentrations show significant variation, ranging from 18 to 100 ng/g (mean 49 ng/g) below the OAE 1a level and in basal OAE strata, before rising slightly to an average of 63 ng/g with a peak of 129 ng/g in the upper part of the OAE level, and further still above it (averaging 86 ng/g with spikes up to 220 ng/g). While TOC and TS contents also vary considerably at DSDP Site 398 (between 0.19–2.09 and 0.10–1.25 wt%, respectively), there is no clear stratigraphic trend. Thus, the Hg enrichments are largely mirrored by peaks in Hg/TOC and Hg/TS ratios. There is a clear Hg/TOC peak in the middle part of the OAE 1a level between 1563 and 1557 mbsf (average Hg/TOC = 197 ng/g/wt%; average Hg/TS = 342 ng/g/wt%), and additional spikes of up to 394 ng/g/wt% and 1054 ng/g/wt%, respectively, above it (Fig. 3a). There is no clear linear relationship between Hg and either TOC or TS (R^2 values of 0.09 and 0.07, respectively).

The $^{187}Os/^{188}Os_{(i)}$ trends documented at Alstätte-1 differ markedly from those of DSDP Site 398, rising from a background average of *c.* 0.77 to over 0.9 at the base of the OAE 1a level, but with values remaining high ($^{187}Os/^{188}Os_{(i)}$ >0.7) throughout the OAE strata (Fig. 3b). A shift to more unradiogenic Os-isotope compositions of *c.* 0.34 (and slight increase in $[Os]_{(i)}$ concentrations from 95 to 173 pg/g) only takes place above OAE 1a strata. Mercury concentrations at Alstätte-1 are also elevated around the OAE 1a level (mean 49 ng/g) with three spikes to *c.* 100 ng/g or more, compared with background contents of 27 ng/g (Fig. 3b). However, the TOC and TS contents also rise in OAE strata; thus, there is no systematic increase in Hg/TOC or Hg/TS in basal OAE 1a strata. There is an increase in Hg/TS from *c.* 32 to 100 ng/g/wt % in the upper part of the OAE level, but this rise is not correlative with any increase in Hg concentrations, rather with a fall to very low TS contents. Some small spikes in Hg/TOC (up to 109 ng/g/wt % compared with a background of 29 ng/g/wt%) do correlate with the three peaks in Hg concentrations; however, those samples also have very high sulfur contents. Indeed, there is a strong linear correlation between Hg and TS concentrations at Alstätte-1 ($R^2 = 0.73$; compared with $R^2 = 0.05$ between Hg and TOC), potentially suggesting that local drawdown with sulfide was the main control on Hg deposition under the highly oxygen-depleted conditions in the Lower Saxony Basin. OAE 1a black shales from Alstätte-1 are known to yield abundant pyrite, suggesting that sulfide sorption was the main control on Hg contents in this oxygen-depleted setting.

Discussion

OAE 1a as a case study of how LIPs impacted the Cretaceous global environment

The $^{187}Os/^{188}Os_{(i)}$ and $[Os]_{(i)}$ trends recorded at DSDP Site 398 closely resemble those from previous studies of OAE 1a. Very low $^{187}Os/^{188}Os_{(i)}$ values recorded in middle–upper OAE 1a strata support a major influx of unradiogenic osmium to the global ocean during that event, probably linked to G-OJP activity (Tejada *et al.* 2009; Bottini *et al.* 2012; Adloff *et al.* 2020; Martínez-Rodríguez *et al.* 2021; Percival *et al.* 2021*b*). Recorded Os-isotope trends from several other sites also document a volcanically triggered shift towards a more unradiogenic seawater composition immediately prior to OAE 1a, with this change also potentially documented at DSDP Site 398 by a single data point (1171.33 mbsf). Basal OAE 1a strata only show a clear mercury enrichment at a single site very close to that LIP (Percival *et al.* 2021*b*). This non-dispersal of mercury is consistent with the short residence time of volcanic Hg emitted directly into seawater (see Bowman *et al.* 2015), and supports submarine volcanism on the G-OJP as the main source of unradiogenic Os to the global ocean during OAE 1a.

The shift to more radiogenic $^{187}Os/^{188}Os_{(i)}$ compositions across OAE 1a strata at Alstätte-1 represents a markedly different trend from that recorded at all other sites. This disparity probably indicates that the Lower Saxony Basin was too hydrographically restricted for significant water–mass exchange with the global ocean, despite having enough connection to permit faunal migration. In this context, the shift to higher $^{187}Os/^{188}Os_{(i)}$ values across the OAE 1a level at Alstätte-1 may highlight a rise in local riverine runoff to the Lower Saxony Basin from enhanced continental weathering in response to elevated atmospheric CO_2 and global temperatures, given that this flux typically represents the main source of radiogenic osmium to seawater. Notably, the radiogenic shift at Alstätte-1 begins at the base of C3 (3.8 m), and age-equivalent C3 strata at DSDP Site 398 (1169.8–1164.54 mbsf) and other locations are also marked by a transient rise in $^{187}Os/^{188}Os_{(i)}$ values between the unradiogenic pulses (Fig. 4). This stratigraphic correlation supports previous interpretations that the transient radiogenic Os-isotope shift recorded in C3 strata at DSDP Site 398 and elsewhere probably reflects a weathering pulse superimposed on an overarching signal of submarine LIP activity, rather than a spell of volcanic quiescence between two distinct pulses of volcanism (e.g. Tejada *et al.* 2009; Bottini *et al.* 2012; Martínez-Rodríguez *et al.* 2021). Strontium-, calcium- and lithium-isotope studies of OAE 1a

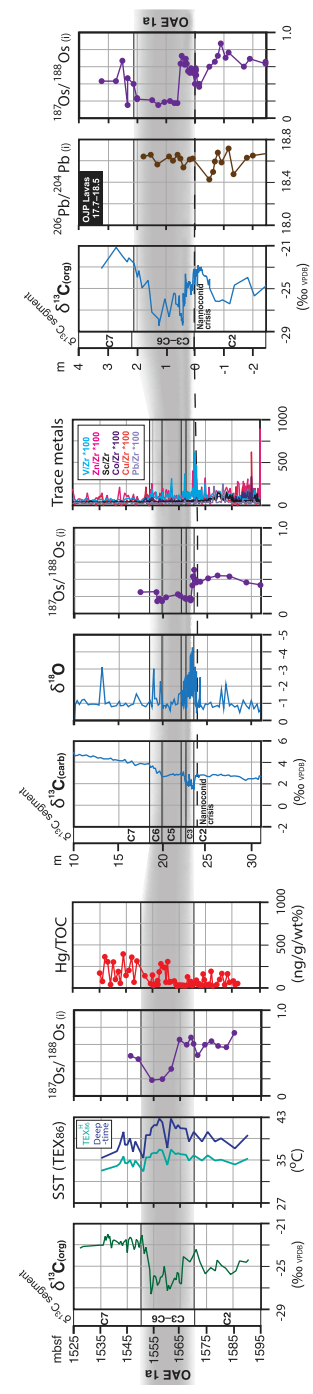

Fig. 4. Stratigraphic correlation of OAE 1a geochemical records from (**a**) DSDP Site 398, (**b**) Cismon, and (**c**) Gorgo a Cerbara. Vertical scales are in metres. The stratigraphic extent of the OAE 1a level (here defined as strata spanning the C3–C6 segments) is marked by the horizontal grey bar. SST, Sea-surface temperature; TOC, total organic carbon. DSDP Site 398 is sourced as for Figure 3. Sources for other sites: Cismon $\delta^{13}C$ and $\delta^{18}O$ data, and the stratigraphic position of the nannoconid crisis, are from Erba *et al.* (2010); $^{187}Os/^{188}Os_{(i)}$ data are from Bottini *et al.* (2012); trace metal data are from Erba *et al.* (2015). Gorgo a Cerbara $^{187}Os/^{188}Os_{(i)}$ data, and the stratigraphic position of the nannoconid crisis, are from Tejada *et al.* (2009); $\delta^{13}C$ and lead-isotope data are from Kuroda *et al.* (2011). The unreliable (TOC < 0.2 wt%) Hg/TOC data point from DSDP Site 398 is not shown.

also support a rise in global weathering rates during the onset of the event (Jones and Jenkyns 2001; Blättler *et al.* 2011; Lechler *et al.* 2015).

When stratigraphic trends in $^{187}Os/^{188}Os_{(i)}$ are compared with temperature proxies from records of OAE 1a, it is clear that the highest temperatures indicated by $\delta^{18}O$ or TEX_{86} data are documented above the radiogenic osmium shift and the C3 excursion, stratigraphically correlative with the most unradiogenic $^{187}Os/^{188}Os_{(i)}$ compositions recorded in OAE 1a strata (upper C3–lower C4; see also Bottini *et al.* 2015). These trends support an intensification in LIP volcanism and associated carbon emissions as the main driver of this further rise in global temperatures during OAE 1a. A pronounced increase in Hg contents and Hg/TOC enrichments across upper C3–lower C4 strata at DSDP Site 398 and some (although not all) other sites across the globe might reflect a potential intensification in volcanic activity or switch to subaerial eruptions after the start of OAE 1a (see Charbonnier and Föllmi 2017; Percival *et al.* 2021*b*; Vickers *et al.* 2023). The latter possibility is consistent with a scenario in which the G-OJP was initially emplaced through submarine volcanism (enabling worldwide dispersal of unradiogenic Os but only nearfield Hg enrichment), before becoming emergent above the sea surface and leading to more global distribution of mercury from subaerial eruptions. However, it should be noted that the C3–C4 Hg enrichments could also reflect localized environmental perturbations such as redox changes or enhanced wildfires/runoff of terrestrial organic matter (see Percival *et al.* 2021*b*). A not exclusively volcanic cause of the C3–C4 mercury enrichments is supported by the enhanced Hg and Hg/TOC values recorded above the OAE 1a level at DSDP Site 398, in strata that post-date the time of LIP volcanism reconstructed from $^{187}Os/^{188}Os_{(i)}$ trends. Unless subaerial eruptions occurred later than and entirely separately from submarine volcanism (which is implausible if both were related to the same LIP), it is highly unlikely that these post-event Hg peaks were volcanically derived. Instead, the post-OAE Hg enrichments may have been caused by variability in the input of terrestrial organic matter from the nearby palaeoshoreline (Hammer *et al.* 2019), or redox fluctuations/the return to a more oxygenated water column (Frieling *et al.* 2023), although there is no direct evidence of major redox change at DSDP Site 398.

There is also a potential correlation between an initial shift towards more unradiogenic Os-isotope values and possible higher sea-surface temperatures below the C3 negative $\delta^{13}C$ excursion at DSDP Site 398. This earlier temperature rise is less pronounced than the later one during the OAE itself, and the fall in $^{187}Os/^{188}Os_{(i)}$ values is based on one data point. Nonetheless, an unradiogenic shift

in the marine Os-isotope composition and rise in surface temperatures just prior to the C3 excursion and onset of OAE 1a is supported by data from other stratigraphic archives in the NW Tethys and the Subbetic margin (e.g. Tejada *et al.* 2009; Keller *et al.* 2011; Bottini *et al.* 2012, 2015; Lorenzen *et al.* 2013; Castro *et al.* 2021; Martínez-Rodríguez *et al.* 2021; Fig. 4). A crisis in nannoconid fauna is also recorded below the base of OAE 1a strata *sensu stricto* in several sites (see the section on the biotic response to Cretaceous LIP formation). Lead-isotope and trace-element datasets further support an onset of volcanic activity that was coeval with the nannoconid crisis but prior to the C3 excursion (Kuroda *et al.* 2011; Erba *et al.* 2015; Figure 4). Assuming that there was a single prolonged pulse in G-OJP activity recorded by the unradiogenic shifts in $^{187}Os/^{188}Os_{(i)}$, which began before and continued after a transient increase in continental weathering rates, the new and previously published geochemical and palaeontological datasets both suggest that magmatic carbon emissions associated with submarine LIP volcanism probably triggered the initial warming and nannoconid crisis immediately prior to the onset of OAE 1a.

These datasets also support a non-volcanic carbon source, probably related to thermogenic emissions or methane clathrate release, as the driver of the C3 $\delta^{13}C$ negative excursion. Osmium-isotope trends in those strata primarily record enhanced continental weathering rather than LIP activity. Furthermore, there is no clear global mercury signal of volcanism at that time. Both methane clathrates and thermogenic carbon are isotopically lighter than magmatic CO_2, with the latter potentially sourced from intrusive magmatism related to the HALIP (see above; also Polteau *et al.* 2016). Thus, either carbon source could potentially have caused the $\delta^{13}C$ negative shift without greatly changing atmospheric CO_2 levels or affecting global temperatures (Méhay *et al.* 2009; Naafs and Pancost 2016; Adloff *et al.* 2020). This scenario is consistent with the geochemical and palaeontological evidence for volcanism as the main driver of climate warming and biota stress prior to and during OAE 1a, but with a non-volcanic carbon source as the driver of the C3 negative excursion (Méhay *et al.* 2009; Adloff *et al.* 2020). However, it is less clear which carbon source (if either) played the dominant role in initiating the widespread marine anoxia that characterized the OAE.

Overview of geochemical evidence for the (variable) links between LIP volcanism and Cretaceous episodes of major environmental change

The entirety of Cretaceous stratigraphic history has been investigated for trends in oceanic strontium-isotope compositions (see reviews by Jones and Jenkyns 2001; McArthur *et al.* 2020), and large parts also for seawater $^{187}Os/^{188}Os_{(i)}$ reconstructions (see e.g. Peucker-Ehrenbrink and Ravizza 2000; Matsumoto *et al.* 2022; and Fig. 5). Reconstructed $^{187}Os/^{188}Os_{(i)}$ trends for most Cretaceous episodes of environmental change are similar to OAE 1a, showing pronounced unradiogenic shifts that are assumed to result from one or more of submarine volcanism, the weathering of juvenile LIP basalts or some other form of basalt–seawater interaction (Fig. 5a, and references therein). Some more local-scale episodes of environmental perturbation are also marked by unradiogenic shifts of a smaller magnitude (Matsumoto *et al.* 2021*b*). Thus, osmium-isotope stratigraphy strongly supports the link between LIP emplacement and Cretaceous climate/environmental change. Additionally, a more gradual $^{187}Os/^{188}Os_{(i)}$ trend towards more unradiogenic compositions in the Late Cretaceous following OAE 2, an interval not coeval with environmental change, has been linked with weathering of Caribbean and Madagascan LIP basalts (Matsumoto *et al.* 2023*a*). Interestingly, clear shifts towards primitive-mantle compositions of strontium isotopes are only documented for OAE 1a and OAE 2 (Fig. 5b), albeit with less sharp stratigraphic trends owing to the longer residence time of strontium in seawater (>2 Myr; Palmer and Edmond 1989). Those intervals are also associated with the highest magnitude unradiogenic Os-isotope shifts in the Cretaceous. Collectively, the strontium and osmium trends may suggest that LIP activity, or at least the flux of mafic elements to seawater, was greater during those intervals than for other Cretaceous events. In addition to strontium and osmium datasets, evidence for some form of magmatic activity during OAEs 1a and 2 has also been inferred on the basis of lead-, neodymium-, chromium- and zinc-isotope studies, and trace-element enrichments (Larson and Erba 1999; Snow *et al.* 2005; Kuroda *et al.* 2007; Zheng *et al.* 2013; Erba *et al.* 2015; Holmden *et al.* 2016; Sweere *et al.* 2018).

Stratigraphic mercury records of Cretaceous events also yield information on the style and/or provenance of magmatic activity. Like OAE 1a, where mercury enrichment in basal C3 strata was only documented at a site proximal to the G-OJP, there is limited global evidence for peaks in Hg and Hg/TOC in OAE 2 strata, with small enrichments at some records deposited relatively proximally to LIPs (Scaife *et al.* 2017, Percival *et al.* 2018). This pattern of a more localized mercury enrichment proximal to a LIP source is consistent with largely submarine volcanism during both events (Scaife *et al.* 2017; Percival *et al.* 2018, 2021*b*). Mercury records associated with OAE 1b are more limited, but spikes have been reported from the

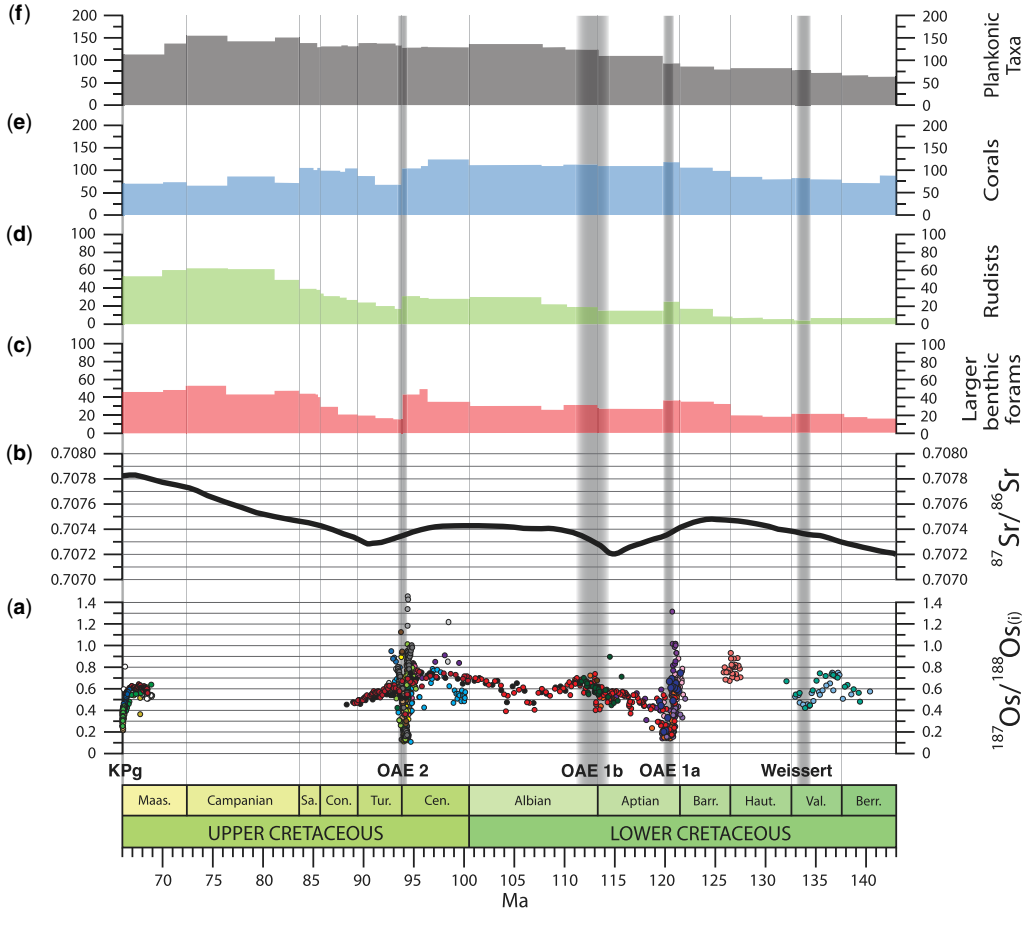

ATLANTIC OCEAN

DSDP Site 398
THIS STUDY

DSDP Site 603
Percival *et al.* (2023)

DSDP Site 534
Percival *et al.* (2023)

ODP Leg 174AX (Bass River)
Percival *et al.* (2020)

IODP Site U1403
Hull *et al.* (2020)

DSDP Site 530
Du Vivier *et al.* (2014)

ODP Site 1260
Turgeon and Creaser (2008)
Du Vivier *et al.* (2014)

DSDP Site 525
Ravizza and Peucker-Ehrenbrink (2003)
Robinson *et al.* (2009)

IODP Site 1262
Ravizza and VonderHaar (2012)

DSDP Site 511
Matsumoto *et al.* (2023b)

NW TETHYS

Poggio le Guaine (Italy)
Matsumoto *et al.* (2020, 2021b, 2022)
Percival *et al.* (2021b)

Fiume Bossa (Italy)
Matsumoto *et al.* (2021a)

Gorgo a Cerbara (Italy)
Tejada *et al.* (2009)

Cismon (Italy)
Bottini *et al.* (2012)

Cau outcrop (Spain)
Adloff *et al.* (2020)

Cau core (Spain)
Martínez-Rodríguez *et al.* (2021)

Bottaccione (Italy)
Robinson *et al.* (2009)
Matsumoto *et al.* (2022, 2023a)

Furlo (Italy)
Turgeon and Creaser (2008)
Du Vivier *et al.* (2014)

SW TETHYS

Gongzha (Tibet)
Li *et al.* (2022)

WESTERN INTERIOR

Portland #1 core (CO, USA)
Du Vivier *et al.* (2014)

Angus core (CO, USA)
Jones *et al.* (2021)

SH #1 core (CO, USA)
Jones *et al.* (2021)

Iona core (TX, USA)
Sullivan *et al.* (2020)

INDIAN OCEAN

ODP Sites 762 and 763
Matsumoto *et al.* (2022, 2023a)

IODP Site U1516
Jones *et al.* (2023)

SOUTHERN OCEAN

ODP Site 690
Ravizza and VonderHaar (2012)
Robinson *et al.* (2009)

ARCTIC OCEAN

Glacier Fjord (Axel Heiberg Island, Canada)
Schröder-Adams *et al.* (2019)

EUROPE

Wunstorf (N Germany)
Du Vivier *et al.* (2014)
Selby *et al.* (2009)

Pont d'Issole (S France)
Du Vivier *et al.* (2014)

Vörhum (N Germany)
Selby *et al.* (2009)

PACIFIC OCEAN

Great Valley Sequence (CA, USA)
Du Vivier *et al.* (2015)

DSDP Site 577
Ravizza and Peucker-Ehrenbrink (2003)
Robinson *et al.* (2009)

IODP Site 1209
Ravizza and VonderHaar (2012)

Yezo Group (Japan)
Du Vivier *et al.* (2015)

DSDP Site 463
Matsumoto *et al.* (2020)
Bottini *et al.* (2012)

Fig. 5. (**a**) compiled $^{187}Os/^{188}Os$ and (**b**) $^{87}Sr/^{86}Sr$ trends from Cretaceous stratigraphic records. The strontium-isotope trend is redrawn from the compilation in McArthur *et al.* (2020). Osmium-isotope data sourced as shown. Changes in biospheric genera throughout the Cretaceous as compiled by Steuber *et al.* (2023) shown for (**c**) larger benthic forams, (**d**) rudists, and (**e**) corals, (**f**) planktonic taxa. Age models for the Os datasets are taken from the respective studies where possible (accounting for updated Stage boundary absolute ages); where no age model exists, a constant sedimentation rate relative to the start and end of the event is assumed.

NW Tethys (Sabatino *et al.* 2018). If these Hg enrichments were indeed volcanically derived, it may indicate that some Kerguelen Plateau volcanism at that time was subaerial. Albian-age mercury enrichments have also been reported from a lacustrine record in North China (Zhao *et al.* 2022), although stratigraphic uncertainties hinder a clear correlation with the Tethys record or a connection to Kerguelen volcanism.

Interestingly, mercury records of Paraná–Etendeka and Deccan volcanism show considerable variability across different sites, despite both LIPs forming through subaerial eruptions (e.g. Percival *et al.* 2018; Fendley *et al.* 2019; Charbonnier *et al.* 2020*b*). Hg enrichments have been reported from strata that record the onset of the Weissert Event (Charbonnier *et al.* 2017, 2020*b*), but because the duration of Paraná–Etendeka volcanism was at least 2–3 Myr (see the section introducing the Paraná-Etendeka LIP; also Dodd *et al.* 2015; Gomes and Vasconcelos 2021; Bacha *et al.* 2022), those peaks cannot reflect the entire eruptive history of that LIP. It is possible that the less clear global mercury signals of the Paraná–Etendeka LIP reflect a generally lower volatile output or slower eruption rate than for other subaerial provinces (see Callegaro *et al.* 2014; Dodd *et al.* 2015). In this case, the Hg enrichments reported by Charbonnier *et al.* (2017, 2020*b*) in basal Weissert Event strata could record a peak in the intensity of Paraná–Etendeka volcanism coeval with the onset of the crisis, consistent with the geochronological models of Gomes and Vasconcelos (2021) and Bacha *et al.* (2022). However, local environmental or sedimentological causes for those Hg peaks cannot be ruled out, particularly if significant Paraná–Etendeka volcanism post-dated the onset of the Weissert event, as suggested by Rocha *et al.* (2020). Similarly, uppermost Maastrichtian Hg peaks have been associated with Deccan eruptions (Keller *et al.* 2020), most notably just below the KPg boundary (e.g. Font *et al.* 2016; Keller *et al.* 2018; Percival *et al.* 2018; Fendley *et al.* 2019). This peak stands in contrast to a comparative lack of evidence for a global-scale systematic enrichment in mercury at the onset of Deccan volcanism 300–400 kyr prior to the end of the Maastrichtian (Percival *et al.* 2018). Thus, it may reflect an intensification of volcanism immediately prior to the extinction, consistent with the U–Pb geochronological model of Deccan eruptions (Schoene *et al.* 2019). However, given that this Hg enrichment is not recorded globally, a non-volcanic cause cannot be excluded (which would be potentially consistent with the Deccan $^{40}Ar/^{39}Ar$ geochronology of Renne *et al.* 2015, and Sprain *et al.* 2019). Mercury enrichments have also been reported for more minor episodes of environmental change, such as OAE 1d and the Faraoni Event (Charbonnier *et al.* 2018; Yao *et al.* 2021), but the possible existence and nature of any causal relationship between those crises and volcanism remains unclear.

Cyclostratigraphic and magnetostratigraphic correlation of KPg records clearly shows that the main phase of Deccan volcanism commenced coevally with the onset of late Maastrichtian climate warming (Schoene *et al.* 2019; Hull *et al.* 2020), as appears to have been the case for LIP activity and global temperature increases during OAE 1a. Geochemical evidence for a causal link between volcanism and climate warming during OAE 2 is also well documented at the stratigraphically condensed record of ODP Site 1260 (Forster *et al.* 2007; Turgeon and Creaser 2008). More expanded OAE 2 records, with better temporal resolution, show that LIP activity began prior to the onset of the OAE *sensu stricto*, leaving the exact chronology of volcanism v. climate warming at that time unclear (e.g. Du Vivier *et al.* 2014). However, evidence of transient cooling pulses during both OAE 1a and OAE 2, such as the Plenus Cold Event (see the section introducing the Caribbean LIP and OAE 2), is recorded in strata which also record Os-isotope evidence of intense LIP activity (Bottini *et al.* 2015; Jenkyns 2018; Percival *et al.* 2020). The late Maastrichtian climate warming was also alleviated while Deccan volcanism was ongoing (e.g. Sprain *et al.* 2019; Hull *et al.* 2020). There are two possible explanations for these transient falls in temperature during times of LIP volcanism. The first model is that the LIP eruptions associated with those events featured spells during which volcanic carbon emissions were reduced (e.g. Sprain *et al.* 2019; Hull *et al.* 2020; Hernandez Nava *et al.* 2021). Alternatively, and more plausibly for the OAEs, magmatic CO_2 output may have been offset by one or both of enhanced organic-carbon burial and an increase in global silicate weathering rates (Pogge von Strandmann *et al.* 2013; Jenkyns *et al.* 2017; Jenkyns 2018; Robinson *et al.* 2019; Percival *et al.* 2020; Papadomanolaki *et al.* 2022). While the latter scenario might be expected to increase the input of radiogenic osmium to the ocean, apparently at odds with the low $^{187}Os/^{188}Os$ values documented during the Plenus Cold Event and other transient intervals of cooling during OAEs 1a and 2, it is possible that any continental weathering signal was overprinted by the unradiogenic Os flux from volcanism, or that primitive LIP basalts were the main lithology being eroded.

Climate cooling associated with the Weissert Event may have been caused by carbon sequestration during weathering of newly erupted Paraná–Etendeka basalts, based on stratigraphic correlations between unradiogenic Os-isotope shifts and evidence of surface temperature decrease in Valanginian strata (Percival *et al.* 2023). Elevated

organic-matter burial in the terrestrial realm may have further drawn down carbon at that time (Westermann *et al.* 2010). Alternatively, volcanic SO_2 emissions might have caused the cooling by leading to the formation of stratospheric sulfate aerosols, which may also have helped cause transient temperature falls during the latest Maastrichtian (see Self *et al.* 2006; Schmidt *et al.* 2016; Callegaro *et al.* 2023). However, the short atmospheric residence time of those compounds and the slow eruption rate and potentially low sulfur content of Paraná–Etendeka basalts do not support this link (Callegaro *et al.* 2014; Dodd *et al.* 2015). Alternatively, the surface-temperature warming reconstructed from some NW Tethyan and proto-Atlantic records of the Weissert Event could suggest significant volcanic emission of CO_2 and other volatiles to the atmosphere, which may be supported by Hg enrichments in sedimentary records of that time (Charbonnier *et al.* 2017, 2020*b*). Direct stratigraphic comparisons between global temperature and volcanic activity are currently lacking for other Cretaceous events. Nonetheless, it is clear that at least some Cretaceous LIPs had a pronounced impact on global climate, through volcanic CO_2 emissions and/or weathering of newly formed basalts.

Aside from changes in global climate, the environmental perturbations associated with the emplacement of Cretaceous LIPs were highly variable. Evidence of ocean acidification has been reported from stratigraphic records of OAEs 1a and 2, and potentially the late Maastrichtian, with this fall in seawater pH probably resulting chiefly from the same carbon emissions that triggered climate warming during those time intervals (e.g. Erba *et al.* 2010; Dameron *et al.* 2017; Jones *et al.* 2023). To date, these postulated episodes of ocean acidification have largely been inferred from sedimentological and palaeontological evidence (see the section on the biotic response to Cretaceous LIP formation), with little geochemical information regarding seawater pH.

While the rises in global temperature during OAEs 1a and 2 were marked by the development of widespread marine anoxia/euxinia in both epicontinental shelf basins and across the global ocean, evidence for similar oceanic redox changes during the Late Maastrichtian warming or Weissert Event is limited. For example, numerous sedimentary records of OAEs 1a and 2 from both epicontinental shelf basins and open-ocean sites are marked by the appearance of organic-rich shales and changes in organic biomarker data, iron speciation and variations in sedimentary elemental contents (particularly P, V, Mn, Mo, U and TOC/P and I/Ca ratios) and N-, S-, Fe-, Mo-, Tl- and U-isotope compositions, all of which are redox-sensitive proxies (e.g. Sinninghe-Damsté and Köster 1998; Kuypers *et al.* 2004; Pancost *et al.* 2004; Jenkyns *et al.* 2007, 2017; Junium and Arthur 2007; Mort *et al.* 2007; van Bentum *et al.* 2009; Lu *et al.* 2010; Montoya-Pino *et al.* 2010; Föllmi 2012; Owens *et al.* 2012, 2013; Ruvalcaba Baroni *et al.* 2015; Dickson *et al.* 2016; Ostrander *et al.* 2017; Clarkson *et al.* 2018; Siebert *et al.* 2021; see also a review by Jenkyns 2010). In the case of the Weissert Event, the limited expansion of anoxic water masses (and lithological/geochemical evidence thereof) may be attributed to the apparent lack of a clear temperature increase and associated seawater stratification/nutrient runoff and eutrophication in many parts of the world. However, the Late Maastrichtian Warming Event featured a temperature rise of 2°C (Hull *et al.* 2020); thus, an increase in seawater deoxygenation and evidence of this phenomenon might be expected. It is possible that the continued break-up of Pangaea through the Cretaceous caused evolution in the global palaeogeography, shelf-basin extent and ocean circulation, potentially decreasing the propensity of marine environments to become oxygen depleted by the Maastrichtian. This mechanism has been proposed to explain the far greater extent of marine anoxia during OAEs 1a and 2 than the Paleocene–Eocene Thermal Maximum (56 Ma), despite the latter event being marked by climate warming of a similar or greater magnitude and at a faster rate than for the Cretaceous events (e.g. Jenkyns 2010; Dickson *et al.* 2014; Clarkson *et al.* 2021).

Another hypothesized trigger of marine anoxia during OAEs 1a and 2 is the enhanced output of trace-metal micronutrients from submarine ocean-plateau volcanism directly into seawater, elevating primary productivity and the consumption of oxygen from the water-column (Sinton and Duncan 1997; Kerr 1998; Snow *et al.* 2005; Erba *et al.* 2015; see Fig. 6). As a mechanism that depends on submarine LIP activity instead of continental volcanism, rather than global temperature increase, this model is consistent with the lack of widespread marine anoxia during the Weissert and Late Maastrichtian events, and is supported by enriched abundances of micronutrient metals in sedimentary records of OAEs 1a and 2, particularly those proximal to the G-OJP and Caribbean LIP (Larson and Erba 1999; Snow *et al.* 2005; Erba *et al.* 2015). However, OAE 1b also coincided with submarine volcanism during emplacement of the Kerguelen Plateau, and has also been associated with climate warming, yet anoxic sediments are largely found in Atlantic and NW Tethyan sites (see the section introducing the Kerguelen Plateau and OAE 1b). It is possible that this distribution may reflect the relative paucity of OAE 1b sites studied thus far. However, the Os-isotope record of OAE 1b documents a much lower magnitude unradiogenic shift than those recorded for OAEs 1a and 2 (see Fig. 4). Thus,

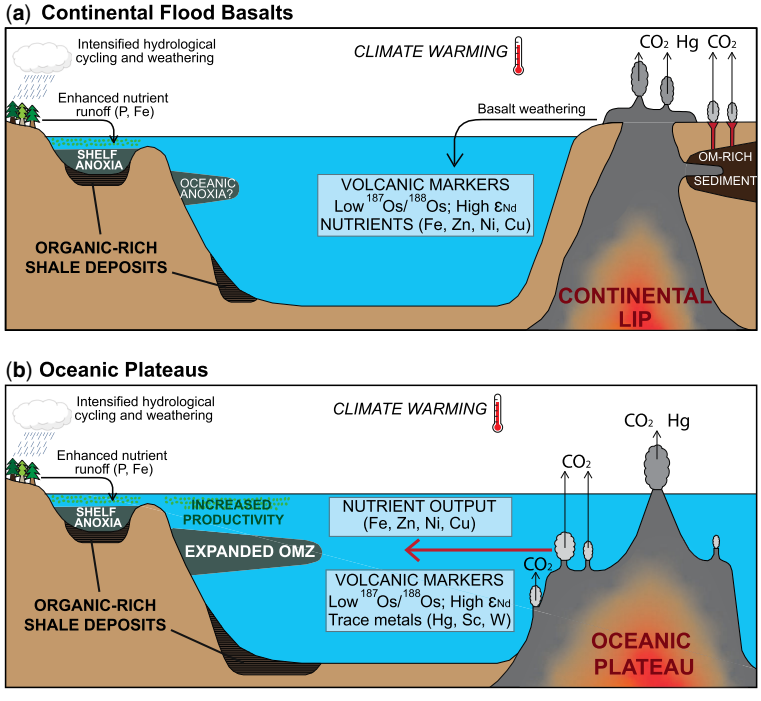

Fig. 6. Simplified schematic of the climatic and environmental influence, and output of elements used as proxies of LIP activity, during the Cretaceous for (**a**) continental flood basalts and (**b**) oceanic plateaus, OMZ, Oxygen Minimum Zone.

submarine LIP volcanism and associated trace metal output was probably more intense at the time of OAEs 1a and 2 than during OAE 1b (or any other time in the Cretaceous, see above). OAE 2 was also coeval with enhanced seasonality related to a peak in orbital eccentricity, which might have increased the susceptibility of the Earth system to the development of marine anoxia (Batenburg *et al.* 2016). Furthermore, the relatively protracted nature of environmental change during OAE 1b (~4 Myr; Gale *et al.* 2020; Ait-Itto *et al.* 2023), compared with the geologically rapid onset of OAEs 1a and 2, may have mitigated the severity of environmental change during the Aptian–Albian transition.

The biotic response to Cretaceous LIP formation

Fossil evidence of biotic changes during times of LIP formation during the Cretaceous highlights considerable variation in the response of the marine biosphere to these major volcanic episodes. Furthermore, diversity patterns of the main planktonic and benthic carbonate producers in the Cretaceous, evaluated at the generic level, document disjunct trends for the two groups (Steuber *et al.* 2023). These differences suggest the importance of distinct environmental parameters in controlling the radiation and decline of marine groups, following different ecological strategies. The terrestrial biosphere was also impacted to some degree by different Cretaceous LIPs, with indications of at least regional vegetation changes during the Weissert Event (Kujau *et al.* 2013) and OAE 1a (e.g. Cors *et al.* 2015; Galloway *et al.* 2022). A rise in terrestrial organic-matter burial associated with the Weissert Event $\delta^{13}C$ positive excursion may also reflect changes in the continental biosphere (Westermann *et al.* 2010). Furthermore, charcoal preservation in Aptian–Albian and OAE 2 strata suggest increased wildfire activity during parts of the Cretaceous (Brown *et al.* 2012; dos Santos *et al.* 2016; Wang *et al.* 2019; Baker *et al.* 2020; Xu *et al.* 2022), potentially resulting from climate warming and elevated atmospheric oxygen levels following enhanced primary productivity in the case of the latter time interval (Baker *et al.* 2020). However, Heimhofer *et al.* (2004) reported relatively stable terrestrial vegetation during and after OAE 1a. Overall, the comparative paucity of the continental stratigraphic record compared with that of the marine realm means that the ocean biosphere is much more studied and better understood, and is the focus of this section hereafter.

A pronounced impact of environmental change associated with Cretaceous LIPs has been

documented for benthic carbonate platform dwellers (dasycladales, larger benthic foraminifera, corals, rudists; see overview by Steuber *et al.* 2023; Figs 5c–e). Shortly before or during the onset of OAE 1a, carbonate platforms and their benthic biota experienced a substantial decline, particularly in the mid latitudes. Dasycladacean algae and large benthic foraminifera are marked by significant diversity declines across OAE 1a and (especially) OAE 2, with aragonitic taxa chiefly affected. Rudist genera disappeared during OAE 1a from higher latitudes but survived in more equatorial settings. This abrupt decline of aragonitic taxa is thought to be related to the major increases in atmospheric CO_2 and very high sea-surface temperatures caused by LIP eruptions, resulting in a shallowing of the carbonate-compensation depth (e.g. Ridgwell 2005; Foster *et al.* 2017), reduced seawater carbonate saturation and a subsequent calcification crisis (Bauer *et al.* 2017).

The same mechanism could have caused the retreat of shallow-water carbonate platforms to low latitudes in the aftermath of OAEs 1a and 2. Coral diversity was significantly reduced in the aftermath of OAE 2, and to a lesser extent after OAE 1a (Fig. 5e), with high sea-surface temperatures and presumably low seawater pH probably reducing the photosymbiotic activity of zooxanthellid corals and large benthic forams (Kiessling and Kocsis 2015; Reddin *et al.* 2021; Steuber *et al.* 2023). This interpretation is supported by an increase of azooxanthellate coral genera after OAE 1a, potentially reflecting a bleaching effect. Corals living in symbioses with dinoflagellates were thus partly replaced by corals missing these symbionts, supporting a decline of photosymbiosis owing to high temperatures (e.g. Kiessling and Kocsis 2015). Carbonate platform drowning has also been documented during several intervals in the Early Cretaceous, particularly in the NW Tethys, and is often linked with increased volcanic activity on one or both of the G-OJP or Kerguelen Plateau (e.g. Föllmi *et al.* 1994; Weissert *et al.* 1998; Föllmi 2012; Charbonnier *et al.* 2018; Matsumoto *et al.* 2020, 2021*b*, 2022). A spread of warm-water scleractinian corals has been documented in uppermost Maastrichtian strata of Belgium and the Netherlands, and is correlative with evidence for rising seawater temperatures (Leloux 1999; O'Hora *et al.* 2022). This relationship supports some benthic response to rising global temperatures associated with early Deccan volcanism. However, the extent of biospheric changes during the Late Maastrichtian Warming Event remains debated (see e.g. Witts *et al.* 2016; Tobin *et al.* 2017 regarding high-latitude molluscs).

The diversity of planktonic carbonate producers (calcareous nannofossils, calcispheres, planktonic foraminifera) was apparently less impacted by environmental change related to Cretaceous LIP volcanism. A major turnover in planktonic carbonate producers did occur during the KPg mass extinction (e.g. Smit 1982; Olsson and Liu 1993; Pospichal 1996), but no specific declines in diversity have been recorded at the generic level for other intervals coeval with Cretaceous LIPs (Steuber *et al.* 2023). Rather, planktonic taxa diversity increased consistently throughout the Cretaceous, reaching a broad maximum between the Albian and Maastrichtian stages, peaking around the Campanian (Suchéras-Marx *et al.* 2019; Steuber *et al.* 2023; Fig. 5f). In general, this trend towards increased diversity applies to both calcareous nannofossils and planktonic foraminifera (Suchéras-Marx *et al.* 2019; Steuber *et al.* 2023), despite their disparate trophic levels. However, phytoplanktonic organisms show some change in records of the Late Maastrichtian warming, with warm-water species tending to spread in favour of cold-water taxa, together with blooms in both dinoflagellate and calcareous nannoplankton highlighting stressed ecosystems in response to the rise in global temperatures caused by Deccan volcanism at that time (e.g. Thibault and Gardin 2007; Sheldon *et al.* 2010; Vellekoop *et al.* 2019). Planktonic foraminifera show a more locally variable response to Maastrichtian warming, possibly related to local controls such as nutrient levels and/or freshwater runoff as well as temperature changes (e.g. Abramovich and Keller 2002; Woelders *et al.* 2017).

Slightly elevated rates of turnover (extinction and speciation) in planktonic foraminifers, and to a lesser extent in calcareous nannofossils, have also been documented for OAEs 1a, 1b, and 2 (Leckie *et al.* 2002), and potentially the Late Maastrichtian (e.g. Li and Keller 1998*b*; Dameron *et al.* 2017; cf, Hart *et al.* 2019). In particular, pronounced changes in the abundance patterns of calcareous nannofossils are recorded in stratigraphic records of the Cretaceous OAEs, particularly OAE 1a, as well as the Weissert Event and OAE 2 (Erba 1994, 2004; Mutterlose and Böckel 1998; Erba *et al.* 2010; Bottini and Mutterlose 2012; Faucher *et al.* 2017; Erba *et al.* 2019). This change is most prominently shown by a significant decline in the heavily calcified nannoconids just prior to OAE 1a (Erba 1994; Erba *et al.* 2010; Erba *et al.* 2019) and around the latest Aptian OAE 1b (nannoconid final collapse: Herrle and Mutterlose 2003; Bottini *et al.* 2015). A nannoconid decline slightly preceeded the Weissert Event, also characterized by a general decrease in micrite production at pelagic and hemipelagic sites associated with an increase in abundance of higher-fertility taxa (Erba *et al.* 2004; Bornemann and Mutterlose 2008; Gréselle *et al.* 2011; Barbarin *et al.* 2012; Pauly *et al.* 2012; Duchamp-Alphonse *et al.* 2014; Mattioli *et al.* 2014; Möller *et al.* 2015, 2020; Erba *et al.* 2019; Shmeit *et al.* 2022).

Extensive study of the nannoconid crisis associated with OAE 1a has shown it to be synchronous at a global scale, and apparently representing the culmination of a decrease in nannofossil calcite production that commenced in the latest Barremian (Erba 1994, 2004; Bottini and Mutterlose 2012; Aguado *et al.* 2014; Erba *et al.* 2015; Bonin *et al.* 2016; Giraud *et al.* 2018; Mahanipour *et al.* 2019). In addition to major changes in nannofossil abundance, species-specific decreases in size have been detected for both OAE 1a and OAE 2. Specifically, *Biscutum constans* shows a marked reduction in coccolith size across OAE 1a at global scale (Erba *et al.* 2010; Lübke *et al.* 2015; Lübke and Mutterlose 2016; Bottini and Faucher 2020). Coccolith dwarfism of *B. constans* during OAE 2 has also been documented globally, alongside a fall in nannofossil abundance and species richness worldwide (Nederbragt and Fiorentino 1999; Hardas and Mutterlose 2007; Linnert *et al.* 2010, 2011; Corbett and Watkins 2013; Faucher *et al.* 2017). It should be noted that these changes did not result in extinctions, with species recovering following the alleviation of environmental changes, and some nannofossil taxa actually increasing in abundance (Erba and Tremolada 2004; Erba *et al.* 2019). Nonetheless, the transient net decrease in carbonate producers reduced the availability of nannofossil micrite and was reflected as a biocalcification crisis, since nannoconids were the main rock-forming nannofossils during the Early Cretaceous (Erba and Tremolada 2004; Weissert and Erba 2004). This interpretation has been challenged recently by Slater *et al.* (2022), who argued that the apparent decrease in nannoplankton preservation results from post-depositional removal of carbonate from the rock record and that diversity increased during OAEs. However, while both of these phenomena did indeed occur, they do not explain the geologically rapid loss of heavily calcified nannoconids compared with other calcifiers (Erba *et al.* 2010), which is more consistent with a biocalcification crisis. Furthermore, fossil evidence of reduced biocalcification during OAE 2 is supported by sedimentological changes consistent with a shallowing of the seawater carbonate compensation depth in response to ocean acidification at that time (Erba 2004; Faucher *et al.* 2017; Jones *et al.* 2023).

While ocean acidification caused by volcanic CO_2 emissions from LIP eruptions is considered to be the main driver of reduced biocalcification during OAEs 1a, and OAE 2 (Erba 2004; Erba *et al.* 2010), alternative processes may also have played a role. Enhanced seawater fertility and subsequent eutrophication have also been proposed as a cause of nannoplankton stress and reduced species richness that favoured smaller taxa (Bersezio *et al.* 2002; Gréselle *et al.* 2011; Aguado *et al.* 2014; Duchamp-Alphonse *et al.* 2014; Mattioli *et al.* 2014; Giraud *et al.* 2018; Shmeit *et al.* 2022). At open oceanic sites, fertilization was potentially driven by the hydrothermal output of biolimiting trace metals from G-OJP or Caribbean LIP activity (Snow *et al.* 2005; Bottini *et al.* 2015; Erba *et al.* 2015; Faucher *et al.* 2017; Bottini and Erba 2018; Bottini and Faucher 2020). Increased runoff of terrestrial material and nutrients caused by volcanically triggered climate warming could have produced the same effect in continental shelf settings, while potentially also reducing light availability in the photic zone (Lübke *et al.* 2015; Lübke and Mutterlose 2016). Alternatively, output of toxic volcanic elements may have suppressed biocalcification.

A more progressive decline in nannoconid biocalcification also occurred during OAE 1b, but has been linked with cold conditions (McAnena *et al.* 2013). Alternatively, volcanic CO_2 output during the formation of the Kerguelen Plateau may have lowered seawater pH enough to reduce carbonate saturation, even if the carbon emissions were insufficient to cause prolonged global temperature rise. Longer-term cooling in the Late Aptian may have been linked to enhanced absorption of CO_2 in seawater, lowering its pH (Bottini *et al.* 2015). The reduction in size, decrease in abundance and species turnover of planktonic foraminifers (Huber and Leckie 2011) might reflect the response of calcareous zooplankton to volcanically triggered ocean acidification (Bottini *et al.* 2015; Bottini and Erba 2018). Analogous changes in the abundance, test size and evolutionary rates of calcareous zooplankton were documented for OAE 1a and OAE 2 (Premoli Silva *et al.* 1989, 1999; Coccioni *et al.* 1992; Leckie *et al.* 2002) and are also consistent with ocean acidification (Kump *et al.* 2009; Hönisch *et al.* 2012). The cause of a nannoconid decline associated with the Weissert Event is less clear, although it has also been linked to increased fertility and seawater acidification related to volcanic CO_2 emissions (Erba and Tremolada 2004; Weissert and Erba 2004). However, there is no independent evidence for decreased seawater pH during that crisis, and as noted above, possible climate warming signals have only been reported for NW Tethyan and proto-Atlantic records of the Weissert Event thus far (see compilations by Charbonnier *et al.* 2020*c*; Cavalheiro *et al.* 2021). At present, the limited evidence for global-scale temperature rise at that time (Meissner *et al.* 2015; Price *et al.* 2018; Cavalheiro *et al.* 2021) hinders argument for a clear causal link between nannoconid stress and climate warming or CO_2 release comparable with that of OAEs 1a and 2.

It is clear that while rapid climate warming itself apparently impacted some marine groups during the Cretaceous, biospheric stress during intervals of LIP volcanism may not have been dependent on increased temperatures (Erba 2006). Nonetheless,

aside from the KPg mass extinction (for which the influence of Deccan Trap volcanism was complicated by the coeval climatic effects of the Chicxulub impact), OAEs 1a and 2 were the intervals associated with LIP emplacement that featured the most severe perturbations to Earth's biosphere. Both OAEs featured significant climate warming, unlike the Weissert Event or OAE 1b. Moreover, the environmental change during OAEs 1a and 2 was also less protracted in nature and had a more rapid onset (probably owing to the more intense LIP activity coeval with those intervals), which may have helped drive a more severe biotic response.

Remaining questions and future perspectives for understanding Cretaceous LIPs

Previous overviews of LIPs and mass extinctions/environmental change have largely focused on continental provinces. It has been hypothesized that the impact of oceanic LIPs was somewhat muted owing to the potentially lower degassing efficiency of submarine eruptions occurring under high seawater pressure (e.g. Courtillot and Renne 2003; Ganino and Arndt 2009; Green *et al.* 2022). However, submarine oceanic-plateau volcanism was probably the main driver of both OAEs 1a and 2, which were marked by the most severe climatic, environmental and biotic changes during the Cretaceous prior to the KPg extinction. Even if the widespread marine anoxia, ocean acidification and biocalcifcation crises during those events were driven by the output of trace-metal micronutrients and volcanic CO_2 and/or halogens into seawater (e.g. Kerr 1998; Erba *et al.* 2004, 2015; Snow *et al.* 2005), both events also featured significant climate warming that was apparently driven by magmatic carbon emissions (Larson and Erba 1999; Jenkyns 2003; Forster *et al.* 2007; Méhay *et al.* 2009; Adloff *et al.* 2020; *this study*; Fig. 6). Thus, submarine LIPs were capable of raising global temperatures as well as triggering oceanic anoxia and acidification, three key processes thought to have helped cause major extinctions.

Recent studies have emphasized that the rate of eruptions (and, consequently, the assumed rate of magmatic CO_2 output) plays a key role in determining the environmental and biotic impact of a LIP (Green *et al.* 2022; Jiang *et al.* 2022). Constraining this CO_2 flux depends on both precise geochronology and robust estimates of the magmatic carbon content. Currently, reconstructed eruption histories vary greatly in terms of detail and precision for different LIPs, both from the Cretaceous and other time intervals (see reviews by Kasbohm *et al.* 2021; Jiang *et al.* 2023). Additionally, the CO_2 content of tholeiitic basalts remains relatively poorly constrained. Current estimates for LIP magma carbon contents range between 0.1 and 2 wt%, based on the study of analogous modern basaltic systems (e.g. Self *et al.* 2006; Saunders 2016), rare olivine melt inclusions (Black *et al.* 2014) and volatile/non-volatile elemental ratios, particularly CO_2/Nb and CO_2/Ba (Black and Gibson 2019; Hernandez Nava *et al.* 2021; Boscaini *et al.* 2022). Thus far, these efforts have only focused on a few continental LIPs, with the Deccan Traps the only Cretaceous province investigated (Hernandez Nava *et al.* 2021). Future studies refining both the eruptive history of Cretaceous LIPs, and their magmatic carbon content, are needed in order to better constrain the rate of CO_2 emissions from LIP volcanism and its importance in determining their impact on Earth's environment/biosphere. Such data are especially required for oceanic LIPs, which have been investigated by relatively few geochronological or geochemical studies thus far (but see compilations by Coffin *et al.* 2002; Kasbohm *et al.* 2021; Davidson *et al.* 2023; Jiang *et al.* 2023). Additional studies of trace-metal and micronutrient distribution from oceanic plateaus are also needed in order to better understand the potential impact of this process in triggering marine anoxia during times of submarine LIP volcanism. In particular, it is unclear whether the distribution of volcanic micronutrients directly into seawater could have enhanced primary productivity and water-column deoxygenation on a global scale. If this effect was largely limited to regions close to the LIP source, anoxia at more distal sites may have depended on terrestrial runoff, upwelling of deepwater nutrients, and/or the development of marine stratification (see Jenkyns 2010; Föllmi 2012).

Finally, the sheer number of Cretaceous LIPs remains something of a mystery. As outlined at the start of this chapter, there were at least seven highly voluminous LIPs during the Cretaceous Period, which have been associated with intervals of profound environmental and/or biosphere disturbance. This represents a significantly higher total than for any other geological period in the last 300 Myr since the formation of Pangaea, even accounting for the longer duration of the Cretaceous v. other periods (Fig. 7). Moreover, seven major Cretaceous LIPs represents a conservative estimate. Some authors have proposed that other extensive igneous formations emplaced geologically rapidly during the Cretaceous represent additional LIPs, or that magmatic areas considered here to be part of the Kerguelen or Greater Ontong–Java plateaus were actually distinct provinces (see compilations by Torsvik 2019; Ernst *et al.* 2021). It may also be noteworthy that the Cretaceous featured the most oceanic LIPs of any known time in the Phanerozoic. This

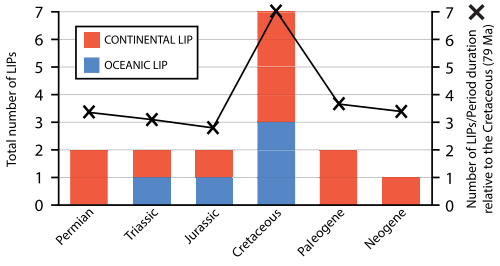

Fig. 7. Summary of the number of mafic LIPs (continental flood basalt provinces or oceanic plateaus) emplaced during each geological period since *c.* 300 Ma, the onset of the Permian. For each period, the total number of mafic LIPs spanning an area of *c.* 0.5 Mkm^2 or more is shown (based on the recent compilation of Ernst *et al.* 2021), together with the ratio between the number of LIPs and proportional duration of the Period relative to the 79 Myr long Cretaceous, i.e. the Jurassic (56.3 Myr) is 0.71 times the duration of the Cretaceous, whereas the Neogene (23.03 Myr) is only 0.29 times that timespan. This compilation includes the Triassic Wrangellia LIP, despite its preservation as relatively small areas of accreted igneous material obducted on to the western margin of North America, since it was probably a large oceanic plateau originally (Kerr 2014, and references therein). Silicic LIPs (see Bryan and Ferrari 2013) are not included, as they are thought to form over very long time intervals, and are less clearly linked to mantle plume activity. LIP, Large igneous province.

peak may result partly from preservation bias given the absence of most pre-Cretaceous ocean crust, but there was no comparable level of oceanic LIP formation in the Cenozoic, for which the available geological record is also good.

Why the Cretaceous was apparently 'a time of LIPs' is unclear. The middle part of the period was also marked by a long interval without magnetic reversals (the Cretaceous Normal superchron), and it has been hypothesized that both the LIPs and the superchron resulted from atypical mantle dynamics, such as the formation of a superplume or significant changes in subduction rates (e.g. Larson 1991; Courtillot and Olson 2007; Yoshimura 2022). Alternatively, this superplume may have been an inevitable consequence of the formation and subsequent break-up of the Pangaean supercontinent (Vaughan and Storey 2007). While these models are speculative, the fact that the Cretaceous was marked by an unusually high number of LIPs, extensive and fast-spreading mid-ocean ridges, enhanced kimberlite emplacement and even the formation of komatiites (the only clear Phanerozoic example of this lithology), suggest that Earth's mantle conditions were highly abnormal during that time (e.g. Kerr 2005; Seton *et al.* 2009; Heaman *et al.* 2019). Given that numerous supercontinent cycles have taken place in the Proterozoic and Phanerozoic eras, it is highly unlikely that there has been only one such spell of high LIP formation in Earth's history. This conclusion raises the tantalising possibility that the Cretaceous Period marked the most recent example of a key mantle phenomenon inherent in Earth's long-term tectonic cycling, which subsequently resulted in profound disturbances to Earth's surface climate, environment, and biosphere.

Summary

Large igneous province volcanism has been hypothesized to be the primary trigger of several intervals of environmental perturbation during the Cretaceous Period, both through eruption of continental flood basalts and the submarine emplacement of oceanic plateaus. This study has generated new mercury-concentration and osmium-isotope datasets to reconstruct the temporal relationships between volcanism, climate warming and environmental change during the Early Aptian oceanic anoxic event (OAE 1a). By incorporating these results into an overview of sedimentary, geochemical and palaeontological evidence of episodes of environmental and biotic change, and the geological, geochronological and geochemical records of LIP activity, the following conclusions are drawn:

(1) Climate warming associated with OAE 1a was probably initiated by magmatic CO_2 emissions prior to the onset of the OAE *sensu stricto*, although volcanic activity and global temperatures did not reach their maximum until the middle part of OAE 1a. The initial carbon was probably sourced from submarine volcanism during formation of the Greater Ontong–Java Plateau. As well as potentially initiating climate warming, this magmatic CO_2 drove biotic stress amongst benthic fauna (dasycladalean algae, larger benthic foraminifera, corals, rudists) and dwarfism in calcareous nannoflora. An additional non-magmatic source such as methane clathrate or thermogenic emissions associated with the High Arctic LIP probably played a key role in further perturbing the global carbon cycle at the onset of the OAE.

(2) The Early Aptian and latest Cenomanian OAEs (OAEs 1a and 2, respectively) represented the episodes of most severe climatic, environmental, and biota stress during the Cretaceous apart from the end-Cretaceous mass extinction (for which the role of volcanism is contested). OAEs 1a and 2 were also coeval with the times of most intense LIP activity and output of mafic trace metals (potentially

including key micronutrients) to the global ocean from oceanic plateaus. Thus, while severe environmental change and mass extinctions are more typically linked with continental LIPs, oceanic plateaus also had the capacity to profoundly impact Earth's surface environment and ecosystems during the Cretaceous Period.

(3) The more limited biosphere impact of some Cretaceous LIPs, such as the Paraná–Etendeka and Kerguelen Plateau, may have resulted from their more protracted formation and lower eruption rate. Kerguelen volcanism was apparently less intense than that of the Greater Ontong–Java and Caribbean/High Arctic LIPs associated with OAEs 1a and 2, potentially leading to lower carbon and trace-metal micronutrient output. Paraná–Etendeka magmas may also have been volatile depleted and did not intrude carbon-rich country rocks. Further work is needed to precisely constrain the eruptive histories and carbon outputs of Cretaceous LIPs (especially oceanic plateaus), and the potential dispersal of micronutrients from submarine volcanism.

(4) The high number of LIP events in the Cretaceous compared with times before or afterwards resulted in Earth's carbon cycle and surface environment being frequently perturbed to an extent not documented for any other geological period in at least the last 300 Myr. Why there was such a high rate of LIP formation (and magmatism in general) during the Cretaceous remains unclear. Further work is needed to determine the cause, and whether there were earlier intervals in Earth's history featuring enhanced Large Igneous Province emplacement, or if the Cretaceous represented a unique 'Age of LIPs'.

Acknowledgements We gratefully acknowledge S. Batenburg for handling this manuscript, and two anonymous reviewers for providing constructive feedback that has improved this overview of Cretaceous LIPs. We greatly appreciate laboratory assistance from Y. Ohtsuki and J. Kikuchi at JAMSTEC (Re–Os analysis) and D. Verstraeten at the VUB (TOC and TS measurements), and further thank P. Claeys, Y. Gao and S. Goderis for providing instrument access for the geochemical analyses undertaken at the VUB. We thank C. Cucciniello and J. Vellekoop for helpful discussions on the Madagascan LIP and Late Maastrichtian Warming Event, respectively.

Competing interests The authors declare that they have no known competing financial interests or personal relationships that could have appeared to influence the work reported in this paper.

Author contributions **LMEP**: conceptualization (lead), data curation (lead), formal analysis (equal), funding acquisition (lead), investigation (lead), methodology (equal), writing – original draft (lead), writing – review & editing (lead); **HM**: data curation (supporting), formal analysis (equal), investigation (supporting), methodology (equal), writing – review & editing (supporting); **SC**: writing – review & editing (supporting); **EE**: writing – review & editing (equal); **ACK**: writing – review & editing (supporting); **JM**: writing – review & editing (equal); **KS**: methodology (equal), writing – review & editing (supporting).

Funding The work was supported by the Research Foundation – Flanders (FWO: grant 12P4522N to LMEP) the Norwegian Research Council (Young Research Talent project number 301096 to SC), the Grant-in-aid for a Japan Society for the Promotion of Science Research Fellow (number 22J00271 to HM), the Japan Society for the Promotion of Science KAKENHI (number 22H01327 to KS), and the Vrije Universiteit Brussel Strategic Research Funding.

Data availability All data generated or analysed during this study are included in this published article (and, if present, its supplementary information files).

References

Abramovich, S. and Keller, G. 2002. High stress late Maastrichtian paleoenvironment: inference from planktonic foraminifera in Tunisia. *Palaeogeography, Palaeoclimatology, Palaeoecology*, **178**, 145–164, https://doi.org/10.1016/S0031-0182(01)00394-7

Adloff, M., Greene, S.E. *et al*. 2020. Unravelling the sources of carbon emissions at the onset of Oceanic Anoxic Event (OAE) 1a. *Earth and Planetary Science Letters*, **530**, 115947, https://doi.org/10.1016/j.epsl.2019.115947

Aguado, R., de Gea, G.A., Castro, J.M., O'Dogherty, L., Quijano, M.L., Naafs, B.D.A. and Pancost, R.D. 2014. Late Barremian–early Aptian dark facies of the Subbetic (Betic Cordillera, southern Spain): calcareous nannofossil quantitative analyses, chemostratigraphy and palaeoceanographic reconstructions. *Palaeogeography, Palaeoclimatology, Palaeoecology*, **395**, 198–221, https://doi.org/10.1016/j.palaeo.2013.12.031

Ait-Itto, F.Z., Martinez, M., Deconinck, J.F. and Bodin, S. 2023. Astronomical calibration of the OAE1b from the Col de Pré-Guittard section (Aptian–Albian), Vocontian Basin, France. *Cretaceous Research*, **150**, 105618, https://doi.org/10.1016/j.cretres.2023.105618

Allègre, C.J., Birck, J.L., Capmas, F. and Courtillot, V. 1999. Age of the Deccan traps using ^{187}Re–^{187}Os systematics. *Earth and Planetary Science Letters*, **170**, 197–204, https://doi.org/10.1016/S0012-821X(99)00110-7

Almeida, V.V., Janasi, V.A., Heaman, L.M., Shaulis, B.J., Hollanda, M.H.B. and Renne, P.R. 2018. Contemporaneous alkaline and tholeiitic magmatism in the Ponta Grossa Arch, Paraná–Etendeka Magmatic Province: Constraints from U–Pb zircon/baddeleyite and

$^{40}Ar/^{39}Ar$ phlogopite dating of the José Fernandes Gabbro and mafic dykes. *Journal of Volcanology and Geothermal Research*, **355**, 55–65, https://doi.org/10.1016/j.jvolgeores.2017.01.018

Alvarez, L.W., Alvarez, W., Asaro, F. and Michel, H.V. 1980. Extraterrestrial cause for the Cretaceous–Tertiary extinction. *Science (New York, NY)*, **208**, 1095–1108, https://doi.org/10.1126/science.208.4448.1095

Ando, A., Kaiho, K., Kawahata, H. and Kakegawa, T. 2008. Timing and magnitude of early Aptian extreme warming: unraveling primary $\delta^{18}O$ variation in indurated pelagic carbonates at Deep Sea Drilling Project Site 463, central Pacific Ocean. *Palaeogeography, Palaeoclimatology, Palaeoecology*, **260**, 463–476, https://doi.org/10.1016/j.palaeo.2007.12.007

Arthur, M.A. 1979. North Atlantic Cretaceous black shales: the record at Site 398 and a brief comparison with other occurrences. *Initial Reports of the Deep Sea Drilling Project*, **47**, 719–751, https://doi.org/10.2973/dsdp.proc.47-2.136.1979

Arthur, M.A., Schlanger, S.T. and Jenkyns, H.C. 1987. The Cenomanian–Turonian Oceanic Anoxic Event, II. Palaeoceanographic controls on organic-matter production and preservation. *Geological Society, London, Special Publications*, **26**, 401–420, https://doi.org/10.1144/GSL.SP.1987.026.01.25

Bacha, R.R., Waichel, B.L. and Ernst, R.E. 2022. The mafic volcanic climax of the Paraná–Etendeka Large Igneous Province as the trigger of the Weissert Event. *Terra Nova*, **34**, 28–36, https://doi.org/10.1111/ter.12558

Baker, S.J., Belcher, C.M., Barclay, R.S., Hesselbo, S.P., Laurin, J. and Sageman, B.B. 2020. CO_2-induced climate forcing on the fire record during the initiation of Cretaceous Oceanic Anoxic Event 2. *Geological Society of America Bulletin*, **132**, 321–333, https://doi.org/10.1130/B35097.1

Baksi, A.K. 1995. Petrogenesis and timing of volcanism in the Rajmahal flood basalt province, northeastern India. *Chemical Geology*, **121**, 73–90, https://doi.org/10.1016/0009-2541(94)00124-Q

Barbarin, N., Bonin, A. *et al*. 2012. Evidence for a complex Valanginian nannoconid decline in the Vocontian basin (south east France). *Marine Micropaleontology*, **84**, 37–53, https://doi.org/10.1016/j.marmicro.2011.11.005

Barnet, J.S., Littler, K., Kroon, D., Leng, M.J., Westerhold, T., Röhl, U. and Zachos, J.C. 2018. A new high-resolution chronology for the late Maastrichtian warming event: establishing robust temporal links with the onset of Deccan volcanism. *Geology*, **46**, 147–150, https://doi.org/10.1130/G39771.1

Barreto, C.J.S., Lafon, J.M., de Lima, E.F. and Sommer, C.A. 2016. Geochemical and Sr–Nd–Pb isotopic insight into the low-Ti basalts from southern Paraná Igneous Province, Brazil: the role of crustal contamination. *International Geology Review*, **58**, 1324–1349, https://doi.org/10.1080/00206814.2016.1147988

Batenburg, S.J., De Vleeschouwer, D. *et al*. 2016. Orbital control on the timing of oceanic anoxia in the Late Cretaceous. *Climate of the Past*, **12**, 1995–2009, https://doi.org/10.5194/cp-12-1995-2016

Bauer, K.W., Zeebe, R.E. and Wortmann, U.G. 2017. Quantifying the volcanic emissions which triggered Oceanic Anoxic Event 1a and their effect on ocean acidification. *Sedimentology*, **64**, 204–214, https://doi.org/10.1111/sed.12335

Bédard, J.H., Saumur, B.M. *et al*. 2021*a*. Geochemical systematics of High Arctic Large Igneous Province continental tholeiites from Canada – evidence for progressive crustal contamination in the plumbing system. *Journal of Petrology*, **62**, https://doi.org/10.1093/petrology/egab042

Bédard, J.H., Troll, V.R. *et al*. 2021*b*. High Arctic Large Igneous Province alkaline rocks in Canada: evidence for multiple mantle components. *Journal of Petrology*, **62**, https://doi.org/10.1093/petrology/egab041

Bersezio, R., Erba, E., Gorza, M. and Riva, A. 2002. Berriasian–Aptian black shales of the Maiolica formation (Lombardian Basin, Southern Alps, northern Italy): local to global events. *Palaeogeography, Palaeoclimatology, Palaeoecology*, **180**, 253–275, https://doi.org/10.1016/S0031-0182(01)00416-3

Birck, J.L., Barman, M.R. and Capmas, F. 1997. Re–Os isotopic measurements at the femtomole level in natural samples. *Geostandards Newsletter*, **21**, 19–27, https://doi.org/10.1111/j.1751-908X.1997.tb00528.x

Black, B.A. and Gibson, S.A. 2019. Deep carbon and the life cycle of large igneous provinces. *Elements*, **15**, 319–324, https://doi.org/10.2138/gselements.15.5.319

Black, B.A., Hauri, E.H., Elkins-Tanton, L.T. and Brown, S.M. 2014. Sulfur isotopic evidence for sources of volatiles in Siberian Traps magmas. *Earth and Planetary Science Letters*, **394**, 58–69, https://doi.org/10.1016/j.epsl.2014.02.057

Black, B.A., Karlstrom, L. and Mather, T.A. 2021. The life cycle of large igneous provinces. *Nature Reviews Earth & Environment*, **2**, 840–857, https://doi.org/10.1038/s43017-021-00221-4

Blättler, C.L., Jenkyns, H.C., Reynard, L.M. and Henderson, G.M. 2011. Significant increases in global weathering during Oxeanic Anoxic Events 1a and 2 indicated by calcium isotopes. *Earth and Planetary Science Letters*, **309**, 77–88, https://doi.org/10.1016/j.epsl.2011.06.029

Bodin, S., Meissner, P., Janssen, N.M., Steuber, T. and Mutterlose, J. 2015. Large igneous provinces and organic carbon burial: controls on global temperature and continental weathering during the Early Cretaceous. *Global and Planetary Change*, **133**, 238–253, https://doi.org/10.1016/j.gloplacha.2015.09.001

Bodin, S., Charpentier, M., Ullmann, C.V., Rudra, A. and Sanei, H. 2023. Carbon cycle during the late Aptian–early Albian OAE 1b: a focus on the Kilian–Paquier levels interval. *Global and Planetary Change*, **222**, 104074, https://doi.org/10.1016/j.gloplacha.2023.104074

Bond, D.P. and Sun, Y. 2021. Global warming and mass extinctions associated with large igneous province volcanism. *In*: Ernst, R.E., Dickson, A.J. and Bekker, A. (eds) *Large Igneous Provinces: a Driver of Global Environmental and Biotic Changes*. AGU, Geophysical Monographs, **255**, 83–102, https://doi.org/10.1002/9781119507444.ch3

Bond, D.P.G. and Wignall, P.B. 2014. Large igneous provinces and mass extinctions: an update. *In*: Keller, G. and Kerr, A.C. (eds) *Volcnanism, Impacts, and Mass Extinctions: Causes and Effects*. Geological Society

of America, Special Papers, **505**, SPE505-02, https://doi.org/10.1130/2014.2505(02)

Bonin, A., Pucéat, E. *et al*. 2016. Cool episode and platform demise in the Early Aptian: new insights on the links between climate and carbonate production. *Paleoceanography*, **31**, 66–80, https://doi.org/10.1002/2015PA002835

Bornemann, A. and Mutterlose, J. 2008. Calcareous nannofossil and $\delta^{13}C$ records from the Early Cretaceous of the Western Atlantic Ocean: evidence for enhanced fertilization across the Berriasian–Valanginian transition. *Palaios*, **23**, 821–832, https://doi.org/10.2110/palo.2007.p07-076r

Boscaini, A., Callegaro, S., Sun, Y. and Marzoli, A. 2022. Late Permian to late Triassic large igneous provinces: timing, eruptive style and paleoenvironmental perturbations. *Frontiers in Earth Science*, **10**, https://doi.org/10.3389/feart.2022.887632

Boschman, L.M., van Hinsbergen, D.J., Torsvik, T.H., Spakman, W. and Pindell, J.L. 2014. Kinematic reconstruction of the Caribbean region since the Early Jurassic. *Earth-Science Reviews*, **138**, 102–136, https://doi.org/10.1016/j.earscirev.2014.08.007

Bottini, C. and Erba, E. 2018. Mid-Cretaceous paleoenvironmental changes in the western Tethys. *Climate of the Past*, **14**, 1147–1163, https://doi.org/10.5194/cp-14-1147-2018

Bottini, C. and Faucher, G. 2020. Biscutum constans coccolith size patterns across the mid Cretaceous in the western Tethys: paleoecological implications. *Palaeogeography, Palaeoclimatology, Palaeoecology*, **555**, 109852, https://doi.org/10.1016/j.palaeo.2020.109852

Bottini, C. and Mutterlose, J. 2012. Integrated stratigraphy of Early Aptian black shales in the Boreal Realm: calcareous nannofossil and stable isotope evidence for global and regional processes. *Newsletters on Stratigraphy*, **45**, 115–137, https://doi.org/10.1127/0078-0421/2012/0017

Bottini, C., Cohen, A.S., Erba, E., Jenkyns, H.C. and Coe, A.L. 2012. Osmium-isotope evidence for volcanism, weathering, and ocean mixing during the early Aptian OAE 1a. *Geology*, **40**, 583–586, https://doi.org/10.1130/G33140.1

Bottini, C., Erba, E., Tiraboschi, D., Jenkyns, H.C., Schouten, S. and Sinninghe Damsté, J.S. 2015. Climate variability and ocean fertility during the Aptian Stage. *Climate of the Past*, **11**, 383–402, https://doi.org/10.5194/cp-11-383-2015

Bowman, K.L., Hammerschmidt, C.R., Lamborg, C.H. and Swarr, G. 2015. Mercury in the North Atlantic Ocean: the U.S. GEOTRACERS zonal and meridional sections. *Deep-Sea Research II*, **116**, 251–261, https://doi.org/10.1016/j.dsr2.2014.07.004

Bralower, T.J., Arthur, M.A., Leckie, R.M., Sliter, W.V., Allard, D.J. and Schlanger, S.O. 1994. Timing and paleoceanography of oceanic dysoxia/anoxia in the Late Barremian to Early Aptian (Early Cretaceous). *Palaios*, **9**, 335–369, https://doi.org/10.2307/3515055

Bréhéret, J.G. 1988. Episodes de sedimentation riche en matière organique dans les marnes bleues d'âge aptien ET ALbien de la partie pélagique du bassin vocontien. *Bulletin de la Société géologique de France*, **4**, 349–356, https://doi.org/10.2113/gssgfbull.IV.2.349

Brown, S.A.E., Scott, A.C., Glasspool, I.J. and Collinson, M.E. 2012. Cretaceous wildfires and their impact on the Earth system. *Cretaceous Research*, **36**, 162–190, https://doi.org/10.1016/j.cretres.2012.02.008

Bryan, S.E. and Ernst, R.E. 2008. Revised definition of large igneous provinces (LIPs). *Earth-Science Reviews*, **86**, 175–202, https://doi.org/10.1016/j.earscirev.2007.08.008

Bryan, S.E. and Ferrari, L. 2013. Large igneous provinces and silicic large igneous provinces: progress in our understanding over the last 25 years. *Geological Society of America Bulletin*, **125**, 1053–1078, https://doi.org/10.1130/B30820.1

Buchan, K.L. and Ernst, R.E. 2006. Giant dyke swarms and the reconstruction of the Canadian Arctic Islands, Greenland, Svalbard and Franz Josef Land. *In*: Hanski, E., Mertanen, S., Rämö, T. and Vuollo, J. (eds) *Dyke Swarms: Time Markers of Crustal Evolution*, 27–48. Taylor and Francis, London.

Buchs, D.M., Kerr, A.C., Brims, J.C., Zapata-Villada, J.P., Correa-Restrepo, T. and Rodríguez, G. 2018. Evidence for subaerial development of the Caribbean oceanic plateau in the Late Cretaceous and palaeo-environmental implications. *Earth and Planetary Science Letters*, **499**, 62–73, https://doi.org/10.1016/j.epsl.2018.07.020

Callegaro, S., Baker, D.R. *et al*. 2014. Microanalyses link sulfur from large igneous provinces and Mesozoic mass extinctions. *Geology*, **42**, 895–898, https://doi.org/10.1130/G35983.1

Callegaro, S., Baker, D.R. *et al*. 2023. Recurring volcanic winters during the latest Cretaceous: sulfur and fluorine budgets of Deccan Traps lavas. *Science Advances*, **9**, https://doi.org/10.1126/sciadv.adg8284

Castro, J.M., Ruiz-Ortiz, P.A. *et al*. 2021. High-resolution C-isotope, TOC and biostratigraphic records of OAE 1a (Aptian) from an expanded hemipelagic cored succession, western Tethys: a new stratigraphic reference for global correlation and paleoenvironmental reconstruction. *Paleoceanography and Paleoclimatology*, **36**, https://doi.org/10.1029/2020PA004004

Cavalheiro, L., Wagner, T. *et al*. 2021. Impact of global cooling on Early Cretaceous high pCO_2 world during the Weissert Event. *Nature Communications*, **12**, https://doi.org/10.1038/s41467-021-25706-0

Chambers, L.M., Pringle, M.S. and Fitton, J.G. 2002. Age and duration of magmatism on the Ontong Java Plateau: ^{40}Ar–^{39}Ar results from ODP Leg 192. AGU Fall Meeting Abstracts, 2002, V71B-1271.

Chambers, L.M., Pringle, M.S. and Fitton, J.G. 2004. Phreatomagmatic eruptions on the Ontong Java Plateau: an Aptian $^{40}Ar/^{39}Ar$ age for volcaniclastic rocks at ODP Site 1184. *Geological Society of London, Special Publications*, **229**, 325–331, https://doi.org/10.1144/GSL.SP.2004.229.01.18

Charbonnier, G. and Föllmi, K.B. 2017. Mercury enrichments in lower Aptian sediments support the link between Ontong Java large igneous province activity and oceanic anoxic episode 1a. *Geology*, **45**, 63–66, https://doi.org/10.1130/G38207.1

Charbonnier, G., Morales, C., Duchamp-Alphonse, S., Westermann, S., Adatte, T. and Föllmi, K.B. 2017. Mercury enrichment indicates volcanic triggering of Valanginian environmental change. *Scientific Reports*, **7**, https://doi.org/10.1038/srep40808

Charbonnier, G., Godet, A., Bodin, S., Adatte, T. and Föllmi, K.B. 2018. Mercury anomalies, volcanic pulses, and drowning episodes along the northern Tethyan margin during the latest Hauterivian–earliest Aptian. *Palaeogeography, Palaeoclimatology, Palaeoecology*, **505**, 337–350, https://doi.org/10.1016/j.palaeo.2018.06.013

Charbonnier, G., Adatte, T., Föllmi, K.B. and Suan, G. 2020*a*. Effect of intense weathering and post-depositional degradation of organic matter on Hg/TOC proxy in organic-rich sediments and its implications for deep-time investigations. *Geochemistry, Geophysics, Geosystems*, **21**, https://doi.org/10.1029/2019GC008707

Charbonnier, G., Adatte, T., Duchamp-Alphonse, S., Spangenberg, J.E. and Föllmi, K.B. 2020*b*. Global mercury enrichment in Valanginian sediments supports a volcanic trigger for the Weissert episode. *In*: Adatte, T., Bond, D.P.G. and Keller, G. (eds) *Mass Extinctions, Volcanism, and Impacts: New Developments*. Geological Society of America, Special Papers, **544**, 85–103, https://doi.org/10.1130/2019.2544(04)

Charbonnier, G., Duchamp-Alphonse, S., Deconinck, J.F., Adatte, T., Spangenberg, J.E., Colin, C. and Föllmi, K.B. 2020*c*. A global palaeoclimatic reconstruction for the Valanginian based on clay mineralogical and geochemical data. *Earth-Science Reviews*, **202**, 103092, https://doi.org/10.1016/j.earscirev.2020.103092

Chenet, A.L., Quidelleur, X., Fluteau, F., Courtillot, V. and Bajpai, S. 2007. ^{40}K–^{40}Ar dating of the Main Deccan large igneous province: further evidence of KTB age and short duration. *Earth and Planetary Science Letters*, **263**, 1–15, https://doi.org/10.1016/j.epsl.2007.07.011

Chenet, A.L., Courtillot, V. *et al*. 2009. Determination of rapid Deccan eruptions across the Cretaceous–Tertiary boundary using paleomagnetic secular variation: 2. Constraints from analysis of eight new sections and synthesis for a 3500-m-thick composite section. *Journal of Geophysical Research: Solid Earth*, **114**, B06103, https://doi.org/10.1029/2008JB005644

Claeys, P., Kiessling, W. and Alvarez, W. 2002. Distribution of Chicxulub ejecta at the Cretaceous–Tertiary boundary. *In*: Koeberl, C. and MacLeod, K.G. (eds) *Catastrophic Events and Mass Extinctions: Impacts and Beyond*. Geological Society of America, Special Papers, **356**, 55–68, https://doi.org/10.1130/0-8137-2356-6.55

Clarkson, M.O., Stirling, C.H. *et al*. 2018. Uranium isotope evidence for two episodes of deoxygenation during Oceanic Anoxic Event 2. *Proceedings of the National Academy of Sciences*, **115**, 2918–2923, https://doi.org/10.1073/pnas.1715278115

Clarkson, M.O., Lenton, T.M., Andersen, M.B., Bagard, M.L., Dickson, A.J. and Vance, D. 2021. Upper limits on the extent of seafloor anoxia during the PETM from uranium isotopes. *Nature Communications*, **12**, https://doi.org/10.1038/s41467-020-20486-5

Coccioni, R., Erba, E. and Premoli-Silva, I. 1992. Barremian–Aptian calcareous plankton biostratigraphy from the Gorgo Cerbara section (Marche, central Italy) and implications for plankton evolution. *Cretaceous Research*, **13**, 517–537, https://doi.org/10.1016/0195-6671(92)90015-I

Coccioni, R., Sabatino, N., Frontalini, F., Gardin, S., Sideri, M. and Sprovieri, M. 2014. The neglected history of Oceanic Anoxic Event 1b: insights and new data from the Poggio le Guaine section (Umbria–Marche Basin). *Stratigraphy*, **11**, 245–282.

Coffin, M.F. and Eldholm, O. 1994. Large igneous provinces: crustal structure, dimensions, and external consequences. *Reviews of Geophysics*, **32**, 1–36, https://doi.org/10.1029/93RG02508

Coffin, M.F., Pringle, M.S., Duncan, R.A., Gladczenko, T.P., Storey, M., Müller, R.D. and Gahagan, L.A. 2002. Kerguelen hotspot magma output since 130 Ma. *Journal of Petrology*, **43**, 1121–1137, https://doi.org/10.1093/petrology/43.7.1121

Cohen, A.S. and Waters, F.G. 1996. Separation of osmium from geological materials by solvent extraction for analysis by thermal ionisation mass spectrometry. *Analytica Chimica Acta*, **332**, 269–275, https://doi.org/10.1016/0003-2670(96)00226-7

Cohen, A.S., Coe, A.L., Bartlett, J.M. and Hawkesworth, C.J. 1999. Precise Re–Os ages of organic-rich mudrocks and the Os isotope composition of Jurassic seawater. *Earth and Planetary Science Letters*, **167**, 159–173, https://doi.org/10.1016/S0012-821X(99)00026-6

Corbett, M.J. and Watkins, D.K. 2013. Calcareous nannofossil paleoecology of the mid-Cretaceous Western Interior Seaway and evidence of oligotrophic surface waters during OAE2. *Palaeogeography, Palaeoclimatology, Palaeoecology*, **392**, 510–523, https://doi.org/10.1016/j.palaeo.2013.10.007

Corfu, F., Polteau, S., Planke, S., Faleide, J.I., Svensen, H., Zayoncheck, A. and Stolbov, N. 2013. U–Pb geochronology of Cretaceous magmatism on Svalbard and Franz Josef Land, Barents Sea large igneous province. *Geological Magazine*, **150**, 1127–1135, https://doi.org/10.1017/S0016756813000162

Cors, J., Heimhofer, U., Adatte, T., Hochuli, P.A., Huck, S. and Bover-Arnal, T. 2015. Climatic evolution across Oceanic Anoxic Event 1a derived from terrestrial palynology and clay minerals (Maestrat Basin, Spain). *Geological Magazine*, **152**, 632–647, https://doi.org/10.1017/S0016756814000557

Cossa, D., Mucci, A. *et al*. 2021. Mercury accumulation in the sediment of the Western Mediterranean abyssal plain: a reliable archive of the late Holocene. *Geochimica et Cosmochimica Acta*, **309**, 1–15, https://doi.org/10.1016/j.gca.2021.06.014

Courtillot, V. and Olson, P. 2007. Mantle plumes link magnetic superchrons to Phanerozoic mass depletion events. *Earth and Planetary Science Letters*, **260**, 495–504, https://doi.org/10.1016/j.epsl.2007.06.003

Courtillot, V. and Renne, P.R. 2003. On the ages of flood basalt events. *Comptes Rendus Geoscience*, **335**, 113–140, https://doi.org/10.1016/S1631-0713(03)00006-3

Courtillot, V., Besse, J., Vandamme, D., Montigny, R., Jaeger, J.J. and Cappetta, H. 1986. Deccan flood basalts at the Cretaceous/Tertiary boundary? *Earth and Planetary Science Letters*, **80**, 361–374, https://doi.org/10.1016/0012-821X(86)90118-4

Courtillot, V., Gallet, Y. *et al*. 2000. Cosmic markers, ^{40}Ar/^{39}Ar dating and paleomagnetism of the KT sections in the Anjar area of the Deccan large igneous province. *Earth and Planetary Science Letters*, **182**,

137–156, https://doi.org/10.1016/S0012-821X(00)00238-7

Cox, A.A. and Keller, C.B. 2023. A Bayesian inversion for emissions and export productivity across the end-Cretaceous boundary. *Science*, **381**, 1446–1451, https://doi.org/10.1126/science.adh3875

Cucciniello, C., Langone, A., Melluso, L., Morra, V., Mahoney, J.J., Meisel, T. and Tiepolo, M. 2010. U–Pb Ages, Pb–Os isotope ratios, and platinum-group element (PGE) composition of the west-central Madagascar flood basalt province. *The Journal of Geology*, **118**, 523–541, https://doi.org/10.1086/655012

Cucciniello, C., Conrad, J. *et al*. 2011. Petrology and geochemistry of Cretaceous mafic and silicic dykes and spatially associated lavas in central-eastern coastal Madagascar. *In*: Srivastava, R.K. (ed.) *Dyke Swarms: Keys for Geodynamic Interpretation: Keys for Geodynamic Interpretation*. 345–375, https://doi.org/10.1007/978-3-642-12496-9_21

Cucciniello, C., Melluso, L., Jourdan, F., Mahoney, J.J., Meisel, T. and Morra, V. 2013. ^{40}Ar–^{39}Ar ages and isotope geochemistry of Cretaceous basalts in northern Madagascar: refining eruption ages, extent of crustal contamination and parental magmas in a flood basalt province. *Geological Magazine*, **150**, 1–17, https://doi.org/10.1017/S0016756812000088

Cucciniello, C., Morra, V., Melluso, L. and Jourdan, F. 2022. Constraints on duration, age and migration of the feeder systems of the Madagascan flood basalt province from high-precision ^{40}Ar/^{39}Ar chronology. *Geological Society, London, Special Publications*, **518**, 325–340, https://doi.org/10.1144/SP518-2020-275

Dameron, S.N., Leckie, R.M., Clark, K., MacLeod, K.G., Thomas, D.J. and Lees, J.A. 2017. Extinction, dissolution, and possible ocean acidification prior to the Cretaceous/Paleogene (K/Pg) boundary in the tropical Pacific. *Palaeogeography, Palaeoclimatology, Palaeoecology*, **485**, 433–454, https://doi.org/10.1016/j.palaeo.2017.06.032

Davidson, P.C., Koppers, A.A., Sano, T. and Hanyu, T. 2023. A younger and protracted emplacement of the Ontong Java Plateau. *Science (New York, NY)*, **380**, 1185–1188, https://doi.org/10.1126/science.ade8666

Deegan, F.M., Bédard, J.H. *et al*. 2022. Magma–shale interaction in large igneous provinces: implications for climate warming and sulfide genesis. *Journal of Petrology*, **63**, https://doi.org/10.1093/petrology/egac094

De Min, A., Callegaro, S., Marzoli, A., Nardy, A.J., Chiaradia, M., Marques, L.S. and Gabbarrini, I. 2018. Insights into the petrogenesis of low-and high-Ti basalts: stratigraphy and geochemistry of four lava sequences from the central Paraná basin. *Journal of Volcanology and Geothermal Research*, **355**, 232–252, https://doi.org/10.1016/j.jvolgeores.2017.08.009

Desmares, D., Crognier, N., Bardin, J., Testé, M., Beaudoin, B. and Grosheny, D. 2016. A new proxy for Cretaceous paleoceanographic and paleoclimatic reconstructions: coiling direction changes in the planktonic foraminifera Muricohedbergella delrioensis. *Palaeogeography, Palaeoclimatology, Palaeoecology*, **445**, 8–17, https://doi.org/10.1016/j.palaeo.2015.12.021

Dickson, A.J., Rees-Owen, R.L. *et al*. 2014. The spread of marine anoxia on the northern Tethys margin during the Paleocene–Eocene Thermal Maximum. *Paleoceanography*, **29**, 471–488, https://doi.org/10.1002/2014PA002629

Dickson, A.J., Cohen, A.S., Coe, A.L., Davies, M., Shcherbinina, E.A. and Gavrilov, Y.O. 2015. Evidence for weathering and volcanism during the PETM from Arctic and Peri-Tethys osmium isotope records. *Palaeogeography, Palaeoclimatology, Palaeoecology*, **438**, 300–307, https://doi.org/10.1016/j.palaeo.2015.08.019

Dickson, A.J., Jenkyns, H.C., Porcelli, D., van den Boorn, S. and Idiz, E. 2016. Basin-scale controls on the molybdenum-isotope composition of seawater during Oceanic Anoxic Event 2 (Late Cretaceous). *Geochimica et Cosmochimica Acta*, **178**, 291–306, https://doi.org/10.1016/j.gca.2015.12.036

Dickson, A.J., Cohen, A.S. and Davies, M. 2021. The osmium isotope signature of phanerozoic large igneous provinces. *In*: Ernst, R.E., Dickson, A.J. and Bekker, A. (eds) *Large Igneous Provinces: a Driver of Global Environmental and Biotic Changes*. AGU, Geophysical Monographs, **255**, 229–246, https://doi.org/10.1002/9781119507444.ch10

Dockman, D.M., Pearson, D.G., Heaman, L.M., Gibson, S.A. and Sarkar, C. 2018. Timing and origin of magmatism in the Sverdrup Basin, Northern Canada – implications for lithospheric evolution in the High Arctic Large Igneous Province (HALIP). *Tectonophysics*, **742**, 50–65, https://doi.org/10.1016/j.tecto.2018.05.010

Dodd, S.C., Mac Niocaill, C. and Muxworthy, A.R. 2015. Long duration (> 4 Ma) and steady-state volcanic activity in the early Cretaceous Paraná–Etendeka Large Igneous Province: new palaeomagnetic data from Namibia. *Earth and Planetary Science Letters*, **414**, 16–29, https://doi.org/10.1016/j.epsl.2015.01.009

dos Santos, ÂCS, Holanda, E.C., de Souza, V., Guerra-Sommer, M., Manfroi, J., Uhl, D. and Jasper, A. 2016. Evidence of palaeo-wildfire from the upper lower Cretaceous (Serra do Tucano Formation, Aptian–Albian) of Roraima (North Brazil). *Cretaceous Research*, **57**, 46–49, https://doi.org/10.1016/j.cretres.2015.08.003

Driscoll, C.T., Mason, R.P., Chan, H.M., Jacob, D.J. and Pirrone, N. 2013. Mercury as a global pollutant: sources, pathways, and effects. *Environmental Science & Technology*, **47**, 4967–4983, https://doi.org/10.1021/es305071v

Duchamp-Alphonse, S., Gardin, S., Fiet, N., Bartolini, A., Blamart, D. and Pagel, M. 2007. Fertilization of the northwestern Tethys (Vocontian basin, SE France) during the Valanginian carbon isotope perturbation: evidence from calcareous nannofossils and trace element data. *Palaeogeography, Palaeoclimatology, Palaeoecology*, **243**, 132–151, https://doi.org/10.1016/j.palaeo.2006.07.010

Duchamp-Alphonse, S., Gardin, S. and Bartolini, A. 2014. Calcareous nannofossil response to the Weissert episode (Early Cretaceous): implications for palaeoecological and palaeoceanographic reconstructions. *Marine Micropaleontology*, **113**, 65–78, https://doi.org/10.1016/j.marmicro.2014.10.002

Dumitrescu, M., Brassell, S.C., Schouten, S., Hopmans, E.C. and Damsté, J.S.S. 2006. Instability in tropical

Pacific sea-surface temperatures during the early Aptian. *Geology*, **34**, 833–836, https://doi.org/10.1130/G22882.1

Duncan, R.A. 1978. Geochronology of basalts from the Ninetyeast Ridge and continental dispersion in the eastern Indian Ocean. *Journal of Volcanology and Geothermal Research*, **4**, 283–305, https://doi.org/10.1016/0377-0273(78)90018-5

Duncan, R.A. 1991. Age distribution of volcanism along aseismic ridges in the eastern Indian Ocean. *In*: Weissel, J., Peirce, J., Taylor, E. and Alt, J. (eds) *Proceedings of the Ocean Drilling Program*. Ocean Drilling Program, College Station, TX, Scientific Results, **121**, 507–517.

Duncan, R.A. 2002. A time frame for construction of the Kerguelen Plateau and Broken Ridge. *Journal of Petrology*, **43**, 1109–1119, https://doi.org/10.1093/petrology/43.7.1109

Du Vivier, A.D.C., Selby, D., Sageman, B.B., Jarvis, I., Gröcke, D.R. and Voigt, S. 2014. Marine $^{187}Os/^{188}Os$ isotope stratigraphy reveals the interaction of volcanism and ocean circulation during Oceanic Anoxic Event 2. *Earth and Planetary Science Letters*, **389**, 23–33, https://doi.org/10.1016/j.epsl.2013.12.024

Du Vivier, A.D.C., Selby, D., Takashima, R. and Nishi, H. 2015. Pacific $^{187}Os/^{188}Os$ isotope geochemistry and U–Pb geochronology: synchroneity of global Os isotope change across OAE 2. *Earth and Planetary Science Letters*, **428**, 204–216, https://doi.org/10.1016/j.epsl.2015.07.020

Eddy, M.P., Schoene, B., Samperton, K.M., Keller, G., Adatte, T. and Khadri, S.F. 2020. U–Pb zircon age constraints on the earliest eruptions of the Deccan Large Igneous Province, Malwa Plateau, India. *Earth and Planetary Science Letters*, **540**, 116249, https://doi.org/10.1016/j.epsl.2020.116249

Eldrett, J.S., Ma, C. *et al*. 2015. An astronomically calibrated stratigraphy of the Cenomanian, Turonian and earliest Coniacian from the Cretaceous Western Interior Seaway, USA: implications for global chronostratigraphy. *Cretaceous Research*, **56**, 316–344, https://doi.org/10.1016/j.cretres.2015.04.010

Erba, E. 1994. Nannofossils and superplumes: the early Aptian 'nannoconid crisis'. *Paleoceanography*, **9**, 483–501, https://doi.org/10.1029/94PA00258

Erba, E. 2004. Calcareous nannofossils and Mesozoic oceanic anoxic events. *Marine Micropaleontology*, **52**, 85–106, https://doi.org/10.1016/j.marmicro.2004.04.007

Erba, E. 2006. The first 150 million years history of calcareous nannoplankton: biosphere–geosphere interactions. *Palaeogeography, Palaeoclimatology, Palaeoecology*, **232**, 237–250, https://doi.org/10.1016/j.palaeo.2005.09.013

Erba, E. and Tremolada, F. 2004. Nannofossil carbonate fluxes during the Early Cretaceous: Phytoplankton response to nutrification episodes, atmospheric CO_2, and anoxia. *Paleoceanography*, **19**, https://doi.org/10.1029/2003PA000884

Erba, E., Bartolini, A. and Larson, R.L. 2004. Valanginian Weissert oceanic anoxic event. *Geology*, **32**, 149–152, https://doi.org/10.1130/G20008.1

Erba, E., Bottini, C., Weissert, H.J. and Keller, C.E. 2010. Calcareous nannoplankton response to surface-water acidification around Oceanic Anoxic Event 1a. *Science (New York, NY)*, **329**, 428–432, https://doi.org/10.1126/science.1188886

Erba, E., Duncan, R.A., Bottini, C., Tiraboschi, D., Weissert, H., Jenkyns, H.C. and Malinverno, A. 2015. Environmental consequences of Ontong Java Plateau and Kerguelen Plateau volcanism. *In*: Neal, C.R., Sager, W.W., Sano, T and Erba, E. (eds) *The Origin, Evolution, and Environmental Impact of Oceanic Large Igneous Provinces*. Geological Society, Special Papers, **511**, 271–303, https://doi.org/10.1130/2015.2511(15)

Erba, E., Bottini, C., Faucher, G., Gambacorta, G. and Visentin, S. 2019. The response of calcareous nannoplankton to oceanic anoxic events: the Italian pelagic record. *Bollettino della Società Paleontologica Italiana*, **58**, 51–71, https://doi.org/10.4435/BPSI.2019.08

Erbacher, J., Huber, B.T., Norris, R.D. and Markey, M. 2001. Increased thermohaline stratification as a possible cause for an ocean anoxic event in the Cretaceous period. *Nature*, **409**, 325–327, https://doi.org/10.1038/35053041

Erbacher, J., Friedrich, O., Wilson, P.A., Birch, H. and Mutterlose, J. 2005. Stable organic carbon isotope stratigraphy across Oceanic Anoxic Event 2 of Demerara Rise, western tropical Atlantic. *Geochemistry, Geophysics, Geosystems*, **6**, Q06010, https://doi.org/10.1029/2004GC000850

Erlank, A.J., Marsh, J.S., Duncan, A.R., Miller, R.M., Hawkesworth, C.J., Betton, P.J. and Rex, D.C. 1984. Geochemistry and petrogenesis of the Etendeka volcanic rocks from SWA/Namibia. *Petrogenesis of the volcanic rocks of the Karoo Province*, **13**, 195–245.

Ernesto, M., Raposo, M.I.B., Marques, L.S., Renne, P.R., Diogo, L.A. and De Min, A. 1999. Paleomagnetism, geochemistry and $^{40}Ar/^{39}Ar$ dating of the Northeastern Paraná Magmatic Province: tectonic implications. *Journal of Geodynamics*, **28**, 321–340, https://doi.org/10.1016/S0264-3707(99)00013-7

Ernst, R.E. 2014. *Large Igneous Provinces*. Cambridge University Press.

Ernst, R.E., Bond, D.P. *et al*. 2021. Large igneous province record through time and implications for secular environmental changes and geological time-scale boundaries. *In*: Ernst, R.E., Dickson, A.J. and Bekker, A. (eds) *Large Igneous Provinces: a Driver of Global Environmental and Biotic Changes*. AGU, Geophysical Monographs, **255**, 3–26, https://doi.org/10.1002/9781119507444.ch1

Esmeray-Senlet, S., Wright, J.D., Olsson, R.K., Miller, K.G., Browning, J.V. and Quan, T.M. 2015. Evidence for reduced export productivity following the Cretaceous/Paleogene mass extinction. *Paleoceanography*, **30**, 718–738, https://doi.org/10.1002/2014PA002724

Estrada, S., Damaske, D. *et al*. 2016. Multistage Cretaceous magmatism in the northern coastal region of Ellesmere Island and its relation to the formation of Alpha Ridge–evidence from aeromagnetic, geochemical and geochronological data. *Norwegian Journal of Geology*, **96**, 65–95, http://doi.org/10.17850/njg96-2-03

Evenchick, C.A., Davis, W.J., Bédard, J.H., Hayward, N. and Friedman, R.M. 2015. Evidence for protracted High Arctic large igneous province magmatism in the central Sverdrup Basin from stratigraphy, geochronology, and paleodepths of saucer-shaped sills. *Geological*

Society of America Bulletin, **127**, 1366–1390, https://doi.org/10.1130/B31190.1

Faucher, G., Erba, E., Bottini, C. and Gambacorta, G. 2017. Calcareous nannoplankton response to the latest Cenomanian Oceanic Anoxic Event 2 perturbation. *Rivista Italiana di Paleontologia e Stratigrafia*, **123**, 159–176.

Fendley, I.M., Mittal, T., Sprain, C.J., Marvin-DiPasquale, M., Tobin, T.S. and Renne, P.R. 2019. Constraints on the volume and rate of Deccan Traps flood basalt eruptions using a combination of high-resolution terrestrial mercury records and geochemical box models. *Earth and Planetary Science Letters*, **524**, 115721, https://doi.org/10.1016/j.epsl.2019.115721

Feyte, S., Tessier, A., Gobeil, C. and Cossa, D. 2010. In situ adsorption of mercury, methylmercury and other elements by iron oxyhydroxides and organic matter in lake sediments. *Applied Geochemistry*, **25**, 984–995, https://doi.org/10.1016/j.apgeochem.2010.04.005

Fitton, J.G. and Godard, M. 2004. Origin and evolution of magmas on the Ontong Java Plateau. *Geological Society, London, Special Publications*, **229**, 151–178, https://doi.org/10.1144/GSL.SP.2004.229.01.10

Florisbal, L.M., Heaman, L.M., de Assis Janasi, V. and de Fatima Bitencourt, M. 2014. Tectonic significance of the Florianópolis dyke Swarm, Paraná–Etendeka Magmatic Province: a reappraisal based on precise U–Pb dating. *Journal of Volcanology and Geothermal Research*, **289**, 140–150, https://doi.org/10.1016/j.jvolgeores.2014.11.007

Föllmi, K.B. 2012. Early Cretaceous life, climate and anoxia. *Cretaceous Research*, **35**, 230–257, https://doi.org/10.1016/j.cretres.2011.12.005

Föllmi, K.B., Weissert, H., Bisping, M. and Funk, H. 1994. Phosphogenesis, carbon-isotope stratigraphy, and carbonate-platform evolution along the Lower Cretaceous northern Tethyan margin. *Geological Society of America Bulletin*, **106**, 729–746, https://doi.org/10.1130/0016-7606(1994)106<0729:PCISAC>2.3.CO;2

Föllmi, K.B., Godet, A., Bodin, S. and Linder, P. 2006. Interactions between environmental change and shallow water carbonate buildup along the northern Tethyan margin and their impact on the Early Cretaceous carbon isotope record. *Paleoceanography*, **21**, https://doi.org/10.1029/2006PA001313

Font, E., Adatte, T., Sial, A.N., de Lacerda, L.D., Keller, G. and Punekar, J. 2016. Mercury anomaly, Deccan volcanism, and the end-Cretaceous mass extinction. *Geology*, **44**, 171–174, https://doi.org/10.1130/G37451.1

Forster, A., Schouten, S., Moriya, K., Wilson, P.A. and Sinninghe Damsté, J.S. 2007. Tropical warming and intermittent cooling during the Cenomanian/Turonian oceanic anoxic event 2: sea surface temperature records from the equatorial Atlantic. *Palaeoceanography*, **22**, A1219, https://doi.org/10.1029/2006PA001349

Foster, G.L., Royer, D.L. and Lunt, D.J. 2017. Future climate forcing potentially without precedent in the last 420 million years. *Nature Communications*, **8**, https://doi.org/10.1038/ncomms14845

Frey, F.A., McNaughton, N.J., Nelson, D.R., deLaeter, J.R. and Duncan, R.A. 1996. Petrogenesis of the Bunbury Basalt, Western Australia: interaction between the Kerguelen plume and Gondwana lithosphere? *Earth and Planetary Science Letters*, **144**, 163–183, https://doi.org/10.1016/0012-821X(96)00150-1

Frieling, J., Mather, T.A. *et al*. 2023. Effects of redox variability and early diagenesis on marine sedimentary Hg records. *Geochimica et Cosmochimica Acta*, **351**, 78–95, https://doi.org/10.1016/j.gca.2023.04.015

Gale, A.S. and Christensen, W.K. 1996. Occurrence of the belemnite Actinocamax plenus in the Cenomanian of SE France and its significance. *Bulletin of the Geological Society of Denmark*, **43**, 68–77.

Gale, A.S., Mutterlose, J., Batenburg, S., Gradstein, F.M., Agterberg, F.P., Ogg, J.G. and Petrizzo, M.R. 2020. The Cretaceous period. *In*: Gradstein, F.M., Ogg, J.G., Schmitz, M.D. and Ogg, G.M. (eds) *Geologic Time Scale 2020*. Elsevier, 1023–1086, https://doi.org/10.1016/B978-0-12-824360-2.00027-9

Galloway, J.M., Fensome, R.A. *et al*. 2022. Exploring the role of High Arctic Large Igneous Province volcanism on Early Cretaceous Arctic forests. *Cretaceous Research*, **129**, 105022, https://doi.org/10.1016/j.cretres.2021.105022

Ganino, C. and Arndt, N.T. 2009. Climate changes caused by degassing of sediments during the emplacement of large igneous provinces. *Geology*, **37**, 323–326, https://doi.org/10.1130/G25325A.1

Gilabert, V., Batenburg, S.J., Arenillas, I. and Arz, J.A. 2022. Contribution of orbital forcing and Deccan volcanism to global climatic and biotic changes across the Cretaceous–Paleogene boundary at Zumaia, Spain. *Geology*, **50**, 21–25, https://doi.org/10.1130/G49214.1

Giraud, F., Pittet, B., Grosheny, D., Baudin, F., Lécuyer, C. and Sakamoto, T. 2018. The palaeoceanographic crisis of the Early Aptian (OAE 1a) in the Vocontian Basin (SE France). *Palaeogeography, Palaeoclimatology, Palaeoecology*, **511**, 483–505, https://doi.org/10.1016/j.palaeo.2018.09.014

Gladczenko, T.P., Coffin, M.F. and Eldholm, O. 1997. Crustal structure of the Ontong Java Plateau: modelling of new gravity and existing seismic data. *Journal of Geophysical Research: Solid Earth*, **102**, 22711–22729, https://doi.org/10.1029/97JB01636

Goderis, S., Sato, H. *et al*. 2021. Globally distributed iridium layer preserved within the Chicxulub impact structure. *Science Advances*, **7**, https://doi.org/10.1126/sciadv.abe3647

Gomes, A.S. and Vasconcelos, P.M. 2021. Geochronology of the Paraná–Etendeka large igneous province. *Earth-Science Reviews*, **220**, 103716, https://doi.org/10.1016/j.earscirev.2021.103716

Grasby, S.E., Beauchamp, B., Bond, D.P.G., Wignall, P.B. and Sanei, H. 2016. Mercury anomalies associated with three extinction events (Capitanian crisis, latest Permian extinction and the Smithian/Spathian extinction) in NW Pangea. *Geological Magazine*, **153**, 285–297, https://doi.org/10.1017/S0016756815000436

Grasby, S.E., Them, T.R., Chen, Z., Yin, R. and Ardakani, O.H. 2019. Mercury as a proxy for volcanic emissions in the geologic record. *Earth-Science Reviews*, **196**, 102880, https://doi.org/10.1016/j.earscirev.2019.102880

Green, T., Renne, P.R. and Keller, C.B. 2022. Continental flood basalts drive Phanerozoic extinctions. *Proceedings of the National Academy of Sciences*, **119**, https://doi.org/10.1073/pnas.2120441119

Gréselle, B., Pittet, B. *et al*. 2011. The Valanginian isotope event: a complex suite of palaeoenvironmental

perturbations. *Palaeogeography, Palaeoclimatology, Palaeoecology*, **306**, 41–57, https://doi.org/10.1016/j.palaeo.2011.03.027

Gröcke, D.R., Hesselbo, S.P. and Jenkyns, H.C. 1999. Carbon-isotope composition of Lower Cretaceous fossil wood: ocean–atmosphere chemistry and relation to sea-level change. *Geology*, **27**, 155–158, https://doi.org/10.1130/0091-7613(1999)027<0155:CICOLC>2.3.CO;2

Gröcke, D.R., Price, G.D., Robinson, S.A., Baraboshkin, E.Y., Mutterlose, J. and Ruffell, A.H. 2005. The Upper Valanginian (Early Cretaceous) positive carbon–isotope event recorded in terrestrial plants. *Earth and Planetary Science Letters*, **240**, 495–509, https://doi.org/10.1016/j.epsl.2005.09.001

Hall, R., Álvarez, J. and Rico, H. 1972. Geología de parte de los departamentos de Antioquia y Caldas (sub-zona II-A). *Boletín Geológico*, **20**, 1–85, https://doi.org/10.32685/0120-1425/bolgeol20.1.1972.326

Hammer, Ø, Jones, M.T., Schneebeli-Hermann, E., Hansen, B.B. and Bucher, H. 2019. Are Early Triassic extinction events associated with mercury anomalies? A reassessment of the Smithian/Spathian boundary extinction. *Earth-Science Reviews*, **195**, 179–190, https://doi.org/10.1016/j.earscirev.2019.04.016

Hardas, P. and Mutterlose, J. 2007. Calcareous nannofossil assemblages of Oceanic Anoxic Event 2 in the equatorial Atlantic: evidence of an eutrophication event. *Marine Micropaleontology*, **66**, 52–69, https://doi.org/10.1016/j.marmicro.2007.07.007

Hart, M.B., Yancey, T.E., Leighton, A.D., Miller, B., Liu, C., Smart, C.W. and Twitchett, R.J. 2012. The Cretaceous-Paleogene boundary on the Brazos River, Texas: New stratigraphic sections and revised interpretations. *Journal of the Gulf Coast Association of Geological Societies*, **1**, 69–80.

Hart, M.B., Leighton, A.D., Hampton, M. and Smart, C.W. 2019. Global bioevents and the Cretaceous/Paleogene boundary in Texas and Alabama: stratigraphy, correlation and ocean acidification. *Global and Planetary Change*, **175**, 129–143, https://doi.org/10.1016/j.gloplacha.2019.01.020

Hasegawa, T. 1997. Cenomanian–Turonian carbon isotope events recorded in terrestrial organic matter from northern Japan. *Palaeogeography, Palaeoclimatology, Palaeoecology*, **130**, 251–273, https://doi.org/10.1016/S0031-0182(96)00129-0

Heaman, L.M., Phillips, D. and Pearson, G. 2019. Dating kimberlites: methods and emplacement patterns through time. *Elements*, **15**, 399–404, https://doi.org/10.2138/gselements.15.6.399

Heimdal, T.H., Svensen, H.H. *et al*. 2018. Large-scale sill emplacement in Brazil as a trigger for the end-Triassic crisis. *Scientific Reports*, **8**, https://doi.org/10.1038/s41598-017-18629-8

Heimhofer, U., Hochuli, P.A., Herrle, J.O., Andersen, N. and Weissert, H. 2004. Absence of major vegetation and palaeoatmospheric pCO_2 changes associated with oceanic anoxic event 1a (Early Aptian, SE France). *Earth and Planetary Science Letters*, **223**, 303–318, https://doi.org/10.1016/j.epsl.2004.04.037

Hernandez Nava, A., Black, B.A., Gibson, S.A., Bodnar, R.J., Renne, P.R. and Vanderkluysen, L. 2021. Reconciling early Deccan Traps CO_2 outgassing and pre-KPB global climate. *Proceedings of the National Academy of Sciences*, **118**, https://doi.org/10.1073/pnas.200779 7118

Herrle, J.O. and Mutterlose, J. 2003. Calcareous nannofossils from the Aptian–Lower Albian of southeast France: palaeoecological and biostratigraphic implications. *Cretaceous Research*, **24**, 1–22, https://doi.org/10.1016/S0195-6671(03)00023-5

Herrle, J.O., Pross, J., Friedrich, O. and Hemleben, C. 2003. Short-term environmental changes in the Cretaceous Tethyan Ocean: micropalaeontological evidence from the Early Albian Oceanic Anoxic Event 1b. *Terra Nova*, **15**, 14–19, https://doi.org/10.1046/j.1365-3121.2003.00448.x

Herrle, J.O., Kößler, P., Friedrich, O., Erlenkeuser, H. and Hemleben, C. 2004. High-resolution carbon isotope records of the Aptian to Lower Albian from SE France and the Mazagan Plateau (DSDP Site 545): a stratigraphic tool for paleoceanographic and paleobiologic reconstruction. *Earth and Planetary Science Letters*, **218**, 149–161, https://doi.org/10.1016/S0012-821X(03)00646-0

Herrle, J.O., Schröder-Adams, C.J., Davis, W., Pugh, A.T., Galloway, J.M. and Fath, J. 2015. Mid-Cretaceous High Arctic stratigraphy, climate, and oceanic anoxic events. *Geology*, **43**, 403–406, https://doi.org/10.1130/G36439.1

Hoernle, K., Hauff, F. *et al*. 2010. Age and geochemistry of volcanic rocks from the Hikurangi and Manihiki oceanic Plateaus. *Geochimica et Cosmochimica Acta*, **74**, 7196–7219, https://doi.org/10.1016/j.gca.2010.09.030

Hoffmann, R. and Mutterlose, J. 2011. Stratigraphie und Cephalopodenfauna des Unter-Apt von Alstätte (NRW). *Geologie und Paläontologie in Westfalen*, **80**, 43–59.

Holmden, C., Jacobson, A.D., Sageman, B.B. and Hurtgen, M.T. 2016. Response of the Cr isotope proxy to Cretaceous Ocean Anoxic Event 2 in a pelagic carbonate succession from the Western Interior Seaway. *Geochimica et Cosmochimica Acta*, **186**, 277–295, https://doi.org/10.1016/j.gca.2016.04.039

Hönisch, B., Ridgwell, A. *et al*. 2012. The geological record of ocean acidification. *Science (New York, NY)*, **335**, 1058–1063, https://doi.org/10.1126/science.1208277

Huber, B.T. and Leckie, R.M. 2011. Planktic foraminiferal species turnover across deep-sea Aptian/Albian boundary sections. *The Journal of Foraminiferal Research*, **41**, 53–95, https://doi.org/10.2113/gsjfr.41.1.53

Huber, B.T., MacLeod, K.G., Gröcke, D.R. and Kucera, M. 2011. Paleotemperature and paleosalinity inferences and chemostratigraphy across the Aptian/Albian boundary in the subtropical North Atlantic. *Paleoceanography*, **26**, https://doi.org/10.1029/2011PA002178

Hull, P.M., Bornemann, A. *et al*. 2020. On impact and volcanism across the Cretaceous–Paleogene boundary. *Science (New York, NY)*, **367**, 266–272, https://doi.org/10.1126/science.aay5055

Ingle, S. and Coffin, M.F. 2004. Impact origin for the greater Ontong Java Plateau? *Earth and Planetary Science Letters*, **218**, 123–134, https://doi.org/10.1016/S0012-821X(03)00629-0

Ingle, S., Mahoney, J.J., Sato, H., Coffin, M.F., Kimura, J.I., Hirano, N. and Nakanishi, M. 2007. Depleted

mantle wedge and sediment fingerprint in unusual basalts from the Manihiki Plateau, central Pacific Ocean. *Geology*, **35**, 595–598, https://doi.org/10.1130/G23741A.1

Ishikawa, A., Senda, R., Suzuki, K., Dale, C.W. and Meisel, T. 2014. Re-evaluating digestion methods for highly siderophile element and ^{187}Os isotope analysis: Evidence from geological reference materials. *Chemical Geology*, **384**, 27–46, https://doi.org/10.1016/j.chemgeo.2014.06.013

Jahren, A.H., Arens, N.C., Sarmiento, G., Guerrero, J. and Amundson, R. 2001. Terrestrial record of methane hydrate dissociation in the Early Cretaceous. *Geology*, **29**, 159–162, https://doi.org/10.1130/0091-7613(2001)029<0159:TROMHD>2.0.CO;2

Janasi, V.d.A., de Freitas, V.A. and Heaman, L.H. 2011. The onset of flood basalt volcanism, Northern Paraná Basin, Brazil: a precise U–Pb baddeleyite/zircon age for a Chapecó-type dacite. *Earth and Planetary Science Letters*, **302**, 147–153, https://doi.org/10.1016/j.epsl.2010.12.005

Jarvis, I., Lignum, J.S., Gröcke, D.R., Jenkyns, H.C. and Pearce, M.A. 2011. Black shale deposition, atmospheric CO_2 drawdown, and cooling during the Cenomanian–Turonian Oceanic Anoxic Event. *Paleoceanography*, **26**, A3201, https://doi.org/10.1029/2010PA002081

Jelby, M.E., Śliwińska, K.K., Koevoets, M.J., Alsen, P., Vickers, M.L., Olaussen, S. and Stemmerik, L. 2020. Arctic reappraisal of global carbon-cycle dynamics across the Jurassic–Cretaceous boundary and Valanginian Weissert Event. *Palaeogeography, Palaeoclimatology, Palaeoecology*, **555**, 109847, https://doi.org/10.1016/j.palaeo.2020.109847

Jenkyns, H.C. 1995. Carbon-isotope stratigraphy and paleoceanographic significance of the Lower Cretaceous shallow-water carbonates of Resolution Guyot, Mid-Pacific Mountains. *In*: Winterer, E.L., Sager, W.W., Firth, J.V. and Sinton, J.M. (eds) *Proceedings of the Ocean Drilling Program*. Ocean Drilling Program, College Station, TX, Scientific Results, **143**, 99–104, https://doi.org/10.2973/odp.proc.sr.143.213.1995

Jenkyns, H.C. 2003. Evidence for rapid climate change in the Mesozoic–Palaeogene greenhouse world. *Philosophical Transactions of the Royal Society of London Series A: Mathematical, Physical and Engineering Sciences*, **361**, 1885–1916, https://doi.org/10.1098/rsta.2003.1240

Jenkyns, H.C. 2010. Geochemistry of oceanic anoxic events. *Geochemistry, Geophysics, Geosystems*, **11**, https://doi.org/10.1029/2009GC002788

Jenkyns, H.C. 2018. Transient cooling episodes during Cretaceous Oceanic Anoxic Events with special reference to OAE 1a (Early Aptian). *Philosophical Transactions of the Royal Society A: Mathematical, Physical and Engineering Sciences*, **376**, 20170073, https://doi.org/10.1098/rsta.2017.0073

Jenkyns, H.C., Matthews, A., Tsikos, H. and Erel, Y. 2007. Nitrate reduction, sulfate reduction, and sedimentary iron isotope evolution during the Cenomanian–Turonian oceanic anoxic event. *Paleoceanography*, **22**, PA3208, https://doi.org/10.1029/2006PA001355

Jenkyns, H.C., Schouten-Huibers, L., Schouten, S. and Sinninghe Damsté, J.S. 2012. Warm Middle Jurassic–Early Cretaceous high-latitude sea-surface temperatures from the Southern Ocean. *Climate of the Past*, **8**, 215–226, https://doi.org/10.5194/cp-8-215-2012

Jenkyns, H.C., Dickson, A.J., Ruhl, M. and Boorn, S.H. 2017. Basalt-seawater interaction, the Plenus Cold Event, enhanced weathering and geochemical change: deconstructing Oceanic Anoxic Event 2 (Cenomanian–Turonian, Late Cretaceous). *Sedimentology*, **64**, 16–43, https://doi.org/10.1111/sed.12305

Jiang, Q., Jourdan, F., Olierook, H.K., Merle, R.E. and Whittaker, J.M. 2021. Longest continuously erupting large igneous province driven by plume–ridge interaction. *Geology*, **49**, 206–210, https://doi.org/10.1130/G47850.1

Jiang, Q., Jourdan, F. *et al*. 2022. Volume and rate of volcanic CO_2 emissions governed the severity of past environmental crises. *Proceedings of the National Academy of Sciences*, **119**, https://doi.org/10.1073/pnas.2202039119

Jiang, Q., Jourdan, F., Olierook, H.K. and Merle, R.E. 2023. An appraisal of the ages of Phanerozoic large igneous provinces. *Earth-Science Reviews*, **237**, 104314, https://doi.org/10.1016/j.earscirev.2023.104314

Jones, C.E. and Jenkyns, H.C. 2001. Seawater strontium isotopes, oceanic anoxic events, and seafloor hydrothermal activity in the Jurassic and Cretaceous. *American Journal of Science*, **301**, 112–149, https://doi.org/10.2475/ajs.301.2.112

Jones, M.T., Jerram, D.A., Svensen, H.H. and Grove, C. 2016. The effects of large igneous provinces on the global carbon and sulphur cycles. *Palaeogeography, Palaeoclimatology, Palaeoecology*, **441**, 4–21, https://doi.org/10.1016/j.palaeo.2015.06.042

Jones, M.M., Sageman, B.B., Selby, D., Jicha, B.R., Singer, B.S. and Titus, A.L. 2021. Regional chronostratigraphic synthesis of the Cenomanian–Turonian Oceanic Anoxic Event 2 (OAE 2) interval, Western Interior Basin (USA): new Re–Os chemostratigraphy and $^{40}Ar/^{39}Ar$ geochronology. *Geological Society of America Bulletin*, **133**, 1090–1104, https://doi.org/10.1130/B35594.1

Jones, M.M., Sageman, B.B. *et al*. 2023. Abrupt episode of mid-Cretaceous ocean acidification triggered by massive volcanism. *Nature Geoscience*, **16**, 169–174, https://doi.org/10.1038/s41561-022-01115-w

Junium, C.K. and Arthur, M.A. 2007. Nitrogen cycling during the Cretaceous, Cenomanian–Turonian oceanic anoxic event II. *Geochemistry, Geophysics, Geosystems*, **8**, https://doi.org/10.1029/2006GC001328

Kasbohm, J., Schoene, B. and Burgess, S. 2021. Radiometric constraints on the timing, tempo, and effects of large igneous province emplacement. *In*: Ernst, R.E., Dickson, A.J. and Bekker, A. (eds) *Large Igneous Provinces: A Driver of Global Environmental and Biotic Changes*. AGU, Geophysical Monographs, **255**, 27–82, https://doi.org/10.1002/9781119507444.ch2

Keller, G. 2012. The Cretaceous–Tertiary mass extinction, Chicxulub impact, and Deccan volcanism. *In*: Talent, J.A. (ed.) *Earth and Life: Global Biodiversity, Extinction Intervals and Biogeographic Perturbations Through Time*. Springer, Dordrecht, 759–793, https://doi.org/10.1007/978-90-481-3428-1_25

Keller, C.E., Hochuli, P.A., Weissert, H., Bernasconi, S.M., Giorgioni, M. and Garcia, T.I. 2011. A volcanically induced climate warming and floral change preceded the onset of OAE1a (Early Cretaceous). *Palaeogeography, Palaeoclimatology, Palaeoecology*, **305**, 43–49, https://doi.org/10.1016/j.palaeo.2011.02.011

Keller, G., Mateo, P. *et al*. 2018. Environmental changes during the Cretaceous–Paleogene mass extinction and Paleocene–Eocene thermal maximum: Implications for the Anthropocene. *Gondwana Research*, **56**, 69–89, https://doi.org/10.1016/j.gr.2017.12.002

Keller, G., Mateo, P. *et al*. 2020. Mercury linked to Deccan Traps volcanism, climate change and the end-Cretaceous mass extinction. *Global and Planetary Change*, **194**, 103312, https://doi.org/10.1016/j.gloplacha.2020.103312

Kent, R.W., Pringle, M.S., Müller, R.D., Saunders, A.D. and Ghose, N.C. 2002. $^{40}Ar/^{39}Ar$ geochronology of the Rajmahal basalts, India, and their relationship to the Kerguelen Plateau. *Journal of Petrology*, **43**, 1141–1153, https://doi.org/10.1093/petrology/43.7.1141

Kerr, A.C. 1998. Oceanic plateau formation: a cause of mass extinction and black shale deposition around the Cenomanian–Turonian boundary? *Journal of the Geological Society of London*, **155**, 619–626, https://doi.org/10.1144/gsjgs.155.4.0619

Kerr, A.C. 2005. La Isla de Gorgona, Colombia: a petrological enigma? *Lithos*, **84**, 77–101, https://doi.org/10.1016/j.lithos.2005.02.006

Kerr, A.C. 2014. Oceanic Plateaus. *In*: Holland, H.D. and Turekian, K.K. (eds) *Treatise on Geochemistry: Vol: 4: the Crust*. Elsevier, Amsterdam, 631–667, https://doi.org/10.1016/B978-0-08-095975-7.00320-X

Kerr, A.C., Tarney, J., Marriner, G.F., Nivia, A. and Saunders, A.D. 1997. The Caribbean–Colombian Cretaceous igneous province: the internal anatomy of an oceanic plateau. *In*: Mahoney, J.J. and Coffin, M.F. (eds) *Large Igneous Provinces, Continental, Oceanic, and Planetary Flood Volcanism*. AGU, Geophysical Monographs, **100**, 123–144.

Kerr, A.C., White, R.V., Thompson, P.M.E., Tarney, J. and Saunders, A.D. 2003. No Oceanic Plateau – no Caribbean Plate? The seminal role of an oceanic plateau in Caribbean Plate evolution. *In*: Bartolini, C., Buffler, R.T. and Blickwede, J. (eds) *The Gulf of Mexico and Caribbean Region: Hydrocarbon Habitats, Basin Formation and Plate Tectonics*. AAPG Memoir, **79**, 126–168.

Kerr, A.C., Tarney, J., Kempton, P.D., Pringle, M. and Nivia, A. 2004. Mafic pegmatites intruding oceanic plateau gabbros and ultramafic cumulates from Bolívar, Colombia: evidence for a 'wet' mantle plume? *Journal of Petrology*, **45**, 1877–1906, https://doi.org/10.1093/petrology/egh037

Kiessling, W. and Kocsis, ÁT . 2015. Biodiversity dynamics and environmental occupancy of fossil azooxanthellate and zooxanthellate scleractinian corals. *Paleobiology*, **41**, 402–414, https://doi.org/10.1017/pab.2015.6

Kim, J.H., Van der Meer, J. *et al*. 2010. New indices and calibrations derived from the distribution of crenarchaeal isoprenoid tetraether lipids: implications for past sea surface temperature reconstructions. *Geochimica et Cosmochimica Acta*, **74**, 4639–4654, https://doi.org/10.1016/j.gca.2010.05.027

Kingsbury, C.G., Kamo, S.L., Ernst, R.E., Söderlund, U. and Cousens, B.L. 2018. U–Pb geochronology of the plumbing system associated with the Late Cretaceous Strand Fiord Formation, Axel Heiberg Island, Canada: part of the 130–90 Ma High Arctic large igneous province. *Journal of Geodynamics*, **118**, 106–117, https://doi.org/10.1016/j.jog.2017.11.001

Kongchum, M., Hudnall, W.H. and Delaune, R.D. 2011. Relationship between sediment clay minerals and total mercury. *Journal of Environmental Science and Health, Part A*, **46**, 534–539, https://doi.org/10.1080/10934529.2011.551745

Kocsis, Á.T. and Scotese, C.R. 2021. Mapping paleocoastlines and continental flooding during the Phanerozoic. *Earth-Science Reviews*, **213**, 103463, https://doi.org/10.1016/j.earscirev.2020.103463

Kuhnt, W., Holbourn, A. and Moullade, M. 2011. Transient global cooling at the onset of early Aptian Oceanic Anoxic Event (OAE) 1a. *Geology*, **39**, 323–326, https://doi.org/10.1130/G31554.1

Kujau, A., Heimhofer, U. *et al*. 2013. Reconstructing Valanginian (Early Cretaceous) mid-latitude vegetation and climate dynamics based on spore–pollen assemblages. *Review of Palaeobotany and Palynology*, **197**, 50–69, https://doi.org/10.1016/j.revpalbo.2013.05.003

Kumar, A., Pande, K., Venkatesan, T.R. and Rao, Y.B. 2001. The Karnataka Late Cretaceous dykes as products of the Marion Hot Spot at the Madagascar–India breakup event: evidence from $^{40}Ar–^{39}Ar$ geochronology and geochemistry. *Geophysical Research Letters*, **28**, 2715–2718, https://doi.org/10.1029/2001GL013007

Kump, L.R., Bralower, T.J. and Ridgwell, A. 2009. Ocean acidification in deep time. *Oceanography*, **22**, 94–107.

Kuroda, J., Ogawa, N.O., Tanimizu, M., Coffin, M.F., Tokuyama, H., Kitazato, H. and Ohkouchi, N. 2007. Contemporaneous massive subaerial volcanism and late cretaceous Oceanic Anoxic Event 2. *Earth and Planetary Science Letters*, **256**, 211–223, https://doi.org/10.1016/j.epsl.2007.01.027

Kuroda, J., Tanimizu, M. *et al*. 2011. Lead isotopic record of Barremian–Aptian marine sediments: implications for large igneous provinces and the Aptian climatic crisis. *Earth and Planetary Science Letters*, **307**, 126–134, https://doi.org/10.1016/j.epsl.2011.04.021

Kuypers, M.M., van Breugel, Y., Schouten, S., Erba, E. and Damsté, J.S.S. 2004. N_2-fixing cyanobacteria supplied nutrient N for Cretaceous oceanic anoxic events. *Geology*, **32**, 853–856, https://doi.org/10.1130/G20458.1

Larson, R.L. 1991. Latest pulse of Earth: evidence for a mid-Cretaceous superplume. *Geology*, **19**, 547–550, https://doi.org/10.1130/0091-7613(1991)019<0547:LPOEEF>2.3.CO;2

Larson, R.L. and Erba, E. 1999. Onset of the Mid-Cretaceous greenhouse in the Barremian–Aptian: igneous events and the biological, sedimentary, and geochemical responses. *Paleoceanography*, **14**, https://doi.org/10.1029/1999PA900040

Leandro, C.G., Savian, J.F. *et al*. 2022. Astronomical tuning of the Aptian stage and its implications for age recalibrations and paleoclimatic events. *Nature Communications*, **13**, https://doi.org/10.1038/s41467-022-30075-3

Lechler, M., Pogge von Strandmann, P.A.E., Jenkyns, H.C., Prosser, G. and Parente, M. 2015. Lithium-isotope evidence for enhanced silicate weathering during OAE 1a (Early Aptian Selli event). *Earth and Planetary Science Letters*, **432**, 210–222, https://doi.org/10.1016/j.epsl.2015.09.052

Leckie, R.M., Bralower, T.J. and Cashman, R. 2002. Oceanic anoxic events and plankton evolution: biotic response to tectonic forcing during the mid-Cretaceous. *Paleoceanography*, **17**, https://doi.org/10.1029/2001PA000623

Leighton, A.D., Hart, M.B., Smart, C.W., Leng, M.J. and Hampton, M. 2017. Timing recovery after the Cretaceous/Paleogene boundary: evidence from the Brazos River, Texas, USA. *Journal of Foraminiferal Research*, **47**, 229–238, https://doi.org/10.2113/gsjfr.47.3.229

Leloux, J. 1999. Numerical distribution of Santonian to Danian corals (Scleractinia, Octocorallia) of southern Limburg, the Netherlands. *Geologie en Mijnbouw*, **78**, 191–195, https://doi.org/10.1023/A:1003743301625

Li, L. and Keller, G. 1998*a*. Abrupt deep-sea warming at the end of the Cretaceous. *Geology*, **26**, 995–998, https://doi.org/10.1130/0091-7613(1998)026<0995:ADSWAT>2.3.CO;2

Li, L. and Keller, G. 1998*b*. Maastrichtian climate, productivity and faunal turnovers in planktic foraminifera in South Atlantic DSDP sites 525A and 21. *Marine Micropaleontology*, **33**, 55–86, https://doi.org/10.1016/S0377-8398(97)00027-3

Li, X., Wei, Y., Li, Y. and Zhang, C. 2016. Carbon isotope records of the early Albian oceanic anoxic event (OAE) 1b from eastern Tethys (southern Tibet, China). *Cretaceous Research*, **62**, 109–121, https://doi.org/10.1016/j.cretres.2015.08.015

Li, Y.X., Bralower, T.J. *et al*. 2008. Toward an orbital chronology for the early Aptian Oceanic Anoxic Event (OAE1a, ~120 Ma). *Earth and Planetary Science Letters*, **271**, 88–100, https://doi.org/10.1016/j.epsl.2008.03.055

Li, Y.X., Liu, X., Selby, D., Liu, Z., Montañez, I.P. and Li, X. 2022. Enhanced ocean connectivity and volcanism instigated global onset of Cretaceous Oceanic Anoxic Event 2 (OAE2) ~94.5 million years ago. *Earth and Planetary Science Letters*, **578**, 117331, https://doi.org/10.1016/j.epsl.2021.117331

Lini, A., Weissert, H. and Erba, E. 1992. The Valanginian carbon isotope event: a first episode of greenhouse climate conditions during the Cretaceous. *Terra Nova*, **4**, 374–384, https://doi.org/10.1111/j.1365-3121.1992.tb00826.x

Linnert, C., Mutterlose, J. and Erbacher, J. 2010. Calcareous nannofossils of the Cenomanian/Turonian boundary interval from the Boreal Realm (Wunstorf, northwest Germany). *Marine Micropaleontology*, **74**, 38–58, https://doi.org/10.1016/j.marmicro.2009.12.002

Linnert, C., Mutterlose, J. and Mortimore, R. 2011. Calcareous nannofossils from Eastbourne (southeastern England) and the paleoceanography of the Cenomanian–Turonian boundary interval. *Palaios*, **26**, 298–313, https://doi.org/10.2110/palo.2010.p10-130r

Littler, K., Robinson, S.A., Bown, P.R., Nederbragt, A.J. and Pancost, R.D. 2011. High sea-surface temperatures during the Early Cretaceous Epoch. *Nature Geoscience*, **4**, 169–172, https://doi.org/10.1038/ngeo1081

Liu, Z., Percival, L.M.E., Vandeputte, D., Selby, D., Claeys, P., Over, D.J. and Gao, Y. 2021. Late Devonian mercury record from North America and its implications for the Frasnian–Famennian mass extinction. *Palaeogeography, Palaeoclimatology, Palaeoecology*, **576**, 110502, https://doi.org/10.1016/j.palaeo.2021.110502

Lorenzen, J., Kuhnt, W., Holbourn, A., Flögel, S., Moullade, M. and Tronchetti, G. 2013. A new sediment core from the Bedoulian (Lower Aptian) stratotype at Roquefort–La Bédoule, SE France. *Cretaceous Research*, **39**, 6–16, https://doi.org/10.1016/j.cretres.2012.03.019

Lu, Z., Jenkyns, H.C. and Rickaby, R.E. 2010. Iodine to calcium ratios in marine carbonate as a paleo-redox proxy during oceanic anoxic events. *Geology*, **38**, 1107–1110, https://doi.org/10.1130/G31145.1

Lübke, N. and Mutterlose, J. 2016. The impact of OAE 1a on marine biota deciphered by size variations of coccoliths. *Cretaceous Research*, **61**, 169–179, https://doi.org/10.1016/j.cretres.2016.01.006

Lübke, N., Mutterlose, J. and Bottini, C. 2015. Size variations of coccoliths in Cretaceous oceans – a result of preservation, genetics and ecology? *Marine Micropaleontology*, **117**, 25–39, https://doi.org/10.1016/j.marmicro.2015.03.002

Mahanipour, A., Mutterlose, J. and Eftekhari, M. 2019. Calcareous nannofossils of the Barremian–Aptian interval from the southeastern Tethys (Zagros Basin, West Iran) and their paleoceanographic implications: A record of Oceanic Anoxic Event 1a. *Marine Micropaleontology*, **149**, 64–74, https://doi.org/10.1016/j.marmicro.2019.04.003

Maher, H.D. 2001. Manifestations of the Cretaceous High Arctic large igneous province in Svalbard. *The Journal of Geology*, **109**, 91–104, https://doi.org/10.1086/317960

Maher, W., Krikowa, F. and Ellwood, M. 2020. Mercury cycling in Australian estuaries and near shore coastal ecosystems: triggers for management. *Elementa Science of the Anthropocene*, **8**, https://doi.org/10.1525/elementa.425

Mahoney, J., Nicollet, C. and Dupuy, C. 1991. Madagascar basalts: tracking oceanic and continental sources. *Earth and Planetary Science Letters*, **104**, 350–363, https://doi.org/10.1016/0012-821X(91)90215-4

Mahoney, J.J., Storey, M., Duncan, R.A., Spencer, K.J. and Pringle, M. 1993. Geochemistry and age of the Ontong Java Plateau. *In*: Pringle, M., Sager, W.W., Sliter, W.V. and Stein, S. (eds) *The Mesozoic Pacific: Geology, Tectonics, and Volcanism*. AGU, Geophysical Monographs, **77**, 233–261, https://doi.org/10.1029/GM077p0233

Mahoney, J.J., Saunders, A.D., Storey, M. and Randriamanantenasoa, A. 2008. Geochemistry of the Volcan de l'Androy basalt–rhyolite complex, Madagascar Cretaceous igneous province. *Journal of Petrology*,

49, 1069–1096, https://doi.org/10.1093/petrology/egn018

Malinverno, A., Erba, E. and Herbert, T.D. 2010. Orbital tuning as an inverse problem: chronology of the early Aptian oceanic anoxic event 1a (Selli Level) in the Cismon APTICORE. *Paleoceanography and Paleoclimatology*, **25**, https://doi.org/10.1029/2009PA001769

Marks, L., Keiding, J., Wenzel, T., Trumbull, R.B., Veksler, I., Wiedenbeck, M. and Markl, G. 2014. F, Cl, and S concentrations in olivine-hosted melt inclusions from mafic dikes in NW Namibia and implications for the environmental impact of the Paraná–Etendeka large igneous province. *Earth and Planetary Science Letters*, **392**, 39–49, https://doi.org/10.1016/j.epsl.2014.01.057

Marsh, J.S., Ewart, A., Milner, S.C., Duncan, A.R. and Miller, R.M. 2001. The Etendeka Igneous Province: magma types and their stratigraphic distribution with implications for the evolution of the Paraná–Etendeka flood basalt province. *Bulletin of Volcanology*, **62**, 464–486, https://doi.org/10.1007/s004450000115

Martinez, M., Deconinck, J.F., Pellenard, P., Riquier, L., Company, M., Reboulet, S. and Moiroud, M. 2015. Astrochronology of the Valanginian–Hauterivian stages (Early Cretaceous): chronological relationships between the Paraná–Etendeka large igneous province and the Weissert and the Faraoni events. *Global and Planetary Change*, **131**, 158–173, https://doi.org/10.1016/j.gloplacha.2015.06.001

Martinez, M., Aguirre-Urreta, B. *et al*. 2023. Synchrony of carbon cycle fluctuations, volcanism and orbital forcing during the Early Cretaceous. *Earth-Science Reviews*, **239**, 104356, https://doi.org/10.1016/j.earscirev.2023.104356

Martínez-Rodríguez, R., Selby, D., Castro, J.M., de Gea, G.A., Nieto, L.M. and Ruiz-Ortiz, P.A. 2021. Tracking magmatism and oceanic change through the early Aptian Anoxic Event (OAE 1a) to the late Aptian: insights from osmium isotopes from the westernmost Tethys (SE Spain) Cau Core. *Global and Planetary Change*, **207**, 103652, https://doi.org/10.1016/j.gloplacha.2021.103652

Matsumoto, H., Kuroda, J., Coccioni, R., Frontalini, F., Sakai, S., Ogawa, N.O. and Ohkouchi, N. 2020. Marine Os isotopic evidence for multiple volcanic episodes during Cretaceous Oceanic Anoxic Event 1b. *Scientific Reports*, **10**, https://doi.org/10.1038/s41598-020-69505-x

Matsumoto, H., Coccioni, R., Frontalini, F., Shirai, K. and Kuroda, J. 2021*a*. Osmium isotopic evidence for eccentricity-paced increases in continental weathering during the Latest Hauterivian, Early Cretaceous. *Geochemistry, Geophysics, Geosystems*, **22**, e2021GC009789, https://doi.org/10.1029/2021GC009789

Matsumoto, H., Coccioni, R. *et al*. 2021*b*. Long-term Aptian marine osmium isotopic record of Ontong Java Nui activity. *Geology*, **49**, 1148–1152, https://doi.org/10.1130/G48863.1

Matsumoto, H., Coccioni, R. *et al*. 2022. Mid-Cretaceous marine Os isotope evidence for heterogeneous cause of oceanic anoxic events. *Nature communications*, **13**, https://doi.org/10.1038/s41467-021-27817-0

Matsumoto, H., Ishikawa, A., Coccioni, R., Frontalini, F. and Suzuki, K. 2023*a*. Fine-grained interplanetary dust input during the Turonian (Late Cretaceous): evidence from osmium isotope and platinum group elements. *Scientific Reports*, **13**, https://doi.org/10.1038/s41598-023-49252-5

Matsumoto, H., Shirai, K., Huber, B.T., MacLeod, K.G. and Kuroda, J. 2023*b*. High-resolution marine osmium and carbon isotopic record across the Aptian–Albian boundary at the southern Atlantic Ocean: implication for the enhanced continental weathering and the acidified oceanic condition across the Aptian–Albian boundary. *Palaeogeography, Palaeoclimatology, Palaeoecology*, **613**, 111414, https://doi.org/10.1016/j.palaeo.2023.111414

Mattioli, E., Pittet, B., Riquier, L. and Grossi, V. 2014. The mid-Valanginian Weissert Event as recorded by calcareous nannoplankton in the Vocontian Basin. *Palaeogeography, Palaeoclimatology, Palaeoecology*, **414**, 472–485, https://doi.org/10.1016/j.palaeo.2014.09.030

Mauffret, A. and Leroy, S. 1997. Seismic stratigraphy and structure of the Caribbean igneous province. *Tectonophysics*, **283**, 61–104, https://doi.org/10.1016/S0040-1951(97)00103-0

McAnena, A., Flögel, S. *et al*. 2013. Atlantic cooling associated with a marine biotic crisis during the mid-Cretaceous period. *Nature Geoscience*, **6**, 558–561, https://doi.org/10.1038/ngeo1850

McArthur, J.M., Janssen, N.M.M., Reboulet, S., Leng, M.J., Thirlwall, M.F. and Van de Schootbrugge, B. 2007. Palaeotemperatures, polar ice-volume, and isotope stratigraphy (Mg/Ca, $\delta^{18}O$, $\delta^{13}C$, $^{87}Sr/^{86}Sr$): the Early Cretaceous (Berriasian, Valanginian, Hauterivian). *Palaeogeography, Palaeoclimatology, Palaeoecology*, **248**, 391–430, https://doi.org/10.1016/j.palaeo.2006.12.015

McArthur, J.M., Howarth, R.J., Shields, G.A. and Zhou, Y. 2020. Strontium isotope stratigraphy. *In*: Gradstein, F.M., Ogg, J.G., Schmitz, M.D. and Ogg, G.M. (eds) *Geologic Time Scale 2020*. Elsevier, 211–238, https://doi.org/10.1016/B978-0-12-824360-2.00027-3

Méhay, S., Keller, C.E., Bernasconi, S.M., Weissert, H., Erba, E., Bottini, C. and Hochuli, P.A. 2009. A volcanic CO_2 pulse triggered the Cretaceous Oceanic Anoxic Event 1a and a biocalcification crisis. *Geology*, **37**, 819–822, https://doi.org/10.1130/G30100A.1

Meissner, P., Mutterlose, J. and Bodin, S. 2015. Latitudinal temperature trends in the northern hemisphere during the Early Cretaceous (Valanginian–Hauterivian). *Palaeogeography, Palaeoclimatology, Palaeoecology*, **424**, 17–39, https://doi.org/10.1016/j.palaeo.2015.02.003

Melluso, L., Morra, V., Brotzu, P. and Mahoney, J.J. 2001. The Cretaceous igneous province of Madagascar: geochemistry and petrogenesis of lavas and dykes from the central-western sector. *Journal of Petrology*, **42**, 1249–1278, https://doi.org/10.1093/petrology/42.7.1249

Melluso, L., Morra, V. *et al*. 2005. Geochronology and petrogenesis of the Cretaceous Antampombato–Ambatovy complex and associated dyke swarm, Madagascar. *Journal of Petrology*, **46**, 1963–1996, https://doi.org/10.1093/petrology/egi044

Mena, M., Goguitchaichvili, A., Solano, M.C. and Vilas, J.F. 2011. Paleosecular variation and absolute geomagnetic paleointensity records retrieved from the Early Cretaceous Posadas Formation (Misiones, Argentina). *Studia Geophysica et Geodaetica*, **55**, 279–309, https://doi.org/10.1007/s11200-011-0016-3

Menegatti, A.P., Weissert, H., Brown, R.S., Tyson, R.V., Farrimond, P., Strasser, A. and Caron, M. 1998. High-resolution $\delta^{13}C$ stratigraphy through the early Aptian 'Livello Selli' of the Alpine Tethys. *Paleoceanography*, **13**, https://doi.org/10.1029/98PA01793

Meyers, S.R., Siewert, S.E. *et al*. 2012. Intercalibration of radioisotopic and astrochronologic time scales for the Cenomanian–Turonian boundary interval, Western Interior Basin, USA. *Geology*, **40**, 7–10, https://doi.org/10.1130/G32261.1

Millán, M.I., Weissert, H.J. and López-Horgue, M.A. 2014. Expression of the late Aptian cold snaps and the OAE1b in a highly subsiding carbonate platform (Aralar, northern Spain). *Palaeogeography, Palaeoclimatology, Palaeoecology*, **411**, 167–179, https://doi.org/10.1016/j.palaeo.2014.06.024

Milner, S.C., Duncan, A.R. and Ewart, A. 1992. Quartz latite rheoignimbrite flows of the Etendeka Formation, north-western Namibia. *Bulletin of Volcanology*, **54**, 200–219, https://doi.org/10.1007/BF00278389

Milner, S.C., Duncan, A.R., Whittingham, A.M. and Ewart, A. 1995. Trans-Atlantic correlation of eruptive sequences and individual silicic volcanic units within the Paraná–Etendeka igneous province. *Journal of Volcanology and geothermal Research*, **69**, 137–157, https://doi.org/10.1016/0377-0273(95)00040-2

Mittal, T., Sprain, C.J., Renne, P.R. and Richards, M.A. 2022. Deccan volcanism at K-Pg time. *In*: Koeberl, C., Claeys, P. and Montanari, A. (eds) *From the Guajira Desert to the Apennines, and from Mediterranean Microplates to the Mexican Killer Asteroid: Honoring the Career of Walter Alvarez*. Geological Society of America, Special Papers, **557**, 471–496, https://doi.org/10.1130/2022.2557(22)

Möller, C., Mutterlose, J. and Alsen, P. 2015. Integrated stratigraphy of Lower Cretaceous sediments (Ryazanian–Hauterivian) from North-East Greenland. *Palaeogeography, Palaeoclimatology, Palaeoecology*, **437**, 85–97, https://doi.org/10.1016/j.palaeo.2015.07.014

Möller, C., Bornemann, A. and Mutterlose, J. 2020. Climate and paleoceanography controlled size variations of calcareous nannofossils during the Valanginian Weissert Event (Early Cretaceous). *Marine Micropaleontology*, **157**, 101875, https://doi.org/10.1016/j.marmicro.2020.101875

Montoya-Pino, C., Weyer, S., Anbar, A.D., Pross, J., Oschmann, W., van de Schootbrugge, B. and Arz, H.W. 2010. Global enhancement of ocean anoxia during Oceanic Anoxic Event 2: A quantitative approach using U isotopes. *Geology*, **38**, 315–318, https://doi.org/10.1130/G30652.1

Moreno-Sanchez, M. and Pardo-Trujillo, A. 2003. Stratigraphical and sedimentological constraints on western Colombia: Implications on the evolution of the Caribbean plate. *In*: Bartolini, C., Buffler, R.T. and Blickwede, J. (eds) *The Circum-Gulf of Mexico and the Caribbean: Hydrocarbon Habitats, Basin Formation, and Plate Tectonics*. AAPG Memoir, **79**, 891–924.

Mort, H.P., Adatte, T. *et al*. 2007. Phosphorus and the roles of productivity and nutrient recycling during Oceanic Anoxic Event 2. *Geology*, **35**, 483–486, https://doi.org/10.1130/G23475A.1

Mutterlose, J. 1998. The Barremian–Aptian turnover of biota in northwestern Europe: evidence from belemnites. *Palaeogeography, Palaeoclimatology, Palaeoecology*, **144**, 161–173, https://doi.org/10.1016/S0031-0182(98)00081-9

Mutterlose, J. and Böckel, B. 1998. The Barremian–Aptian interval in NW Germany: a review. *Cretaceous Research*, **19**, 539–568, https://doi.org/10.1006/cres.1998.0119

Mutterlose, J., Bottini, C., Schouten, S. and Sinninghe Damsté, J.S. 2014. High sea-surface temperatures during the early Aptian Oceanic Anoxic Event 1a in the boreal realm. *Geology*, **42**, 439–442, https://doi.org/10.1130/G35394.1

Naafs, B.D.A. and Pancost, R.D. 2016. Sea-surface temperature evolution across Aptian Oceanic Anoxic Event 1a. *Geology*, **44**, 959–962, https://doi.org/10.1130/G38575.1

Naafs, B.D.A., Castro, J.M., De Gea, G.A., Quijano, M.L., Schmidt, D.N. and Pancost, R.D. 2016. Gradual and sustained carbon dioxide release during Aptian Oceanic Anoxic Event 1a. *Nature Geoscience*, **9**, 135–139, https://doi.org/10.1038/ngeo2627

Naber, T.V., Grasby, S.E., Cuthbertson, J.P., Rayner, N. and Tegner, C. 2021. New constraints on the age, geochemistry, and environmental impact of High Arctic Large Igneous Province magmatism: tracing the extension of the Alpha Ridge onto Ellesmere Island, Canada. *Geological Society of America Bulletin*, **133**, 1695–1711, https://doi.org/10.1130/B35792.1

Navarro-Ramirez, J.P., Bodin, S., Heimhofer, U. and Immenhauser, A. 2015. Record of Albian to early Cenomanian environmental perturbation in the eastern subequatorial Pacific. *Palaeogeography, Palaeoclimatology, Palaeoecology*, **423**, 122–137, https://doi.org/10.1016/j.palaeo.2015.01.025

Neal, C.R., Mahoney, J.J., Kroenke, L.W., Duncan, R.A. and Petterson, M.G. 1997. The Ontong–Java Plateau. *In*: Mahoney, J.J. and Coffin, M.F. (eds) *Large Igneous Provinces: Continental, Oceanic and Planetary Flood Volcanism*. American Geophysical Union, Washington, DC, 183–216, https://doi.org/10.1029/GM100p0183

Nederbragt, A.J. and Fiorentino, A. 1999. Stratigraphy and palaeoceanography of the Cenomanian–Turonian boundary event in Oued Mellegue, north-western Tunisia. *Cretaceous Research*, **20**, 47–62, https://doi.org/10.1006/cres.1998.0136

Nerlich, R., Clark, S.R. and Bunge, H.P. 2014. Reconstructing the link between the Galapagos hotspot and the Caribbean Plateau. *GeoResJ*, **1**, 1–7, https://doi.org/10.1016/j.grj.2014.02.001

Nozaki, T., Suzuki, K., Ravizza, G., Kimura, J.I. and Chang, Q. 2012. A method for rapid determination of Re and Os isotope compositions using ID–MC–ICP–MS combined with the sparging method. *Geostandards and Geoanalytical Research*, **36**, 131–148, https://doi.org/10.1111/j.1751-908X.2011.00125.x

O'Connor, L.K., Jenkyns, H.C., Robinson, S.A., Remmelzwaal, S.R., Batenburg, S.J., Parkinson, I.J. and Gale, A.S. 2020. A re-evaluation of the Plenus Cold Event,

and the links between CO_2, temperature, and seawater chemistry during OAE 2. *Paleoceanography and Paleoclimatology*, **35**, https://doi.org/10.1029/2019PA003631

O'Connor, L.K., Crampton-Flood, E.D. *et al*. 2023. Steady decline in mean annual air temperatures in the first 30 ky after the Cretaceous–Paleogene boundary. *Geology*, **51**, 486–490, https://doi.org/10.1130/G50588.1

O'Hora, H.E., Petersen, S.V., Vellekoop, J., Jones, M.M. and Scholz, S.R. 2022. Clumped-isotope-derived climate trends leading up to the end-Cretaceous mass extinction in northwestern Europe. *Climate of the Past*, **18**, 1963–1982, https://doi.org/10.5194/cp-18-1963-2022

Olsson, R.K. and Liu, C. 1993. Controversies on the placement of Cretaceous–Paleogene boundary and the K/P mass extinction of planktonic foraminifera. *Palaios*, **8**, 127–139, https://doi.org/10.2307/3515167

Ostrander, C.M., Owens, J.D. and Nielsen, S.G. 2017. Constraining the rate of oceanic deoxygenation leading up to a Cretaceous Oceanic Anoxic Event (OAE-2: ~94 Ma). *Science Advances*, **3**, https://doi.org/10.1126/sciadv.1701020

Owens, J.D., Lyons, T.W., Li, X., Macleod, K.G., Gordon, G., Kuypers, M.M., Anbar, A., Kuhnt, W. and Severmann, S. 2012. Iron isotope and trace metal records of iron cycling in the proto-North Atlantic during the Cenomanian-Turonian oceanic anoxic event (OAE-2). *Paleoceanography*, **27**, https://doi.org/10.1029/2012PA002328

Owens, J.D., Gill, B.C. *et al*. 2013. Sulfur isotopes track the global extent and dynamics of euxinia during Cretaceous Oceanic Anoxic Event 2. *Proceedings of the National Academy of Sciences*, **110**, 18407–18412, https://doi.org/10.1073/pnas.1305304110

Palmer, M.R. and Edmond, J.M. 1989. The strontium isotope budget of the modern ocean. *Earth and Planetary Science Letters*, **92**, 11–26, https://doi.org/10.1016/0012-821X(89)90017-4

Pancost, R.D., Crawford, N., Magness, S., Turner, A., Jenkyns, H.C. and Maxwell, J.R. 2004. Further evidence for the development of photic-zone euxinic conditions during Mesozoic oceanic anoxic events. *Journal of the Geological Society*, **161**, 353–364, https://doi.org/10.1144/0016764903-059

Pande, K., Sheth, H.C. and Bhutani, R. 2001. ^{40}Ar–^{39}Ar age of the St. Mary's Islands volcanics, southern India: record of India–Madagascar break-up on the Indian subcontinent. *Earth and Planetary Science Letters*, **193**, 39–46, https://doi.org/10.1016/S0012-821X(01)00495-2

Papadomanolaki, N.M., van Helmond, N.A., Pälike, H., Sluijs, A. and Slomp, C.P. 2022. Quantifying volcanism and organic carbon burial across Oceanic Anoxic Event 2. *Geology*, **50**, 511–515, https://doi.org/10.1130/G49649.1

Paquay, F.S. and Ravizza, G. 2012. Heterogeneous seawater $^{187}Os/^{188}Os$ during the late Pleistocene glaciations. *Earth and Planetary Science Letters*, **349**, 126–138, https://doi.org/10.1016/j.epsl.2012.06.051

Parisio, L., Jourdan, F., Marzoli, A., Melluso, L., Sethna, S.F. and Bellieni, G. 2016. $^{40}Ar/^{39}Ar$ ages of alkaline and tholeiitic rocks from the northern Deccan Traps: implications for magmatic processes and the K–Pg boundary. *Journal of the Geological Society*, **173**, 679–688, https://doi.org/10.1144/jgs2015-133

Paul, C.R.C., Lamolda, M.A., Mitchell, S.F., Vaziri, M.R., Gorostidi, A. and Marshall, J.D. 1999. The Cenomanian–Turonian boundary at Eastbourne (Sussex, UK): a proposed European reference section. *Palaeogeography, Palaeoclimatology, Palaeoecology*, **150**, 83–121, https://doi.org/10.1016/S0031-0182(99)00009-7

Pauly, S., Mutterlose, J. and Alsen, P. 2012. Early Cretaceous palaeoceanography of the Greenland–Norwegian Seaway evidenced by calcareous nannofossils. *Marine Micropaleontology*, **90**, 72–85, https://doi.org/10.1016/j.marmicro.2012.04.004

Pauly, S., Mutterlose, J. and Wray, D.S. 2013. Palaeoceanography of Lower Cretaceous (Barremian–Lower Aptian) black shales from northwest Germany evidenced by calcareous nannofossils and geochemistry. *Cretaceous Research*, **42**, 28–43, https://doi.org/10.1016/j.cretres.2013.01.001

Peate, D.W. 1997. The Paraná–Etendeka Province. *In*: Mahoney, J.J. and Coffin, M.F. (eds) *Large Igneous Provinces: Continental, Oceanic, and Planetary Volcanism*. AGU, Geophysical Monographs, **100**, 217–245.

Percival, L.M.E., Jenkyns, H.C. *et al*. 2018. Does large igneous province volcanism always perturb the mercury cycle? Comparing the records of Oceanic Anoxic Event 2 and the end-Cretaceous to other Mesozoic events. *American Journal of Science*, **318**, 799–860, https://doi.org/10.2475/08.2018.01

Percival, L.M.E., van Helmond, N.A.G.M., Selby, D., Goderis, S. and Claeys, P. 2020. Complex interactions between large igneous province emplacement and global temperature changes during the Cenomanian–Turonian oceanic anoxic event (OAE 2). *Paleoceanography and Paleoclimatology*, **35**, https://doi.org/10.1029/2020PA004016

Percival, L.M.E., Bergquist, B.A., Mather, T.A. and Sanei, H. 2021*a*. Sedimentary mercury enrichments as a tracer of large igneous province volcanism. *In*: Ernst, R.E., Dickson, A.J. and Bekker, A. (eds) *Large Igneous Provinces: a Driver of Global Environmental and Biotic Changes*. AGU, Geophysical Monographs, **255**, 247–262, https://doi.org/10.1002/9781119507444.ch11

Percival, L.M.E., Tedeschi, L.R. *et al*. 2021*b*. Determining the style and provenance of magmatic activity during the Early Aptian Oceanic Anoxic Event (OAE 1a). *Global and Planetary Change*, **200**, 103461, https://doi.org/10.1016/j.gloplacha.2021.103461

Percival, L.M.E., Ownsworth, E.M., Selby, D., Robinson, S.A., Goderis, S. and Claeys, P. 2023. Valanginian climate cooling and environmental change driven by Paraná–Etendeka basalt erosion. *Geology*, **51**, 753–757, https://doi.org/10.1130/G51202.1

Petersen, S.V., Dutton, A. and Lohmann, K.C. 2016. End-Cretaceous extinction in Antarctica linked to both Deccan volcanism and meteorite impact via climate change. *Nature Communications*, **7**, https://doi.org/10.1038/ncomms12079

Peucker-Ehrenbrink, B. and Jahn, B.M. 2001. Rhenium-osmium isotope systematics and platinum group

element concentrations: loess and the upper continental crust. *Geochemistry, Geophysics, Geosystems*, **2**, https://doi.org/10.1029/2001GC000172

Peucker-Ehrenbrink, B. and Ravizza, G. 2000. The marine osmium isotope record. *Terra Nova*, **12**, 205–219, https://doi.org/10.1046/j.1365-3121.2000.00295.x

Phelps, R.M., Kerans, C., Da-Gama, R.O., Jeremiah, J., Hull, D. and Loucks, R.G. 2015. Response and recovery of the Comanche carbonate platform surrounding multiple Cretaceous oceanic anoxic events, northern Gulf of Mexico. *Cretaceous Research*, **54**, 117–144, https://doi.org/10.1016/j.cretres.2014.09.002

Pinto, V.M., Hartmann, L.A., Santos, J.O.S., McNaughton, N.J. and Wildner, W. 2011. Zircon U–Pb geochronology from the Paraná bimodal volcanic province support a brief eruptive cycle at ~135Ma. *Chemical Geology*, **281**, 93–102, https://doi.org/10.1016/j.chemgeo.2010.11.031

Pogge von Strandmann, P.A.E., Jenkyns, H.C. and Woodfine, R.G. 2013. Lithium isotope evidence for enhanced weathering during Ocean Anoxic Event 2. *Nature Geoscience*, **6**, 668–672, https://doi.org/10.1038/ngeo1875

Polteau, S., Hendriks, B.W.H. *et al*. 2016. The Early Cretaceous Barents Sea sill complex: distribution, $^{40}Ar/^{39}Ar$ geochronology, and implications for carbon gas formation. *Palaeogeography, Palaeoclimatology, Palaeoecology*, **441**, 83–95, https://doi.org/10.1016/j.palaeo.2015.07.007

Pospichal, J.J. 1996. Calcareous nannoplankton mass extinction at the Cretaceous/Tertiary boundary: an update. *In*: Ryder, G., Fastovsky, D.E. and Gartner, S. (eds) *The Cretaceous–Tertiary Event and Other Catastrophes in Earth History*. Geological Society of America, Special Papers, **307**, 335–360, https://doi.org/10.1130/0-8137-2307-8.335

Premoli Silva, L., Ripepe, M. and Tornaghi, M.E. 1989. Planktonic foraminiferal distribution record productivity cycles: evidence from the Aptian-Albian Piobbico core (central Italy). *Terra Nova*, **1**, 443–448, https://doi.org/10.1111/j.1365-3121.1989.tb00407.x

Premoli Silva, I., Erba, E., Salvini, G., Locatelli, C. and Verga, D. 1999. Biotic changes in Cretaceous oceanic anoxic events of the Tethys. *The Journal of Foraminiferal Research*, **29**, 352–370.

Price, G.D. and Mutterlose, J. 2004. Isotopic signals from late Jurassic–early Cretaceous (Volgian–Valanginian) sub-Arctic belemnites, Yatria River, Western Siberia. *Journal of the Geological Society*, **161**, 959–968, https://doi.org/10.1144/0016-764903-169

Price, G.D., Janssen, N.M., Martinez, M., Company, M., Vandevelde, J.H. and Grimes, S.T. 2018. A high-resolution belemnite geochemical analysis of Early Cretaceous (Valanginian–Hauterivian) environmental and climatic perturbations. *Geochemistry, Geophysics, Geosystems*, **19**, 3832–3843, https://doi.org/10.1029/2018GC007676

Punekar, J., Keller, G., Khozyem, H.M., Adatte, T., Font, E. and Spangenberg, J. 2016. A multi-proxy approach to decode the end-Cretaceous mass extinction. *Palaeogeography, Palaeoclimatology, Palaeoecology*, **441**, 116–136, https://doi.org/10.1016/j.palaeo.2015.08.025

Pyle, D.M. and Mather, T.A. 2003. The importance of volcanic emissions for the global atmospheric mercury cycle. *Atmospheric Environment*, **37**, 5115–5124, https://doi.org/10.1016/j.atmosenv.2003.07.011

Quémerais, B., Cossa, D., Rondeau, B., Pham, T.T. and Fortin, B. 1998. Mercury distribution in relation to iron and manganese in the waters of the St. Lawrence river. *Science of The Total Environment*, **213**, 193–201, https://doi.org/10.1016/S0048-9697(98)00092-8

Raup, D.M. and Sepkoski, J.J. 1982. Mass extinction in the marine fossil record. *Science (New York, NY)*, **215**, 1501–1503, https://doi.org/10.1126/science.215.4539.1501

Ravizza, G. and Peucker-Ehrenbrink, B. 2003. Chemostratigraphic evidence of Deccan volcanism from the marine osmium isotope record. *Science (New York, NY)*, **302**, 1392–1395, https://doi.org/10.1126/science.1089209

Ravizza, G. and VonderHaar, D. 2012. A geochemical clock in earliest Paleogene pelagic carbonates based on the impact-induced Os isotope excursion at the Cretaceous–Paleogene boundary. *Paleoceanography*, **27**, https://doi.org/10.1029/2012PA002301

Reddin, C.J., Kocsis, ÁT, Aberhan, M. and Kiessling, W. 2021. Victims of ancient hyperthermal events herald the fates of marine clades and traits under global warming. *Global Change Biology*, **27**, 868–878, https://doi.org/10.1111/gcb.15434

Renne, P.R., Ernesto, M., Pacca, I.G., Coe, R.S., Glen, J.M., Prévot, M. and Perrin, M. 1992. The age of Paraná flood volcanism, rifting of Gondwanaland, and the Jurassic–Cretaceous boundary. *Science (New York, NY)*, **258**, 975–979, https://doi.org/10.1126/science.258.5084.975

Renne, P.R., Glen, J.M., Milner, S.C. and Duncan, A.R. 1996. Age of Etendeka flood volcanism and associated intrusions in southwestern Africa. *Geology*, **24**, 659–662, https://doi.org/10.1029/2000PA000541

Renne, P.R., Sprain, C.J., Richards, M.A., Self, S., Vanderkluysen, L. and Pande, K. 2015. State shift in Deccan volcanism at the Cretaceous–Paleogene boundary, possibly induced by impact. *Science (New York, NY)*, **350**, 76–78, https://doi.org/10.1126/science.aac7549

Richards, M.A., Alvarez, W. *et al*. 2015. Triggering of the largest Deccan eruptions by the Chicxulub impact. *Geological Society of America Bulletin*, **127**, 1507–1520, https://doi.org/10.1130/B31167.1

Ridgwell, A. 2005. A Mid Mesozoic Revolution in the regulation of ocean chemistry. *Marine Geology*, **217**, 339–357, https://doi.org/10.1016/j.margeo.2004.10.036

Robinson, N., Ravizza, G., Coccioni, R., Peucker-Ehrenbrink, B. and Norris, R. 2009. A high-resolution marine $^{187}Os/^{188}Os$ record for the late Maastrichtian: distinguishing the chemical fingerprints of Deccan volcanism and the KP impact event. *Earth and Planetary Science Letters*, **281**, 159–168, https://doi.org/10.1016/j.epsl.2009.02.019

Robinson, S.A., Clarke, L.J., Nederbragt, A. and Wood, I.G. 2008. Mid-Cretaceous oceanic anoxic events in the Pacific Ocean revealed by carbon-isotope stratigraphy of the Calera Limestone, California, USA. *Geological Society of America Bulletin*, **120**, 1416–1426, https://doi.org/10.1130/B26350.1

Robinson, S.A., Heimhofer, U., Hesselbo, S.P. and Petrizzo, M.R. 2017. Mesozoic climates and oceans – a

tribute to Hugh Jenkyns and Helmut Weissert. *Sedimentology*, **64**, 1–15, https://doi.org/10.1111/sed.12349

Robinson, S.A., Dickson, A.J., Pain, A., Jenkyns, H.C., O'Brien, C.L., Farnsworth, A. and Lunt, D.J. 2019. Southern Hemisphere sea-surface temperatures during the Cenomanian–Turonian: implications for the termination of Oceanic Anoxic Event 2. *Geology*, **47**, 131–134, https://doi.org/10.1130/G45842.1

Rocha, B.C., Davies, J.H. *et al*. 2020. Rapid eruption of silicic magmas from the Paraná magmatic province (Brazil) did not trigger the Valanginian event. *Geology*, **48**, 1174–1178, https://doi.org/10.1130/G47766.1

Ruvalcaba Baroni, I., Van Helmond, N.A.G.M., Tsandev, I., Middelburg, J.J. and Slomp, C.P. 2015. The nitrogen isotope composition of sediments from the proto-North Atlantic during Oceanic Anoxic Event 2. *Paleoceanography*, **30**, 923–937, https://doi.org/10.1002/2014PA002744

Ryan, W.B.F. *et al*. 1979. Site 398. *Initial Reports of the Deep Sea Drilling Project*, **47**, 25–233, https://doi.org/10.2973/dsdp.proc.47-2.102.1979

Sabatino, N., Ferraro, S., Coccioni, R., Bonsignore, M., Del Core, M., Tancredi, V. and Sprovieri, M. 2018. Mercury anomalies in upper Aptian–lower Albian sediments from the Tethys realm. *Palaeogeography, Palaeoclimatology, Palaeoecology*, **495**, 163–170, https://doi.org/10.1016/j.palaeo.2018.01.008

Sageman, B.B., Meyers, S.R. and Arthur, M.A. 2006. Orbital time scale and new C-isotope record for Cenomanian–Turonian boundary stratotype. *Geology*, **34**, 125–128, https://doi.org/10.1130/G22074.1

Saunders, A.D. 2016. Two LIPs and two Earth-system crises: the impact of the North Atlantic Igneous Province and the Siberian Traps on the Earth-surface carbon cycle. *Geological Magazine*, **153**, 201–222, https://doi.org/10.1017/S0016756815000175

Saunders, A.D., Tarney, J., Kerr, A.C. and Kent, R.W. 1996. The formation and fate of large oceanic igneous provinces. *Lithos*, **37**, 81–95, https://doi.org/10.1016/0024-4937(95)00030-5

Scaife, J.D., Ruhl, M. *et al*. 2017. Sedimentary mercury enrichments as a marker for submarine large igneous province volcanism? Evidence from the Mid-Cenomanian event and Oceanic Anoxic Event 2 (Late Cretaceous). *Geochemistry, Geophysics, Geosystems*, **18**, https://doi.org/10.1002/2017GC007153

Schlanger, S.O. and Jenkyns, H.C. 1976. Cretaceous oceanic anoxic events: causes and consequences. *Geologie en Mijnbouw*, **55**, 179–184.

Schlanger, S.O., Jenkyns, H.C. and Premoli-Silva, I. 1981. Volcanism and vertical tectonics in the Pacific Basin related to global Cretaceous transgressions. *Earth and Planetary Science Letters*, **52**, 435–449, https://doi.org/10.1016/0012-821X(81)90196-5

Schmidt, A., Skeffington, R.A. *et al*. 2016. Selective environmental stress from sulphur emitted by continental flood basalt eruptions. *Nature Geoscience*, **9**, 77–82, https://doi.org/10.1038/ngeo2588

Schoene, B., Samperton, K.M. *et al*. 2015. U–Pb geochronology of the Deccan Traps and relation to the end-Cretaceous mass extinction. *Science (New York, NY)*, **347**, 182–184, https://doi.org/10.1126/science.aaa0118

Schoene, B., Eddy, M.P., Samperton, K.M., Keller, C.B., Keller, G., Adatte, T. and Khadri, S.F.R. 2019. U–Pb constraints on pulsed eruption of the Deccan Traps across the end-Cretaceous mass extinction. *Science (New York, NY)*, **363**, 862–866, https://doi.org/10.1126/science.aau2422

Scholle, P.A. and Arthur, M.A. 1980. Carbon isotope fluctuations in Cretaceous pelagic limestones: potential stratigraphic and petroleum exploration tool. *AAPG Bulletin*, **64**, 67–87, https://doi.org/10.1306/2F91892D-16CE-11D7-8645000102C1865D

Schröder-Adams, C.J., Herrle, J.O., Selby, D., Quesnel, A. and Froude, G. 2019. Influence of the High Arctic Igneous Province on the Cenomanian/Turonian boundary interval, Sverdrup Basin, High Canadian Arctic. *Earth and Planetary Science Letters*, **511**, 76–88, https://doi.org/10.1016/j.epsl.2019.01.023

Schroeder, W.H. and Munthe, J. 1998. Atmospheric mercury – an overview. *Atmospheric Environment*, **32**, 809–822, https://doi.org/10.1016/S1352-2310(97)00293-8

Schulte, P. *et al*. 2010. The Chicxulub asteroid impact and mass extinction at the Cretaceous–Paleogene boundary. *Science (New York, NY)*, **327**, 1214–1218, https://doi.org/10.1126/science.1177265

Selby, D., Mutterlose, J. and Condon, D.J. 2009. U–Pb and Re–Os geochronology of the Aptian/Albian and Cenomanian/Turonian stage boundaries: implications for timescale calibration, osmium isotope seawater composition and Re–Os systematics in organic-rich sediments. *Chemical Geology*, **265**, 394–409, https://doi.org/10.1016/j.chemgeo.2009.05.005

Self, S., Widdowson, M., Thordarson, T. and Jay, A.E. 2006. Volatile fluxes during flood basalt eruptions and potential effects on the global environment: a Deccan perspective. *Earth and Planetary Science Letters*, **248**, 518–532, https://doi.org/10.1016/j.epsl.2006.05.041

Self, S., Schmidt, A. and Mather, T.A. 2014. Emplacement characteristics, time scales, and volcanic gas release rates of continental flood basalt eruptions on Earth. *In*: Keller, G. and Kerr, A.C. (eds) *Volcanism, Impacts, and Mass Extinctions: Causes and Effects*. Geological Society of America, Special Papers, **505**, https://doi.org/10.1130/2014.2505(16)

Selin, N.E. 2009. Global biogeochemical cycling of mercury: a review. *Annual Review of Environment and Resources*, **34**, 43–63, https://doi.org/10.1146/annurev.environ.051308.084314

Senel, C.B., Kaskes, P. *et al*. 2023. Chicxulub impact winter sustained by fine silicate dust. *Nature Geoscience*, **16**, 1033–1040, https://doi.org/10.1038/s41561-023-01290-4

Senger, K. and Galland, O. 2022. Stratigraphic and spatial extent of HALIP magmatism in central Spitsbergen. *Geochemistry, Geophysics, Geosystems*, **23**, https://doi.org/10.1029/2021GC010300

Senger, K., Tveranger, J., Ogata, K., Braathen, A. and Planke, S. 2014. Late Mesozoic magmatism in Svalbard: a review. *Earth-Science Reviews*, **139**, 123–144, https://doi.org/10.1016/j.earscirev.2014.09.002

Seton, M., Gaina, C., Müller, R.D. and Heine, C. 2009. Mid-Cretaceous seafloor spreading pulse: fact or fiction? *Geology*, **37**, 687–690, https://doi.org/10.1130/G25624A.1

Sheldon, E., Ineson, J. and Bown, P. 2010. Late Maastrichtian warming in the Boreal Realm: calcareous nannofossil evidence from Denmark. *Palaeogeography, Palaeoclimatology, Palaeoecology*, **295**, 55–75, https://doi.org/10.1016/j.palaeo.2010.05.016

Shen, J., Algeo, T.J., Chen, J., Planavsky, N.J., Feng, Q., Yu, J. and Liu, J. 2019. Mercury in marine Ordovician/Silurian boundary sections of South China is sulfide-hosted and non-volcanic in origin. *Earth and Planetary Science Letters*, **511**, 130–140, https://doi.org/10.1016/j.epsl.2019.01.028

Shen, J., Feng, Q. *et al*. 2020. Sedimentary host phases of mercury (Hg) and implications for use of Hg as a volcanic proxy. *Earth and Planetary Science Letters*, **543**, 116333, https://doi.org/10.1016/j.epsl.2020.116333

Shmeit, M., Giraud, F., Jaillard, E., Reboulet, S., Masrour, M., Spangenberg, J.E. and El-Samrani, A. 2022. The Valanginian Weissert Event on the south Tethyan margin: a dynamic paleoceanographic evolution based on the study of calcareous nannofossils. *Marine Micropaleontology*, **175**, 102134, https://doi.org/10.1016/j.marmicro.2022.102134

Siebert, C., Scholz, F. and Kuhnt, W. 2021. A new view on the evolution of seawater molybdenum inventories before and during the Cretaceous Oceanic Anoxic Event 2. *Chemical Geology*, **582**, https://doi.org/10.1016/j.chemgeo.2021.120399

Sigal, J. 1979. Chronostratigraphy and ecostratigraphy of cretaceous formations recovered on DSDP Leg 47B, Site 398. *Initial Reports of the Deep Sea Drilling Project*, **47**, 287–326, https://doi.org/10.2973/dsdp.proc.47-2.105.1979

Sinninghe-Damsté, J.S. and Köster, J. 1998. A euxinic southern North Atlantic Ocean during the Cenomanian/Turonian oceanic anoxic event. *Earth and Planetary Science Letters*, **158**, 165–173, https://doi.org/10.1016/S0012-821X(98)00052-1

Sinninghe-Damsté, J.S., Kuypers, M.M., Pancost, R.D. and Schouten, S. 2008. The carbon isotopic response of algae, (cyano) bacteria, archaea and higher plants to the late Cenomanian perturbation of the global carbon cycle: insights from biomarkers in black shales from the Cape Verde Basin (DSDP Site 367). *Organic Geochemistry*, **39**, 1703–1718, https://doi.org/10.1016/j.orggeochem.2008.01.012

Sinton, C.W. and Duncan, R.A. 1997. Potential links between ocean plateau volcanism and global ocean anoxia at the Cenomanian–Turonian boundary. *Economic Geology*, **92**, 836–842, https://doi.org/10.2113/gsecongeo.92.7-8.836

Sinton, C.W., Duncan, R., Storey, M., Lewis, J. and Estrada, J.J. 1998. An oceanic flood basalt province within the Caribbean plate. *Earth and Planetary Science Letters*, **155**, 221–235, https://doi.org/10.1016/S0012-821X(97)00214-8

Slater, S.M., Bown, P., Twitchett, R.J., Danise, S. and Vajda, V. 2022. Global record of "ghost" nannofossils reveals plankton resilience to high CO_2 and warming. *Science*, **376** (6595), 853–856, https://doi.org/10.1126/science.abm7330

Smit, J. 1982. Extinction and evolution of planktonic foraminifera after a major impact at the Cretaceous/Tertiary boundary. *In*: Silver, L.T. and Schultz, P.H. (eds) *Geological Implications of Impacts of Large Asteroids and Comets on the Earth*. Geological Society of America, Special Papers, **190**, 329–352, https://doi.org/10.1130/SPE190-p329

Snow, L.J., Duncan, R.A. and Bralower, T.J. 2005. Trace element abundances in the Rock Canyon Anticline, Pueblo, Colorado, marine sedimentary section and their relationship to Caribbean plateau construction and oxygen anoxic event 2. *Paleoceanography*, **20**, PA3005, https://doi.org/10.1029/2004PA001093

Sprain, C.J., Renne, P.R., Vanderkluysen, L., Pande, K., Self, S. and Mittal, T. 2019. The eruptive tempo of Deccan volcanism in relation to the Cretaceous–Paleogene boundary. *Science (New York, NY)*, **363**, 866–870, https://doi.org/10.1126/science.aav1446

Steuber, T., Löser, H., Mutterlose, J. and Parente, M. 2023. Biogeodynamics of Cretaceous marine carbonate production. *Earth-Science Reviews*, **238**, 104341, https://doi.org/10.1016/j.earscirev.2023.104341

Storey, M., Mahoney, J.J., Saunders, A.D., Duncan, R.A., Kelley, S.P. and Coffin, M.F. 1995. Timing of hot spot related volcanism and the breakup of Madagascar and India. *Science (New York, NY)*, **267**, 852–855, https://doi.org/10.1126/science.267.5199.852

Stüben, D., Kramar, U. *et al*. 2003. Late Maastrichtian paleoclimatic and paleoceanographic changes inferred from Sr/Ca ratio and stable isotopes. *Palaeogeography, Palaeoclimatology, Palaeoecology*, **199**, 107–127, https://doi.org/10.1016/S0031-0182(03)00499-1

Suchéras-Marx, B., Mattioli, E., Allemand, P., Giraud, F., Pittet, B., Plancq, J. and Escarguel, G. 2019. The colonization of the oceans by calcifying pelagic algae. *Biogeosciences (online)*, **16**, 2501–2510, https://doi.org/10.5194/bg-16-2501-2019

Sullivan, D.L., Brandon, A.D., Eldrett, J., Bergman, S.C., Minisini, D. and Wright, S. 2020. High resolution osmium data record three distinct pulses of magmatic activity during Cretaceous Ocean Anoxic Event 2 (OAE 2). *Geochimica et Cosmochimica Acta*, **285**, 257–273, https://doi.org/10.1016/j.gca.2020.04.002

Svensen, H., Planke, S., Malthe-Sørenssen, A., Jamtveit, B., Myklebust, R., Eidem, T.R. and Rey, S.S. 2004. Release of methane from a volcanic basin as a mechanism for initial Eocene global warming. *Nature*, **429**, 542–545, https://doi.org/10.1038/nature02566

Svensen, H., Planke, S., Polozov, A.G., Schmidbauer, N., Corfu, F., Podladchikov, Y.Y. and Jamtveit, B. 2009. Siberian gas venting and the end-Permian environmental crisis. *Earth and Planetary Science Letters*, **277**, 490–500, https://doi.org/10.1016/j.epsl.2008.11.015

Svensen, H.H., Jerram, D.A., Polozov, A.G., Planke, S., Neal, C.R., Augland, L.E. and Emeleus, H.C. 2019. Thinking about LIPs: a brief history of ideas in Large igneous province research. *Tectonophysics*, **760**, 229–251, https://doi.org/10.1016/j.tecto.2018.12.008

Sweere, T.C., Dickson, A.J., Jenkyns, H.C., Porcelli, D., Elrick, M., van den Boorn, S.H. and Henderson, G.M. 2018. Isotopic evidence for changes in the zinc cycle during Oceanic Anoxic Event 2 (Late Cretaceous). *Geology*, **46**, 463–466, https://doi.org/10.1130/G40226.1

Tarduno, J. 1998. The High Arctic Large Igneous Province. Paper presented at the Third International Conference

on Arctic Margins, Federal Institute for Geosciences and Natural Resources, Celle, Germany, 12–16.

Taylor, B. 2006. The single largest oceanic plateau: Ontong Java–Manihiki–Hikurangi. *Earth and Planetary Science Letters*, **241**, 372–380, https://doi.org/10.1016/j.epsl.2005.11.049

Tegner, C., Storey, M., Holm, P.M., Thorarinsson, S.B., Zhao, X., Lo, C.H. and Knudsen, M.F. 2011. Magmatism and Eurekan deformation in the High Arctic Large Igneous Province: ^{40}Ar–^{39}Ar age of Kap Washington Group volcanics, North Greenland. *Earth and Planetary Science Letters*, **303**, 203–214, https://doi.org/10.1016/j.epsl.2010.12.047

Tejada, M.L.G., Mahoney, J.J., Duncan, R.A. and Hawkins, M.P. 1996. Age and geochemistry of basement and alkalic rocks of Malaita and Santa Isabel, Solomon Islands, southern margin of Ontong Java Plateau. *Journal of Petrology*, **37**, 361–394, https://doi.org/10.1093/petrology/37.2.361

Tejada, M.L.G., Mahoney, J.J., Neal, C.R., Duncan, R.A. and Petterson, M.G. 2002. Basement geochemistry and geochronology of Central Malaita, Solomon Islands, with implications for the origin and evolution of the Ontong Java Plateau. *Journal of Petrology*, **43**, 449–484, https://doi.org/10.1093/petrology/43.3.449

Tejada, M.L.G., Suzuki, K. *et al*. 2009. Ontong Java Plateau eruption as a trigger for the early Aptian oceanic anoxic event. *Geology*, **37**, 855–858, https://doi.org/10.1130/G25763A.1

Them, T.R., Jagoe, C.H. *et al*. 2019. Terrestrial sources as the primary delivery mechanism of mercury to the oceans across the Toarcian Oceanic Anoxic Event (Early Jurassic). *Earth and Planetary Science Letters*, **507**, 62–72, https://doi.org/10.1016/j.epsl.2018.11.029

Thibault, N. and Gardin, S. 2007. The late Maastrichtian nannofossil record of climate change in the South Atlantic DSDP Hole 525A. *Marine Micropaleontology*, **65**, 163–184, https://doi.org/10.1016/j.marmicro.2007.07.004

Thiede, D.S. and Vasconcelos, P.M. 2010. Paraná flood basalts: rapid extrusion hypothesis confirmed by new ^{40}Ar/^{39}Ar results. *Geology*, **38**, 747–750, https://doi.org/10.1130/G30919.1

Thórarinsson, S.B., Söderlund, U., Døssing, A., Holm, P.M., Ernst, R.E. and Tegner, C. 2015. Rift magmatism on the Eurasia basin margin: U–Pb baddeleyite ages of alkaline dyke swarms in North Greenland. *Journal of the Geological Society*, **172**, 721–726, https://doi.org/10.1144/jgs2015-049

Thordarson, T. 2004. Accretionary-lapilli-bearing pyroclastic rocks at ODP Leg 192 Site 1184: a record of subaerial phreatomagmatic eruptions on the Ontong Java Plateau. *Geological Society of London, Special Publications*, **229**, 275–306, https://doi.org/10.1144/GSL.SP.2004.229.01.16

Tierney, J.E. and Tingley, M.P. 2014. A Bayesian, spatially-varying calibration model for the TEX_{86} proxy. *Geochimica et Cosmochimica Acta*, **127**, 83–106, https://doi.org/10.1016/j.gca.2013.11.026

Timm, C., Hoernle, K. *et al*. 2011. Age and geochemistry of the oceanic Manihiki Plateau, SW Pacific: new evidence for a plume origin. *Earth and Planetary Science Letters*, **304**, 135–146, https://doi.org/10.1016/j.epsl.2011.01.025

Tobin, T.S., Bitz, C.M. and Archer, D. 2017. Modeling climatic effects of carbon dioxide emissions from Deccan Traps volcanic eruptions around the Cretaceous–Paleogene boundary. *Palaeogeography, Palaeoclimatology, Palaeoecology*, **478**, 139–148, https://doi.org/10.1016/j.palaeo.2016.05.028

Torsvik, T.H. 2019. Earth history: A journey in time and space from base to top. *Tectonophysics*, **760**, 297–313, https://doi.org/10.1016/j.tecto.2018.09.009

Torsvik, T.H., Tucker, R.D., Ashwal, L.D., Eide, E.A., Rakotosolofo, N.A. and De Wit, M.J. 1998. Late Cretaceous magmatism in Madagascar: palaeomagnetic evidence for a stationary Marion hotspot. *Earth and Planetary Science Letters*, **164**, 221–232, https://doi.org/10.1016/S0012-821X(98)00206-4

Torsvik, T.H., Tucker, R.D., Ashwal, L.D., Carter, L.M., Jamtveit, B., Vidyadharan, K.T. and Venkataramana, P. 2000. Late Cretaceous India–Madagascar fit and timing of break-up related magmatism. *Terra Nova*, **12**, 220–224, https://doi.org/10.1046/j.1365-3121.2000.00300.x

Trabucho Alexandre, J., van Gilst, R.I., Rodríguez-López, J.P. and De Boer, P.L. 2011. The sedimentary expression of oceanic anoxic event 1b in the North Atlantic. *Sedimentology*, **58**, 1217–1246, https://doi.org/10.1111/j.1365-3091.2010.01202.x

Tsikos, H., Jenkyns, H.C. *et al*. 2004*a*. Carbon-isotope stratigraphy recorded by the Cenomanian–Turonian Oceanic Anoxic Event: correlation and implications based on three key localities. *Journal of the Geological Society of London*, **161**, 711–719, https://doi.org/10.1144/0016-764903-077

Tsikos, H., Karakitsios, V. *et al*. 2004*b*. Organic-carbon deposition in the Cretaceous of the Ionian Basin, NW Greece: the Paquier Event (OAE 1b) revisited. *Geological Magazine*, **141**, 401–416, https://doi.org/10.1017/S0016756804009409

Turgeon, S.C. and Creaser, R.A. 2008. Cretaceous Oceanic Anoxic Event 2 triggered by a massive magmatic episode. *Nature*, **454**, 323–326, https://doi.org/10.1038/nature07076

van Bentum, E.C., Hetzel, A., Brumsack, H.J., Forster, A., Reichart, G.J. and Damste, J.S.S. 2009. Reconstruction of water column anoxia in the equatorial Atlantic during the Cenomanian–Turonian oceanic anoxic event using biomarker and trace metal proxies. *Palaeogeography, Palaeoclimatology, Palaeoecology*, **280**, 489–498, https://doi.org/10.1016/j.palaeo.2009.07.003

van Breugel, Y., Schouten, S., Tsikos, H., Erba, E., Price, G.D. and Sinninghe Damsté, J.S. 2007. Synchronous negative carbon isotope shifts in marine and terrestrial biomarkers at the onset of the early Aptian Oceanic Anoxic Event 1a: Evidence for the release of ^{13}C-depleted carbon into the atmosphere. *Paleoceanography*, **22**, https://doi.org/10.1029/2006PA001341

van Helmond, N.A.G.M., Sluijs, A., Reichart, G.J., Sinninghe Damsté, J.S., Slomp, C.P. and Brinkhuis, H. 2014. A perturbed hydrological cycle during Oceanic Anoxic Event 2. *Geology*, **42**, 123–126, https://doi.org/10.1130/G34929.1

van Helmond, N.A.G.M., Sluijs, A. *et al*. 2015. Freshwater discharge controlled deposition of Cenomanian–Turonian black shales on the NW European epicontinental shelf (Wunstorf, northern Germany). *Climate of the Past*, **11**, 495–508, https://doi.org/10.5194/cp-11-495-2015

van Helmond, N.A.G.M., Sluijs, A. *et al*. 2016. Equatorward phytoplankton migration during a cold spell within the Late Cretaceous super-greenhouse. *Biogeosciences (online)*, **13**, 2859–2872, https://doi.org/10.5194/bg-13-2859-2016

Vaughan, A.P. and Storey, B.C. 2007. A new supercontinent self-destruct mechanism: evidence from the Late Triassic–Early Jurassic. *Journal of the Geological Society*, **164**, 383–392, https://doi.org/10.1144/0016-76492005-109

Vellekoop, J., Esmeray-Senlet, S. *et al*. 2016. Evidence for Cretaceous–Paleogene boundary bolide 'impact winter' conditions from New Jersey, USA. *Geology*, **44**, 619–622, https://doi.org/10.1130/G37961.1

Vellekoop, J., Woelders, L., Sluijs, A., Miller, K.G. and Speijer, R.P. 2019. Phytoplankton community disruption caused by latest Cretaceous global warming. *Biogeosciences (online)*, **16**, 4201–4210, https://doi.org/10.5194/bg-16-4201-2019

Vickers, M.L., Price, G.D., Jerrett, R.M. and Watkinson, M. 2016. Stratigraphic and geochemical expression of Barremian–Aptian global climate change in Arctic Svalbard. *Geosphere*, **12**, 1594–1605, https://doi.org/10.1130/GES01344.1

Vickers, M.L., Jelby, M.E. *et al*. 2023. Volcanism and carbon cycle perturbations in the High Arctic during the Late Jurassic–Early Cretaceous. *Palaeogeography, Palaeoclimatology, Palaeoecology*, **613**, 111412, https://doi.org/10.1016/j.palaeo.2023.111412

Wagreich, M. 2012. 'OAE 3'–regional Atlantic organic carbon burial during the Coniacian–Santonian. *Climate of the Past*, **8**, 1447–1455, https://doi.org/10.5194/cp-8-1447-2012

Walker, R.J., Echeverria, L.M., Shirey, S.B. and Horan, M.F. 1991. Re–Os isotopic constraints on the origin of volcanic rocks, Gorgona Island, Colombia: Os isotopic evidence for ancient heterogeneities in the mantle. *Contributions to Mineralogy and Petrology*, **107**, 150–162, https://doi.org/10.1007/BF003 10704

Walker, R.J., Storey, M., Kerr, A.C., Tarney, J. and Arndt, N.T. 1999. Implications of ^{187}Os isotopic heterogeneities in a mantle plume: evidence from Gorgona Island and Curaçao. *Geochimica et Cosmochimica Acta*, **63**, 713–728, https://doi.org/10.1016/S0016-7037(99)00041-1

Wallace, P.J., Frey, F.A., Weis, D. and Coffin, M.F. 2002. Origin and evolution of the Kerguelen Plateau, Broken Ridge and Kerguelen archipelago. *Journal of Petrology*, **43**, 1105–1108, https://doi.org/10.1093/petrology/43.7.1105

Wang, S., Shao, L.Y., Yan, Z.M., Shi, M.J. and Zhang, Y.H. 2019. Characteristics of Early Cretaceous wildfires in peat-forming environment. *NE China Journal of Palaeogeography*, **8**, 1–13, https://doi.org/10.1186/s42501-019-0035-5

Weissert, H. 1989. C-isotope stratigraphy, a monitor of paleoenvironmental change: a case study from the Early Cretaceous. *Surveys in Geophysics*, **10**, 1–61, https://doi.org/10.1007/BF01901664

Weissert, H. and Erba, E. 2004. Volcanism, CO_2 and palaeoclimate: a Late Jurassic–Early Cretaceous carbon and oxygen isotope record. *Journal of the Geological Society*, **161**, 695–702, https://doi.org/10.1144/0016-764903-087

Weissert, H., Lini, A., Föllmi, K.B. and Kuhn, O. 1998. Correlation of Early Cretaceous carbon isotope stratigraphy and platform drowning events: a possible link? *Palaeogeography, Palaeoclimatology, Palaeoecology*, **137**, 189–203, https://doi.org/10.1016/S0031-0182(97)00109-0

Westerhold, T., Röhl, U., Donner, B., McCarren, H.K. and Zachos, J.C. 2011. A complete high-resolution Paleocene benthic stable isotope record for the central Pacific (ODP Site 1209). *Paleoceanography*, **26**, https://doi.org/10.1029/2010PA002092

Westermann, S., Föllmi, K.B. *et al*. 2010. The Valanginian δ^{13}C excursion may not be an expression of a global oceanic anoxic event. *Earth and Planetary Science Letters*, **290**, 118–131, https://doi.org/10.1016/j.epsl.2009.12.011

Whitechurch, H., Montigny, R., Sevigny, J., Storey, M. and Salters, V. 1992. K-Ar and ^{40}Ar/^{39}Ar ages of central Kerguelen Plateau basalts. *In*: Wise, S.W., Jr., Schlich, R. *et al*. (eds) *Proceedings of the Ocean Drilling Program, Scientific Results*, **120**, 71–77, College Station, TX (Ocean Drilling Program), https://doi.org/10.2973.odp.proc.sr.120.119.1992

Widdowson, M., Walsh, J.N. and Subbarao, K.V. 1997. The geochemistry of Indian bole horizons: palaeoenvironmental implications of Deccan intravolcanic palaeosurfaces. *Geological Society, London, Special Publications*, **120**, 269–281, https://doi.org/10.1144/GSL.SP.1997.120.01.17

Wignall, P.B. 2001. Large igneous provinces and mass extinctions. *Earth-Science Reviews*, **53**, 1–33, https://doi.org/10.1016/S0012-8252(00)00037-4

Witts, J.D., Whittle, R.J., Wignall, P.B., Crame, J.A., Francis, J.E., Newton, R.J. and Bowman, V.C. 2016. Macrofossil evidence for a rapid and severe Cretaceous–Paleogene mass extinction in Antarctica. *Nature Communications*, **7**, https://doi.org/10.1038/ncomms11738

Woelders, L., Vellekoop, J. *et al*. 2017. Latest Cretaceous climatic and environmental change in the South Atlantic region. *Paleoceanography*, **32**, 466–483, https://doi.org/10.1002/2016PA003007

Woelders, L., Vellekoop, J. *et al*. 2018. Robust multi-proxy data integration, using late Cretaceous paleotemperature records as a case study. *Earth and Planetary Science Letters*, **500**, 215–224, https://doi.org/10.1016/j.epsl.2018.08.010

Xu, X., Shao, L. *et al*. 2022. Widespread wildfires linked to early Albian Ocean Anoxic Event 1b: Evidence from the Fuxin lacustrine basin, NE China. *Global and Planetary Change*, **215**, 103858, https://doi.org/10.1016/j.gloplacha.2022.103858

Yao, H., Chen, X., Yin, R., Grasby, S.E., Weissert, H., Gu, X. and Wang, C. 2021. Mercury evidence of intense volcanism preceded Oceanic Anoxic Event 1d. *Geophysical Research Letters*, **48**, https://doi.org/10.1029/2020GL091508

Yoshimura, Y. 2022. The Cretaceous normal superchron: a mini-review of its discovery, short reversal events, paleointensity, paleosecular variations, paleoenvironment, volcanism, and mechanism. *Frontiers in Earth Science*, **10**, https://doi.org/10.3389/feart.2022.834024

Zhao, X., Zheng, D., Wang, H., Fang, Y., Xue, N. and Zhang, H. 2022. Carbon cycle perturbation and mercury anomalies in terrestrial Oceanic Anoxic Event 1b

from Jiuquan Basin, NW China. *Geological Society, London, Special Publications*, **521**, 185–196, https://doi.org/10.1144/SP521-2021-149

Zheng, X.-Y., Jenkyns, H.C., Gale, A.S., Ward, D.J. and Henderson, G.M. 2013. Changing ocean circulation and hydrothermal inputs during Ocean Anoxic Event 2 (Cenomanian–Turonian): Evidence from Nd-isotopes in the European shelf sea. *Earth and Planetary Science Letters*, **375**, 338–348, https://doi.org/10.1016/j.epsl.2013.05.053